Universidade do Minho
Escola de Medicina

Inês Caetano Costa Campos

MRI biomarkers of the stressed brain: disclosing interactions between perception, morphology and functioning

dezembro de 2021

MRI biomarkers of the stressed brain: disclosing interactions between perception, morphology and functioning

Inês Caetano Costa Campos

UMinho | 2021

Universidade do Minho
Escola de Medicina

Inês Caetano Costa Campos

MRI biomarkers of the stressed brain: disclosing interactions between perception, morphology and functioning

Tese de Doutoramento
Ciências da Saúde

Trabalho efetuado sob a orientação do
Professor Doutor Nuno Jorge Carvalho Sousa

dezembro de 2021

DIREITOS DE AUTOR E CONDIÇÕES DE UTILIZAÇÃO DO TRABALHO POR TERCEIROS

Acknowledgments

To my mom, repeating the words I said in March 2017. To my number one fan, my niece Maria, which always tells me that I can do everything and by who I always try to be and do my best. To my sister, for all the things that we have shared as children. To my partner, Peter, to whom I do not know what to say but who knows everything I mean. To Bete and Joca, for being like second parents. To "Arius, the dog" for being always by my side (literally) and for being my best coping strategy. To Elsa and Bruno for still being the best friends I could ever ask. To Deolinda, my (new Ph.D.) friend for life.

Luck and success are made by effort, work, and good people. Professor Nuno, thank you for all your guidance, support, and availability. Besides being an amazing researcher (and professional), you were an outstanding supervisor. For that, you will always have my most sincere respect and gratitude. My dear neuroimaging team, you are the best! A special thanks to Maria, Ana, Rita, Sónia, Madalena, Liliana, Teresa and Ricardo. Thanks for everything (particularly the friendship); this work is also yours. To the School of Medicine, for their values, and to all the Professors that have been involved in my journey: "A good Ph.D. is a finished Ph.D.", and I could not be prouder.

The work presented in this thesis was performed in the Life and Health Sciences Research Institute (ICVS), School of Medicine, University of Minho, Braga, Portugal, the Clinical Academic Center (2CA), Braga, Portugal, and *Hospital de Braga*, Braga, Portugal.

Financial support was provided by grants from the Foundation for Science and Technology (FCT) [fellowship SFRH/BD/133006/2017, from Health Science program; projects UIDB/50026/2020, UIDP/50026/2020, PTDC/MED-NEU/29071/2017 and POCI-01-0145-FEDER-016428]; by BIAL Foundation [grants PT/FB/BL-2016-206, BIAL Foundation 30-16]; by Fundação Calouste Gulbenkian [contract grant P-139977]; and by the European Commission (FP7) [contract HEALTH-F2-2010-259772].

STATEMENT OF INTEGRITY

I hereby declare having conducted this academic work with integrity. I confirm that I have not used plagiarism or any form of undue use of information or falsification of results along the process leading to its elaboration.

I further declare that I have fully acknowledged the Code of Ethical Conduct of the University of Minho.

Assinado por : **Inês Caetano Costa Campos**
Num. de Identificação: BI13848061
Data: 2021.12.15 17:09:00 +0000

Biomarcadores de RM do cérebro stressado: revelando interações entre perceção, morfologia e funcionamento

Resumo

O stress crónico e maladaptativo é um importante precursor para o desenvolvimento de doenças psiquiátricas como a ansiedade, depressão major e perturbação bipolar. De facto, a maioria dos indivíduos considera que as suas rotinas diárias são cada vez mais stressantes, estimando-se que 1 em cada 5 anos de vida seja atualmente vivido com incapacidade devido a doença mental. A resposta ao stress é uma reação multisistémica que conta com o envolvimento primário do eixo hipotálamo-hipófise-suprarrenal, que desempenha um papel fulcral na adaptação do indivíduo a situações imprevisíveis. No entanto, a exposição a stress crónico pode causar a desregulação de mecanismos internos do corpo, que, a longo prazo, podem potencializar o desenvolvimento de doença. Mesmo partilhando o mesmo antecedente, cada doença neuropsiquiátrica tem características únicas. Assim, é de extrema importância investigar não só o que acontece durante e após a patologia, mas também o que a antecede. De facto, o estudo contínuo é altamente benéfico para um melhor entendimento da neurofisiologia do stress. É ainda essencial se considerarmos terapias preventivas. Até à data, são poucos os estudos que avaliam o impacto do stress em populações não clínicas. Para além disso, existem algumas discrepâncias na literatura que poderão estar relacionadas com o tamanho reduzido da amostragem dos estudos atualmente publicados. Assim, esta Tese teve como objetivo providenciar novos conhecimentos sobre as alterações que o stress (e em particular, o stress percebido) provoca na morfologia e função cerebral, procurando também encontrar novos sinais que possam ser utilizados como biomarcadores do cérebro stressado. Os nossos resultados mostram que existe uma relação forte entre o tamanho da amígdala direita e a perceção de stress. Esta associação positiva é estável quer a curto-prazo, quer ao longo da idade. Para além disso, esta Tese também mostra que aumentos na perceção de stress estão relacionados com aumentos na conetividade funcional da amígdala com regiões corticais, tal como com diminuições na ocorrência de um padrão de atividade contrabalançada entre um subsistema que engloba a amígdala e o hipocampo, e o resto do cérebro. Em suma, esta Tese demonstra que a perceção de stress se relaciona substancialmente quer com a morfologia do cérebro, quer com o seu funcionamento, sobretudo nas regiões da amígdala e hipocampo; interações que podem, em última análise, ser usadas como biomarcadores do cérebro stressado.

Palavras-chave: Amígdala, Conectividade funcional, Indivíduos saudáveis, Morfometria, Stresse percebido

MRI biomarkers of the stressed brain: disclosing interactions between perception, morphology and functioning

Abstract

Chronic, maladaptive, stress is a major precursor for the development of psychiatric diseases such as anxiety, major depression, and bipolar disorder. Importantly, daily routines are perceived as increasingly stressful by most individuals, being estimated that 1 out of 5 years is lived with incapacity due to mental disorders.

The stress response is a multisystemic reaction with the primary involvement of the HPA axis, which usually helps individuals overcome unpredictable situations. However, exposure to chronic stress may cause the dysregulation of internal mechanisms, which in the long run, may exacerbate disease development. Notably, even sharing the same precursor, each neuropsychiatric condition presents unique characteristics. Therefore, disclosing how the brain is altered before, during, and after the disease is highly beneficial to understanding stress neurophysiology and even crucial if considering mental preventive therapies.

To date, few stress studies focus on non-pathological populations, with literature showing significant discrepancies that may have been fostered by the small sample size of published works. Therefore, this Thesis aimed to provide new insights about the changes induced by stress (particularly the perceived stress) on the healthy brain structure and functioning, as well as pursuing the development of new in-vivo biomarkers of the stressed brain. Our findings revealed the existence of a strong link between amygdala size and stress perception, in which a positive association is stable across time, and across age. Moreover, our results also show that increases in perceived stress relate to increases in amygdala-cortical connectivity, as to decreases in the occurrence of a pattern of counterbalanced activity between the amygdala-hippocampal subsystem and the rest of the brain. Altogether, this Thesis shows that stress perception exhibits a substantial interaction with brain morphology and functioning, particularly in amygdalae and hippocampal regions, which can ultimately be used as biomarkers of the stressed brain.

Keywords: Amygdala, Functional connectivity, Healthy subjects, Morphometry, Perceived stress

Table of Contents

List of Abbreviations

A

ACC – Anterior cingulate cortex

ACh – Acetylcholine

ACTH – Adrenocorticotrophic hormone

Amy – Amygdala

AN – Auditory network

AVP – Arginine-vasopressin

B

BLA – Basolateral amygdala

BNST – Bed nucleus of the stria terminalis

BOLD – Blood oxygen level-dependent

C

CC – Cingulate cortex

CeA – Central amygdala

CG – Cingulate gyrus

CRH – Corticotrophin-releasing hormone

CSF – Cerebrospinal fluid

D

3D – 3-Dimensional

DAN – Dorsal attention network

DASS – Depression Anxiety Stress Scales

dlPFC – Dorsolateral prefrontal cortex

DMN – Default Mode Network

E

eTIV – Estimated total intracranial volume

F

FC – Functional connectivity

FG – Frontal gyrus

fMRI – Functional magnetic resonance imaging

FSG – Frontal superior gyrus

FSL – FMRIB Software Library

FWE-R – Family-wise error rate

G

GC – Glucocorticoid

GLM – General linear model

GM – Gray matter

GMV – Gray matter volume

GR – Glucocorticoid receptor

H

Hip – Hippocampus

HPA – Hypothalamic-pituitary-adrenal

I

INU – Intensity non-uniformity

ITG – Inferior temporal gyrus

L

LEiDA – Leading Eigenvector Dynamics Analysis

M

M – Mean

MC – Mineralocorticoids

MCG – Middle cingulate gyrus

MFG – Middle frontal gyrus

MR – Mineralocorticoid receptor

mPFC – Medial prefrontal cortex

MPRAGE – Magnetization-Prepared Rapid Acquisition with Gradient Echo

MRI – Magnetic resonance imaging

O

OFC – Orbitofrontal cortex

P

pCC – Posterior cingulate cortex

PFC – Prefrontal cortex

PSS – Perceived Stress Scale

PSS10 – 10-items Perceived Stress Scale

PVN – Paraventricular nucleus of the hypothalamus

R

ROI – Region-of-interest

Rs-fMRI – Resting-state functional magnetic resonance imaging

RSN – Resting state networks

S

SD – Standard deviation

SE – Standard error

SMN – Sensorimotor network

SNS – Sympathetic Nervous System

T

T1w – T1-weighted

TFCE – Threshold-free cluster enhancement

V

VAN – Ventral attention network

VBM – Voxel-based morphometry

vlPFC – Ventrolateral prefrontal cortex

vmPFC – Ventromedial prefrontal cortex

VN – Visual network

W

WB – Whole-brain

WHO – World Health Organization

WM – White matter

WMV – White matter volume

List of Figures

Supplementary Figure A1. Association of the left amygdala seed-based connectivity with PSS10 scores for a statistical significance of α = 0.1.

Supplementary Figure A2. Results from the association of LEiDA states with the PSS10 scores.

List of Tables

CHAPTER I

CHAPTER II

CHAPTER III

CHAPTER IV

CHAPTER V

CHAPTER I

1. Introduction

Daily routines are perceived as increasingly stressful by most individuals. Importantly, this perception triggers new challenges for mental health, with the number of people with stress symptoms growing day by day (Fett et al., 2019; Lederbogen et al., 2011). Importantly, chronic, maladaptive, stress is a major precursor for the development of psychiatric diseases such as anxiety (Pêgo et al., 2009), major depression (Welberg, 2014), and bipolar disorder (Kim et al., 2007). Furthermore, according to the World Health Organization (WHO), mental disorders are now responsible for 1 out of 5 years lived with incapacity. Future prospects are discouraging with around 20% of the world's children and adolescents already having a mental health disease (World Health Organization, 2021).

The stress response is multisystemic, being primarily recognized by the activation hypothalamic-pituitary-adrenal (HPA) axis and the release of glucocorticoids (GC). Although the stress response contributes to survival in acute life-threatening situations, exposure to chronic stress can dysregulate internal body mechanisms, causing maladaptive stress reactions that may exacerbate disease development. Notably, stressors vary in type, time, recurrence, and intensity, with the subject's outcome being highly variable due to individual susceptibility (Sousa, 2016).

The relevant link between stress and disease has always captured the research community's interest. The development of advanced techniques such as Magnetic Resonance Imaging (MRI), as well as powerful tools to study the brain (particularly in humans), have certainly helped our knowledge in this field (Soares et al., 2016; Sousa, 2016). Of relevance, disclosing how the brain is altered before, during, and after the disease is highly beneficial to the understanding of stress neurophysiology and even crucial if considering mental preventive therapies (Avvenuti et al., 2020; Bergdahl et al., 2005; Kaul et al., 2021).

2. Stress and Brain

2.1. Definition of stress

At the beginning of the XX century, Walter Cannon defined homeostasis as the tendency of our body to respond to the environment as a way of maintaining the internal physical and chemical conditions (such as fluid balance, temperature, pH, ions concentration, and blood sugar levels) within a range that allows to keep life going (Cannon, 1929, 1926). Years later, Hans Selye introduced the concept of stress as a

physiological response that aims to restore the homeostasis disrupted by an external stimulus, usually called stressor (Goldstein and Kopin, 2007; Selye, 1956). A stressor can vary in type (e.g., physical or psychological), duration (e.g., minutes to months), and occurrence (e.g., acute event or prolonged). Notably, it triggers a variable response on the subject, with the stressor's impact being highly conditioned by the susceptibility of each individual (Novais et al., 2017; Sousa, 2016). Interestingly, in acute situations and in moderate levels, stress contributes to the individual's survival and success. On the contrary, prolonged stress may lead to a maladaptive stress response, jeopardizing the subject's well-being and ultimately triggering the development of diverse neurological and psychiatric conditions (Lucassen et al., 2014; Sousa, 2016).

2.2. The Stress Response

The stress response is a multisystemic process also known as the fight-or-flight response (Cannon and Cannon, 1967). It counts with the primary involvement of the neuronal and endocrine systems, particularly on the HPA axis, as well as the Sympathetic Nervous System (SNS), which optimize the body for survival in the acute phase (Figure 1). It is worth noting that the stress response is mediated in two different ways: by neurotransmitters (in synapses, on neuron-to-neuron or neuron-to-effector communication) or through hormones (secreted by glands and released into the bloodstream). These substances act through receptors in distinct target tissues/organs. Interestingly, the same substance can either trigger an inhibitory or excitatory response (e.g., norepinephrine causes the contraction of smooth muscle with α_1 receptors [e.g., abdominal viscera vasoconstriction], and β_2 smooth muscle relaxation [e.g., bronchioles dilatation]).

The physiological response to daily stressors (such as professional, economic, and social questions) is mostly the same as life-threatening situations. Yet, ironically, in the long term, non-life-threatening situations are enabled to compromise subject health precisely due to the body's effectiveness in responding to stress.

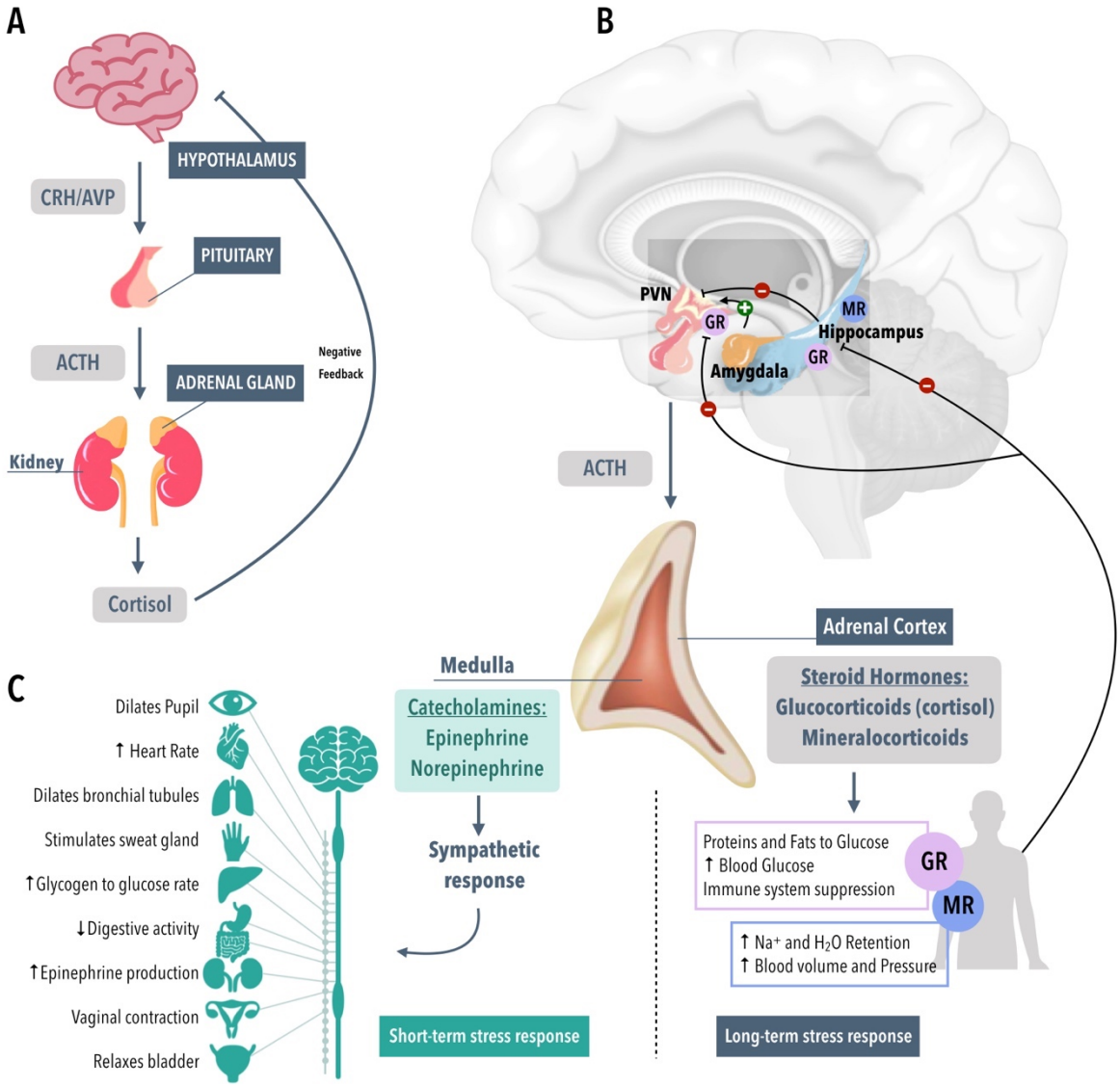

Figure 1. Physiology of Stress Response. A) General representation of the Hypothalamic-Pituitary-Adrenal axis. **B)** Schematic representation of the neuroendocrine response to stress and its regulation. **C)** Sympathetic acute response.

2.2.1. Physiology of Stress Response

The HPA axis (Figure 1A) is the major player in the stress response (Sapolsky et al., 1986). It is composed of hormone-secreting glands from the nervous and endocrine systems that, in the presence of a stimulus, are crucial for the occurrence of a cascade of events, also called stress response. In short, when a threat is recognized, different secretagogues, as the corticotrophin-releasing hormone (CRH) and arginine-

vasopressin (AVP), are released by the hypothalamus. These hormones will act on the pituitary gland, leading it to secrete the adrenocorticotrophic hormone (ACTH) into the bloodstream. The ACTH will then travel until the adrenal glands, where it prompts the release of different corticosteroids, such as cortisol (Keller-Wood and Dallman, 1984; Pêgo et al., 2009; Raabe and Spengler, 2013). This causes many physiological changes in the body that will help the individual face the stressor (e.g., use of body resources to deal with prolonged stressor by the production of glucose from non-carbohydrate sources) (Hannibal and Bishop, 2014). The final act of the stress response is led by a negative feedback mechanism to shut off the HPA activation when increased cortisol levels in the bloodstream are sensed by receptors in the brain (Raabe and Spengler, 2013).

The SNS, represented in Figure 1C, is the primary system to be recruited in the fight-or-flight response (Cannon and Cannon, 1967; Even et al., 2012). It is part of the Autonomic Nervous system responsible for the unconscious regulation of body functions, such as heart and respiratory rate, digestion, or pupillary response (Jänig, 1989). Indeed, in normal conditions, the SNS operates continuously at a basic level taking advantage of different neurotransmitters to regulate the body and maintain homeostasis (Brodal, 2004; Hall et al., 2015; Kreibig, 2010). In the presence of a stimulus, brain signals are sent through the spinal cord until the preganglionic neuronal axons, where acetylcholine (ACh) release occurs. Then, depending on the amount of ACh present in the synaptic cleft (i.e., if enough to generate a response), an action potential is sent throughout the postganglionic fiber until the effector organ, where the release of catecholamines (epinephrine and norepinephrine) will trigger the effector response (e.g., blood vessel or muscles contraction) (Kreibig, 2010; Sturmberg et al., 2015).

2.2.2. The central role of the brain and GC

Although considering the major importance of the HPA axis, the stress response begins with the stressor perception (Goldstein and Kopin, 2007). Notably, when facing a threat, the limbic system integrates different sensorial modalities to engage the stress response (Herman et al., 2005). This anticipated response counts with the involvement of the amygdala (which is primarily involved in emotional processing), the hippocampus (relating to memory and learning), and the prefrontal cortex (PFC) (involved in higher executive and cognitive functions) (Cerqueira et al., 2007; LeDoux, 2000; Maier et al., 2006). Notably, when facing a physical or psychological threat, these regions trigger the activation of the HPA axis through an indirect excitatory pathway. Therefore, regions as the bed nucleus of the stria terminalis (BNST) (part of the extended amygdala) (Herman et al., 2003, 1994) and the locus coeruleus (Plotsky et

al., 1989) are also known for being related to the stress response, due to their involvement in these indirect pathways (Cullinan and Herman, 1993; Herman et al., 2005; Pêgo et al., 2009; Prewitt and Herman, 1998). Of relevance for this Thesis, as demonstrated in Figure 1B, the amygdala has an excitatory effect on the HPA axis, promoting the release of CRH and AVP by the paraventricular nucleus of the hypothalamus (PVN). On the contrary, the hippocampus exerts an inhibitory action over the PVN to refrain the activation of the HPA axis.

As previously referred, upon the stimulation of the HPA axis, the CRH and AVP neuropeptides act on the pituitary gland, promoting the release of ACTH into the bloodstream that acts on the adrenal gland. As a result, the adrenal cortex releases two major types of steroid hormones: glucocorticoids (GC), where cortisol is included; and mineralocorticoids (MC). Briefly, GC are, amongst other actions, involved in the metabolization of proteins and fats, which will be reflected in the increased blood glucose. Besides increasing the body's energy levels, GC are also responsible for suppressing the immune system. In parallel, MC cause the retention of water and sodium molecules by the kidneys, also contributing to increased blood volume and pressure (Hall et al., 2015).

The brain expresses both glucocorticoids receptors (GR) and mineralocorticoids receptors (MR), namely in different limbic structures (Sousa et al., 2008). Importantly, it is suggested that MC are involved in stimuli perception and evaluation, linking hippocampal MR to the onset of the stress response (Raabe and Spengler, 2013). On the other hand, GC entails the normalization of the adaptive stress responses (playing an active role in fear learning and memory encoding), being responsible for shutting down the stress reaction. Indeed, high levels of GR are seen in the PVN and anterior pituitary, which corroborate the negative feedback hypothesis (de Kloet et al., 2005; Raabe and Spengler, 2013).

Importantly, the hippocampus, the amygdala, and the PFC present both GR and MR receptors, which, in case of dysregulation, can compromise the adequate balance of activity of the HPA axis (Sousa, 2016; van Ast et al., 2013). For example, under the persistent exposure to stress, changes in the hippocampal GC receptor's sensitivity can damage the HPA negative feedback mechanism and ultimately result in the development of neuropsychiatric disorders as affective diseases (Finsterwald and Alberini, 2014; Hall et al., 2015; McEwen et al., 2015; Merkulov et al., 2017). A note to highlight that CRH neurons on the amygdala indirectly potentiate the stress response (with the central amygdala projections to the locus coeruleus causing an increase of norepinephrine, which will, in turn, trigger the stimulation of the CHR PVN neurons) (de Kloet et al., 2005; Pêgo et al., 2009; Plotsky et al., 1989; Raabe and Spengler, 2013).

2.3. How Stress impacts the Brain

The pathophysiology repercussions of stress in the brain differ significantly under the influence of different elements such as the stressor type and intensity, and individual's susceptibility (Lee and Sawa, 2014; Sousa, 2016). Interestingly, due to brain neuroplasticity (and its ability to adapt structurally and functionally), many of the abnormalities caused by stress are reversible (Lee and Sawa, 2014; Soares et al., 2012; Weaver et al., 2006). Nevertheless, regardless of the possibility of recovery, acute and chronic stress impact brain structure and function, contributing to the emergence of neuropsychological diseases such as post-traumatic stress disorder (Brewin et al., 2000; Bryant, 2019; Davidson et al., 1991), anxiety (Melchior et al., 2007; Pêgo et al., 2009; Shin and Liberzon, 2010), major depression (Hammen, 2005; Kendler et al., 1999; Melchior et al., 2007; Welberg, 2014), bipolar disorder (Carvalho et al., 2020; Kim et al., 2007) or schizophrenia (Betensky et al., 2008; Gispen-de Wied, 2000; Walker et al., 2008). Notably, even sharing the same precursor, these pathologies present distinct characteristics (Kaul et al., 2021), with no specific illness or neurological sign being solely attributed as the result of stress exposure. Indeed, depending on several factors, GC and neurotransmitters can cause dendritic and synaptic density reduction or increase in distinct brain region targets (McEwen et al., 2015; Novais et al., 2017; Oliveira et al., 2012; Sharp, 2017). Here, we will briefly review the role of three limbic structures that are of extreme relevance for the stress response.

The amygdala has a vital role in the alarm system, being responsible for focusing attention on new stimuli and activating stress hormones. It is involved in the different behavioral, autonomic, and neuroendocrine processes, causing anxiety, triggering fear, and unleashing aggressiveness (Ventura-Silva et al., 2020; Zhang et al., 2021). Importantly, the amygdala has excitatory but also inhibitory effects in response to acute stimuli, which are, among other factors, dependent on the projections that are being stimulated (Zhang et al., 2021). Indeed, it is thought that the information initially reaches the lateral and the basolateral amygdala, following to the central amygdala (CeA), which will initiate the response on the effector systems (Sharp, 2017). As a consequence of the different interactions, there are reports of increases in dendritic density in the basolateral amygdala (BLA) in the face of acute stress, or increases in dendritic density and spinogenesis in response to chronic stress (Mitra et al., 2005; Radley et al., 2015; Zhang et al., 2021). Contrarily to other structures, the structural and functional changes in the amygdala are maintained after the cessation of stress (at least in the short term). This characteristic is responsible for the subject adaptation and learning (e.g., creation of aversive memories of harmful stimuli); however, in the long-term, it can lead to maladaptive states of anxiety and hypervigilance, which

can result in disease development (Farrell et al., 2013; Lucassen et al., 2014; Pêgo et al., 2009; Sousa, 2016). In short, the amygdala contributes to the affective and emotional aspects of cognition during the stress response (Lucassen et al., 2014; McEwen et al., 2015; Pêgo et al., 2009; Sousa, 2016).

The hippocampus is largely associated with the encoding and retrieving of spatial and episodic memories. Due to the high GR concentrations, this region helps in the inhibition of the stress response and restoration of GC levels. In prolonged stress situations, however, the high levels of GC can cause hippocampal dysfunction, which leads to the liberation of the HPA activation (Lucassen et al., 2014; Reser, 2016; Sousa, 2016; Sousa et al., 2008). Furthermore, morphological changes are also noted, particularly with the atrophy of the dorsal CA3 and CA1 components and increases in ventral regions (Pinto et al., 2015). The structural and functional changes in the hippocampus are usually reversible. Nonetheless, it is speculated that after recovery, the basal reactivity of the subject to stressors is altered, in part due to the genetic modulation that occurs as a consequence of the prolonged (or intense acute) stress (Joss et al., 2020; Lucassen et al., 2014; Sousa, 2016).

The PFC is a major responsible for higher cognitive functions, including cognitive and emotional regulation, behavioral flexibility, working memory, and decision-making. Of relevance, it modulates the amygdala and hippocampal activity, performing a mediating role in stressful situations (Cerqueira et al., 2008). Indeed, due to extensive connections between PFC and both cortical and subcortical regions, the brain usually follows a PFC top-down control. However, under situations of uncontrollable stress, the PFC connections become weakened, and the top-down control mechanism is lost. As a consequence, impairments in cognitive functions are noted, such as decreased self-regulation and inhibitory control, difficulty in concentrating, decreased empathy and optimist, as well as heightened alertness (Arnsten and Shanafelt, 2021; Cerqueira et al., 2008; Dias-Ferreira et al., 2009; Morgado et al., 2015). Regarding morphology, the improved alertness in the face of potential new stressors is associated with the dendritic expansion in the orbitofrontal cortex (OFC). On the other hand, cognitive impairments relate to dendritic atrophy and loss in other components (e.g., cingulate cortex) of the PFC (Lucassen et al., 2014; McEwen et al., 2016; Reser, 2016; Sousa, 2016).

3. Measures for quantifying Stress

As previously referred, different threats can induce stress (Selye, 1998). Of relevance, there are different types, categorizations, and measures of stressors (Crosswell and Lockwood, 2020; Iqbal et al., 2021). Importantly, there are two main ways of measuring (and classifying) stress: 1) through the physiological body response (e.g., hormonal measurements) or; 2) by considering the individual self-perception of the stressor (e.g., self-administered questionnaires).

The body's physiological response is usually measured through cortisol, the "primary stress hormone". From non-invasive approaches such as salivary or urinary cortisol to more invasive procedures, such as blood collection (Nicolson, 2008), the main drawback common to all these techniques relies on the momentary dimension of the measurement. Indeed, it is true that external stressors promote the release of GC. However, due to the circadian and the ultradian cycles (for instance), the GC secretion oscillates over the day regardless of external stresses (Kassi and Chrousos, 2013), which may justify the difficulty in establishing reliable links between cortisol and psychosocial stressors (Chida and Steptoe, 2009; Halford et al., 2012; Iqbal et al., 2021). Importantly, these cortisol measurements reflect a particular moment in time (with the exception of hair cortisol, which poses other challenges), being the reflex of an acute endocrine response.

On the other hand, subjective instruments rely on the individual perception of the stressor and not on an objective quantification of stress itself. Contrasting with the Depression Anxiety Stress Scales (DASS), which is more focused on physical symptomatology (Lovibond and Lovibond, 1995; Pais-Ribeiro et al., 2014), the Perceived Stress Scale (PSS) is centered on the individual's feelings as well as on the way stress is integrated by the subject (Cohen et al., 1983; Trigo et al., 2010). As of great interest for this Thesis, the PSS is a reliable instrument largely used to assess chronic psychosocial stress both in clinical and healthy adult populations (Cohen et al., 1983; Fliege et al., 2005; Lee, 2012; Liston et al., 2009; Soares et al., 2012; Trigo et al., 2010). Instead of focusing on a particular life event, this questionnaire determines how frequently people felt stressed, overburdened, or out of control in the previous month (which can be considered as a prolonged/chronic exposure). Therefore, the PSS is sensitive to the absence of events, ordinary daily living, concerns regarding friends and relatives, and anticipation about future events (Cohen, 1988). The scale is available in 14-item, 10-item, and 4-item forms (10 and 4 are subsets of the 14) with each item rated on a 5-point frequency scale (Likert), ranging from ''never" (0) to ''very often" (4) (Ezzati et al., 2014). Importantly, PSS has emerged as one of the most widely used ways

of measuring psychological stress in health research (Sharp et al., 2007, p. 2007), with the 10-item Perceived Stress Scale (PSS10) being the most used and recommendable version (particularly in older adults cohorts) (Ezzati et al., 2014; Lee, 2012). In this version, the total score is obtained by reversing the scoring of 4 positive items and then summing across all 10 items, with higher scores indicating higher perceived stress (maximum of 40). The Portuguese version of the PSS10 was validated by Trigo and colleagues (Trigo et al., 2010). They established that scores above the 80th percentile are indicators of pathology (with cut-off values indicating pathology defined as 20 for males and 22 for females).

As referred by Crosswell and Lockwood, researchers should ascertain the sort of stress response that is most relevant to their research question and determine the method for stress quantification accordingly (Crosswell and Lockwood, 2020). Herein, we are focused on the physiological impact that chronic stress has on brain morphology and function, for which the way how stress is perceived by the individual is of greatest interest.

4. Magnetic Resonance Imaging

As a way of understanding stress effects on the brain, different works at molecular, cellular, and network levels have been conducted in the past (Cerqueira et al., 2007; Magalhães et al., 2018; Popoli et al., 2012; Sousa et al., 2000; Yuen et al., 2012). Notably, the development of MRI techniques (Dill, 2008; Geva, 2006; Liang and Lauterbur, 2000) boosted the research on brain pathophysiology by allowing the non-invasive and longitudinal collection of information on the stressed brain (Koenig et al., 2011; Kogler et al., 2015; Lucassen et al., 2006; Magalhães et al., 2019; Novais et al., 2017; Soares et al., 2017; Sousa, 2016). Also of relevance is the introduction of novel neuroimaging processing techniques, which have nowadays a vital role in expanding our ways to understand the processes (and their dynamics) at the whole-brain level (Cabral et al., 2017; Esteban et al., 2018; Lv et al., 2018; Soares et al., 2016).

4.1. MRI acquisition

The MRI technique takes advantage of the body's magnetic properties to produce 3-Dimensional (3D) images (Berger, 2002). Depending on the protocol established, which is defined according to the information that is pretended to be collected, an MRI scanner can perform different types of acquisitions (Yousaf et al., 2018). Of relevance for this Thesis, the structural T1-weighted (T1w) acquisitions are

commonly used to evaluate brain morphology (Yousaf et al., 2018) and the functional MRI (fMRI) to explore the spatio-temporal brain dynamics (Sutton et al., 2009). Whereas T1w images are created directly through the signal obtained with the T1 contrast (resulted from differences in tissue properties), fMRI acquisitions use (mainly) the blood oxygen level-dependent (BOLD) contrast to obtain an indirect quantification of brain activity. Shortly, when a brain region is active, an increase of the oxygenated blood supply in that region occurs, causing differences in the oxyhemoglobin and deoxyhemoglobin levels responsible for the BOLD signal creation (Sutton et al., 2009). Notably, this technique can be used when a subject is performing a task or at rest. The latter situation is usually known as resting-state fMRI (rs-fMRI).

4.2. Data preprocessing

After the MRI acquisition, it is necessary to extract the raw data from the scanner and prepare it for statistical analysis. This intermediate process is called preprocessing, and it is, indeed, one of the most important stages in neuroimaging research. The preprocessing pipeline depends on the MRI image type. Importantly, it aims to improve image quality and is mandatory to compare results across studies (Yousaf et al., 2018).

The common pipeline for structural images is initiated by brain extraction (also known as skullstripping). Then, the brain image is segmented into cerebrospinal fluid (CSF), gray matter (GM), and white matter (WM) tissues. After the segmentation, the images are normalized to standard space (e.g., MNI space), and finally, it is applied spatial filtering (Yuan et al., 2018). Herein, it should be noted that the standardization for a common space is what allows us to compare results across different studies and acquisitions, including data from different scanners even if they have distinct magnetic fields (e.g., 1.5T and 3T) (Yousaf et al., 2018).

The fMRI preprocessing includes several more steps than the preprocessing of a structural image. Indeed, it should be noticed that a structural image consists of a single acquisition (1 volume), whereas a functional series is composed of several repeated acquisitions (a series of volumes). More importantly, the structural acquisition has a higher spatial resolution, whereas in fMRI, the spatial resolution is lost on behalf of the temporal resolution. Therewith, it is common to use a structural image on the preprocessing of fMRI data (Sutton et al., 2009; Yousaf et al., 2018).

Regarding the fMRI pipeline itself, it is composed of several images and signal processing algorithms in order to increase the signal-to-noise ratio as well as to remove artifacts. Besides the normalization for standard space, most of the pipelines include slice-timing correction (correcting for the acquisition times between slices), motion correction (re-alignment of images across the section to minimize distortions caused by subject's movement), spatial smoothing (smoothing the neighboring data points to remove potential artifacts and increasing the signal-to-noise ratio), mean intensity adjustment (which normalizes signal drifts over time) and temporal filtering (removal of low-frequency drifts over time, as well as unwanted components of a time series) (Jenkinson and Smith, 2006; Soares et al., 2016).

As noted in a guide produced in our laboratory, there are several tools available for preprocessing (Soares et al., 2016). Importantly, it is usual the customization of *ad hoc* preprocessing pipelines for each dataset, or even the adjustment of some parameters individually. If by one side, the customization allowed researchers to improve image quality, on the other hand, it was also noted an escalated complexity in the conductance of preprocessing steps. With this in mind, a group of investigators developed the fMRIPrep, a software known for its ability to preprocess MRI data in an almost independent way, ensuring highly robustness and reproducibility (Esteban et al., 2018). Although its ability to run without manual intervention (automatic adaptation of the pipeline internally), fMRIPrep also allows users to visually inspect data at several stages of the preprocessing pipeline. In sum, this recent, freely available, and easy-to-use preprocessing tool is a valuable resource for neuroscience and neuroimaging communities (Esteban et al., 2018).

4.3. Structural Analysis

The link between brain morphology and disease has been known for a long. Indeed, this relationship has driven the development of (currently archaic) methods to study brain volume in the past (Harper et al., 1984). With the discovery of the MRI technique, and considering its non-invasive advantages, the structural analysis, and particularly of the gray matter volume (GMV) estimation, became one of the most widely used methods in neuroimaging research (Giuliani et al., 2005; Mills and Tamnes, 2014; Seyedi et al., 2020). Of interest to this Thesis, there are two main approaches to compute GM volumes: 1) the voxel-based morphometry (VBM) and; 2) the region-of-interest (ROI).

Introduced by Ashburner and Friston, the VBM method uses a voxel-wise estimation to detect changes in GM concentrations (Ashburner and Friston, 2000). Thus, after the segmentation (GM images),

normalization (to the standard space), and smoothing (to increase the signal-to-noise ratio), the preprocessed MRI images are used to perform the statistical analysis, in which both parametric (e.g., general linear model), or nonparametric (e.g., randomise) tests can be applied (Ashburner and Friston, 2000; Nichols and Holmes, 2002; Rorden et al., 2007). Importantly, it is usually conducted across the whole-brain (WB), with results in the form of a 3D statistical map. Using tools from the FMRIB Software Library (Smith et al., 2004) together with an optimized VBM protocol (Good et al., 2001), the FSL-VBM (Douaud et al., 2007) technique is nowadays widely employed.

The ROI method is used to compute the volume of specific pre-defined brain regions from probabilistic brain atlases (Seyedi et al., 2020). This means that in ROI analysis, individual anatomical templates are created while retaining quantitative inter-subject variability (Mazziotta et al., 1995; Seyedi et al., 2020). Allowing the reconstruction of cortical surfaces and segmentation of subcortical structures, the FreeSurfer (Fischl, 2012) software is often used to conduct ROI analysis. Contrarily to the VBM-FSL method, FreeSurfer returns the individual volume quantification for each region (and subject), in which statistical analysis can be then applied.

4.4. Functional Analysis

Due to their ability to provide information on how the brain operates, fMRI analyses are also quite popular among researchers and clinicians (Soares et al., 2016). Notably, it has been shown that resting-state oscillations (low frequencies) are linked to spontaneous neuronal activity (Biswal et al., 1995), which triggered the interest in this type of analysis (Lv et al., 2018).

There are numerous ways to analyze functional data (e.g., synchronization or spontaneous activation of resting-state networks [RSN]) (Lv et al., 2018; Soares et al., 2016). Pertinent to this Thesis, functional analysis is classified into two types: static or dynamic. Static analyses have an interesting spatial resolution but no temporal definition (i.e., they return a single value independently of sequences' size). On the other hand, dynamic analyses can provide spatiotemporal information (although generally with lower spatial resolution) by identifying patterns of spontaneous brain activity fluctuations (Bassett and Sporns, 2017; Biswal et al., 1995; Menon and Krishnamurthy, 2019).

A well-known static analysis method is seed-based connectivity. Herein, a specific region (which is thought to be important at a functional level) is chosen as ROI, and the connectivity with other ROIs or with all the other voxels of the brain (whole-brain voxel-based connectivity) is computed. Importantly, for each pair of

brain regions analyzed, only one measure is obtained, indicating, on average, how these brain regions were synchronized (Lv et al., 2018; Soares et al., 2016).

Notably, in the last years, neuroscience research has been prompted by the emergence of dynamic algorithms with an exceptional ability to provide new insights into brain functioning, both in health and in disease conditions (Alonso Martínez et al., 2020; Bassett and Sporns, 2017; Figueroa et al., 2019). Of relevance, the Leading Eigenvector Dynamics Analysis (LEiDA) (Alonso Martínez et al., 2020; Figueroa et al., 2019; Larabi et al., 2020), which detects recurrent phase-locking patterns of a population, and distinguished which patters associate with variables of interest in a data-driven approach (Cabral et al., 2017; Magalhães et al., 2021; Vohryzek et al., 2020).

5. Neuroimaging studies in non-pathological cohorts

Considering that one of the main goals of this Thesis is to better understand the impact of chronic stress on brain morphology and function, as well as the particular importance of PSS10 as a measure of perceived chronic stress exposure (Iqbal et al., 2021; Trigo et al., 2010), we decided to review a priori the existent literature in the field by conducting a systematic research across the ISI Web of Knowledge, PubMed and Scopus databases (we kept this task open throughout the duration of Thesis and the last research date was 2/11/2021; see Appendix B - Ongoing Work for details). Briefly, neuroimaging studies that evaluate the stress impact on the healthy brain were included: 1) if the stress was assessed through PSS10 (prolonged stress); 2) if considering young adult or older populations (i. e., 18+ years) and; 3) and if a volumetric or resting-state functional (rs-fMRI) analysis was conducted. Both regressive analyses and between-group comparisons were considered, as well as cross-sectional and longitudinal studies. The overview of studies that fulfilled the criteria is presented in Table 1.

Table 1. Findings from Structural and Resting-State Imaging Studies of the 10-item Perceived Stress Scale questionnaire. (See abbreviations list in page ix).

Type of study	Study	N (Females)	Age (SD)	PSS (SD/*SE)	Methods	Findings in structural and rs-fMRI
Structural cross-sectional	(Li et al., 2014)	304 (166)	19.2 (1.24)	23.10 (6.48*)	WB GMV and WMV (VBM)	↑**PSS:** ↑GMV L/R Parahippocampal G, FC, Entorhinal C; ↓GMV R Insular C; ↓WMV Corpus Callosum
	(Sherman et al., 2016)	40 (27)	67.2 (5.1)	9.53 (5.2)	Amy GMV (ROI)	↑**PSS** ↑Amy (total and L/R)
	(Moreno et al., 2017)	28 (14)	78.41 (4.1)	13.1 (5.1)	PFC, OFC, Hip, Amy GMV and WMV (ROI)	↑**PSS:** ↓Overal R/L PFC; ↓L/R WM in PFC, vlPFC, dlPFC; ↓L WM vmPFC; ↓R WM OFC; ↓L/R GM vlPFC
	(Wu et al., 2020)	26 (13)	36.74 (5.23)	23.38 (8.84)	WB GMV (VBM)	PSS x Age interaction in insula, OFC and L Amy ↑**PSS** ↓OFC, insula, L Amy in adults
Structural longitudinal	(Hölzel et al., 2010)	26 (15)	35.2 (6.7)	Pre: 20.7 (5.6) Pos: 15.2 (4.7)	WB GMV (VBM)	↓ **PSS** ↓ R Amy
	(Soares et al., 2012)	Case: 12 (6) Control: 12 (6)	Case: 23.9 (0.70) Control: 23.6 (2.11)	Case Pre > Case Pos Case Pre > Control Case Pos ≈ Control	Corticostriatal GMV (ROI)	**Case Pre vs Controls:** ↑**PSS** ↓ R Caudate ↑L/R Putamen ↓L medial OFC; ↑ Caudate-to-putamen ratio in controls **Case Pre vs Case Pos:** ↓**PSS** caused recovery of Caudate, Putamen and OFC
	(Joss et al., 2020)	21 (16)	26.05 (2.25)	Pre: 22.421 (8.375) Pos: 16.895 (8.055)	Hip GMV (VBM)	↓ **PSS** ↑L Hip
	(Joss et al., 2021)	15 (12)	26.27 (0.47)	Pre: 19.7 (2.91) Pos: 12.5 (2.91)	Amy GMV (VBM)	↓ **PSS** ↑L Amy
Structural and Functional	(Soares et al., 2013a)	Case: 8 (6) Control: 8 (6)	Case: 23.86 (0.35) Control: 24.25 (1.98)	Case > Control	rs-networks ICA rs-networks GMV (ROI)	↑ **rs-networks FC Case vs Controls (↑PSS) in:** DMN: mPFC, medial OFC, pCC and precuneus; DAN: S parietal, R middle occipital and L medial and SF; VAN: L angular, S parietal and middle F; SMN: L paracentral lobule, precentral, R postcentral and the L cerebellum; VN: Calcarine ↓**rs-networks GMV Case vs Controls (↑PSS) in:** DMN: L pCC, L/R parietal I
	(Soares et al., 2013b)	Case: 6 (3) Control: 6 (3)	Case: 23.83 (0.37) Control: 24.33 (1.24)	Case Pre: 35.50 (2.59) Case Pos: 30.00 (3.03) Control: 30.17 (4.49)	rs-networks ICA rs-networks GMV (ROI)	↓ DMN GMV (L pCC and R Parietal I) in Case Pre vs Controls (↑PSS) ↑ **rs-networks FC Case Pre vs Case Pos (↑PSS) in:** DMN: L aCC, L medial OFC, R precuneus, L Lingual; VAN: L I/S Parietal, R middle and S F; Sensorimotor: L Cerebellum ↓ **rs-networks FC Case Pre vs Case Pos (↑PSS) in:** DAN: R I Parietal, R Supramarginal, R FI opercularis, R Precentral; AN: L Temporal S **≈ PSS but ↑ rs-network FC Case Pos vs Controls in:** DAN: L Occipital S, L Parietal S, R Parietal S, R Postcentral, L middle and S F, L/R F I opercularis, L/R Precentral; VAN: L Parietal I, L/R Angular; Sensorimotor: L/R Precentral, L Paracentral, R Postcentral, L/R Cerebellum **≈ PSS but ↓ rs-network FC Pos < Controls in:** DMN: R ACC; VAN: L/R Parietal I, L Angular, L/R F middle, L F I Triangularis
	(Soares et al., 2017)	104 (52)	65.20 (8.07)	21.49 (8.18)	DMN ICA DMN GMV (ROI)	↑**PSS** (trend for ↓ DMN GMV) ↑DMN FC in L FSG and medial OFC, middle CG, occipital middle G; and in R middle FG, posterior CC and precuneus
Functional	(Taren et al., 2015)	130 (59)	40.15 (6.14)	13.3 (6.1)	Amy seed-based FC	↑**PSS:** ↑FC R Amy - R subgenual ACC; ↑FC L Amy: L subgenual ACC, L parahippocampal G, R S Temporal, L Insula, R Perigenual A Cingulum
	(Archer et al., 2018)	26 (22)	M: 45.04 (13.25) F: 48.81 (15.21)	M: 11.37 (5.68) F: 12.59 (6.04)	Amy, Hip and ACC seed-based FC	↑ **PSS rs-fMRI in Females:** ↑ FC in L ACC - L/R MCG and in R ACC - L/R MCG; ↓ FC in L Hip - L/R Precuneus and in R Hip - L ITG/MTG/FG ↑ **PSS-FC association in F>M in:** L Amy - R Paracentral Lobule and L Hip - L MFG ↑ **PSS-FC association in M>F in**: L /R ACC - L Cerebellum Lobule VIIIA
	(Wu et al., 2018)	Young adults: 22 (9) Adults: 21 (9)	Young adults: 19.55 (0.43) Adults: 35.21 (4.19)	Young adults: 23.14 (6.18) Adults: 21.24 (7.84)	Amy seed-based FC	PSS x Age interaction in R Amy FC with subgenual ACC and vmPFC: **Young adults:** ↑PSS ↓R Amy-vmPFC FC (trend ↓R Amy- subgenual ACC FC) **Adults:** no significant correlations were found
	(McDermott et al., 2019)	22 (14)	71.2 (9.61)	9.7 (6.6)	Hip seed-based FC	↓**PSS** ↑ FC L Hip - L Parietal Lobe

One of the first pieces of evidence of a possible association between stress perception and brain structure comes from the volumetric longitudinal study of Hölzel et al. (Hölzel et al., 2010). To investigate this association, a group of healthy, otherwise stressed, adults were invited to participate in an 8-week mindfulness-based stress reduction intervention. Interestingly, following a WB VBM approach, Hölzel and colleagues have shown that reductions in PSS positively correlated with volumetric decreases in the right basolateral amygdala. Following this, Soares et al. have decided to explore the interaction between corticostriatal regions and psychological stress (Soares et al., 2012). For that, a small group of medical students and matched controls were assessed respectively after preparing for the residence selection exam and under normal academic activities. Between-group comparisons revealed that increased levels of PSS matched with a medial PFC and caudate atrophy, and with putamen increases. More importantly, stressed participants were re-evaluated after a stress-free period of 6 weeks, in which almost a full (morphological) recovery was observed (Soares et al., 2012).

Following a similar case-control and longitudinal cohort study methodology, our lab has also explored the interaction of perceived stress with RSNs (Soares et al., 2013a, 2013b). In the case-control condition, increased activity in the anterior components of the default mode network (DMN) was observed in stressed participants, which suggests an enhanced interaction between emotional processing and cognitive functions (Soares et al., 2013a). Furthermore, when compared to themselves immediately after stress, partial functional recovery was observed in the DMN, ventral attention network (VAN), and sensorimotor network (SMN), which was not seen in the dorsal attention network (DAN) and primary visual network (VN) (Soares et al., 2013b). In sum, findings show that stress affects the activation-deactivation pattern of RSNs, which may help explain the stress-induced alterations observed on the multiple dimensions of brain functioning (Soares et al., 2013a, 2013b).

Among all the studies found, the work of Li et al. is the one with the largest sample size (Li et al., 2014). Using a cohort of 304 students, the authors show that higher PSS scores were related to GM increases in the bilateral parahippocampal gyrus, fusiform cortex (FC), and entorhinal cortex, as well as decreases in the right insular cortex. Besides that, higher PSS scores were also associated with lower WM in the corpus callosum body. Although with a much smaller sample size ($N = 28$), the research of Moreno et al. was the only one following the same methodology, looking both at GM and WM volumes (Moreno et al., 2017). Results have shown a clear link between PFC volume and perceived stress levels, with increases in PSS being associated with decreases in WM (and no significant GM changes being reported).

If by one side, making a direct relationship with Li's study (Li et al., 2014) is impossible due to the use of an elderly cohort, on the other hand, Moreno's research significantly contributed to the literature regarding stress and healthy aging. In truth, a previous study from our lab has focused on non-pathological aging research involving a cohort of 104 older adults (Soares et al., 2017). In line with previous results, our group saw associations regarding DMN deactivation and perceived stress, which highlighted the strong interactions of stress and mood during the aging process (Soares et al., 2017).

Interestingly, other functional studies were focused directly on the role of the amygdala and hippocampus by conducting seed-based connectivity analysis in these key regions of the stress response (Archer et al., 2018; McDermott et al., 2019; Taren et al., 2015; Wu et al., 2018). Herein, a negative interaction between stress perception and hippocampal functional connectivity seems to be replicated (Archer et al., 2018; Taren et al., 2015). However, on the other hand, discrepancies were also observed, with some studies showing positive associations between perceived stress and amygdala connectivity (Taren et al., 2015), as well as negative or inexistent associations (Archer et al., 2018; Wu et al., 2018).

Notably, recent morphological studies in these key regions (Joss et al., 2021, 2020) also show inconsistencies with the previous literature. In fact, in contrast to previous studies (Hölzel et al., 2010; Sherman et al., 2016; Wu et al., 2020), Joss and colleagues have demonstrated that reductions in the perception of stress were associated with increases both in the amygdala (Joss et al., 2021) and hippocampal (Joss et al., 2020) GM volumes.

Altogether, studies in the literature demonstrated an inherent link between the way individuals perceive stress and the brain's structure and functioning. However, the direction of these associations remains unclear, with observed discrepancies possibly resulting from the small sample size of non-pathological studies available. Thus, at the beginning of the Thesis, we thought of interest to conduct a more systematic neuroimaging study to unravel the impact of perceived stress in the structure and connectivity of the amygdala.

6. Objectives

Despite the existence of some anatomical neuroimaging studies investigating the influence of perceived stress in non-pathological populations, there are significant discrepancies in the literature that may have been fostered by the small sample size of published works. With a reduced number and also lacking replicability, functional studies at resting-state are only focused on static connectivity metrics, missing the temporal resolution of dynamic analysis that is crucial in the study of stress repercussions at the network level. Therefore, this Thesis aims to provide new insights about the changes induced by stress on healthy brain structure and functioning but also to pursue the development of new in-vivo biomarkers of the stressed brain to be used in preventive mental interventions (Avvenuti et al., 2020; Kaul et al., 2021).

In order to accomplish the main aim of this Thesis, a combination of the most conservative morphological analysis and sophisticated dynamic algorithms were used in a large non-pathological cohort with a broad age range.

The detailed tasks performed in this Thesis are presented below:

1. Characterize the impact of perceived and physiological stress on the morphology of subcortical regions in a healthy cohort of young adults (Chapter 2);

2. Explore the significant association found (in Chapter 2) throughout lifespan using a healthy cohort with a large age range (Chapter 3);

3. Investigate the association of stress perception with altered brain resting-state connectivity using a seed-based analysis (drift from morphological results of Chapter 2 and 3), as well as a whole-brain data-driven approach to detect altered patterns of dynamic connectivity (Chapter 4).

7. References

Alonso Martínez, S., Deco, G., Ter Horst, G.J., Cabral, J., 2020. The Dynamics of Functional Brain Networks Associated With Depressive Symptoms in a Nonclinical Sample. Front. Neural Circuits 14, 570583. https://doi.org/10.3389/fncir.2020.570583

Archer, J.A., Lee, A., Qiu, A., Chen, S.-H.A., 2018. Functional connectivity of resting-state, working memory and inhibition networks in perceived stress. Neurobiol. Stress 8, 186–201. https://doi.org/10.1016/j.ynstr.2017.01.002

Arnsten, A.F.T., Shanafelt, T., 2021. Physician Distress and Burnout: The Neurobiological Perspective. Mayo Clin Proc 96, 763–769. https://doi.org/10.1016/j.mayocp.2020.12.027

Ashburner, J., Friston, K.J., 2000. Voxel-Based Morphometry—The Methods. NeuroImage 11, 805–821. https://doi.org/10.1006/nimg.2000.0582

Avvenuti, G., Leo, A., Cecchetti, L., Franco, M.F., Travis, F., Caramella, D., Bernardi, G., Ricciardi, E., Pietrini, P., 2020. Reductions in perceived stress following Transcendental Meditation practice are associated with increased brain regional connectivity at rest. Brain Cogn. 139, 105517. https://doi.org/10.1016/j.bandc.2020.105517

Bassett, D.S., Sporns, O., 2017. Network neuroscience. Nat Neurosci 20, 353–364. https://doi.org/10.1038/nn.4502

Bergdahl, J., Larsson, A., Nilsson, L.-G., Ahlström, K.R., Nyberg, L., 2005. Treatment of chronic stress in employees: subjective, cognitive and neural correlates. Scand J Psychol 46, 395–402. https://doi.org/10.1111/j.1467-9450.2005.00470.x

Berger, A., 2002. How does it work?: Magnetic resonance imaging. BMJ 324, 35–35. https://doi.org/10.1136/bmj.324.7328.35

Biswal, B., Zerrin Yetkin, F., Haughton, V.M., Hyde, J.S., 1995. Functional connectivity in the motor cortex of resting human brain using echo-planar mri. Magn. Reson. Med. 34, 537–541. https://doi.org/10.1002/mrm.1910340409

Brodal, P., 2004. The central nervous system: structure and function, 3rd ed. ed. Oxford University Press, Oxford ; New York.

Cabral, J., Vidaurre, D., Marques, P., Magalhães, R., Silva Moreira, P., Miguel Soares, J., Deco, G., Sousa, N., Kringelbach, M.L., 2017. Cognitive performance in healthy older adults relates to spontaneous switching between states of functional connectivity during rest. Sci Rep 7, 5135. https://doi.org/10.1038/s41598-017-05425-7

Cannon, W.B., 1929. Organization for Physiological Homeostasis. Physiological Reviews 9, 399–431. https://doi.org/10.1152/physrev.1929.9.3.399

Cannon, W.B., 1926. Physiological Regulation of Normal States: Some Tentative Postulates Concerning Biological Homeostatics. Ses Amis, ses Colleges, ses Eleves.

Cannon, W.B., Cannon, C.J., 1967. The wisdom of the body: how the human body reacts to disturbance and danger and maintains the stability essential to life, Rev. and enl. ed. Renewed. ed, The Norton library. Norton, New York.

Cerqueira, J.J., Almeida, O.F.X., Sousa, N., 2008. The stressed prefrontal cortex. Left? Right! Brain, Behavior, and Immunity 22, 630–638. https://doi.org/10.1016/j.bbi.2008.01.005

Cerqueira, J.J., Mailliet, F., Almeida, O.F.X., Jay, T.M., Sousa, N., 2007. The Prefrontal Cortex as a Key Target of the Maladaptive Response to Stress. Journal of Neuroscience 27, 2781–2787. https://doi.org/10.1523/JNEUROSCI.4372-06.2007

Chida, Y., Steptoe, A., 2009. Cortisol awakening response and psychosocial factors: A systematic review and meta-analysis. Biological Psychology 80, 265–278. https://doi.org/10.1016/j.biopsycho.2008.10.004

Cohen, S., 1988. Perceived stress in a probability sample of the United States., in: The Social Psychology of Health., The Claremont Symposium on Applied Social Psychology. Sage Publications, Inc, Thousand Oaks, CA, US, pp. 31–67.

Cohen, S., Kamarck, T., Mermelstein, R., 1983. A Global Measure of Perceived Stress. Journal of Health and Social Behavior 24, 385. https://doi.org/10.2307/2136404

Crosswell, A.D., Lockwood, K.G., 2020. Best practices for stress measurement: How to measure psychological stress in health research. Health Psychology Open 7, 205510292093307. https://doi.org/10.1177/2055102920933072

Cullinan, W.E., Herman, J.P., 1993. Ventral subicular interaction with the hypothalamic paraventricular nucleus: Evidence for a relay in the bed nucleus of the stria terminalis. J. Comp. Neurol. 332, 1–20. https://doi.org/10.1002/cne.903320102

de Kloet, E.R., Joëls, M., Holsboer, F., 2005. Stress and the brain: from adaptation to disease. Nat Rev Neurosci 6, 463–475. https://doi.org/10.1038/nrn1683

Dias-Ferreira, E., Sousa, J.C., Melo, I., Morgado, P., Mesquita, A.R., Cerqueira, J.J., Costa, R.M., Sousa, N., 2009. Chronic Stress Causes Frontostriatal Reorganization and Affects Decision-Making. Science 325, 621–625. https://doi.org/10.1126/science.1171203

Dill, T., 2008. Contraindications to magnetic resonance imaging. Heart 94, 943–948. https://doi.org/10.1136/hrt.2007.125039

Douaud, G., Smith, S., Jenkinson, M., Behrens, T., Johansen-Berg, H., Vickers, J., James, S., Voets, N., Watkins, K., Matthews, P.M., James, A., 2007. Anatomically related grey and white matter abnormalities in adolescent-onset schizophrenia. Brain 130, 2375–2386. https://doi.org/10.1093/brain/awm184

Esteban, O., Markiewicz, C.J., Blair, R.W., Moodie, C.A., Isik, A.I., Erramuzpe, A., Kent, J.D., Goncalves, M., DuPre, E., Snyder, M., Oya, H., Ghosh, S.S., Wright, J., Durnez, J., Poldrack, R.A., Gorgolewski, K.J., 2018. fMRIPrep: a robust preprocessing pipeline for functional MRI. Nat Methods 16, 111–116. https://doi.org/10.1038/s41592-018-0235-4

Even, N., Devaud, J.-M., Barron, A., 2012. General Stress Responses in the Honey Bee. Insects 3, 1271–1298. https://doi.org/10.3390/insects3041271

Ezzati, A., Jiang, J., Katz, M.J., Sliwinski, M.J., Zimmerman, M.E., Lipton, R.B., 2014. Validation of the Perceived Stress Scale in a community sample of older adults: Perceived Stress Scale in older adults. Int J Geriatr Psychiatry 29, 645–652. https://doi.org/10.1002/gps.4049

Farrell, M.R., Sengelaub, D.R., Wellman, C.L., 2013. Sex differences and chronic stress effects on the neural circuitry underlying fear conditioning and extinction. Physiol Behav 122, 208–215. https://doi.org/10.1016/j.physbeh.2013.04.002

Fett, A.-K.J., Lemmers-Jansen, I.L.J., Krabbendam, L., 2019. Psychosis and urbanicity: a review of the recent literature from epidemiology to neurourbanism. Current Opinion in Psychiatry 32, 232–241. https://doi.org/10.1097/YCO.0000000000000486

Figueroa, C.A., Cabral, J., Mocking, R.J.T., Rapuano, K.M., Hartevelt, T.J., Deco, G., Expert, P., Schene, A.H., Kringelbach, M.L., Ruhé, H.G., 2019. Altered ability to access a clinically relevant control network in patients remitted from major depressive disorder. Hum Brain Mapp 40, 2771–2786. https://doi.org/10.1002/hbm.24559

Finsterwald, C., Alberini, C.M., 2014. Stress and glucocorticoid receptor-dependent mechanisms in long-term memory: From adaptive responses to psychopathologies. Neurobiology of Learning and Memory 112, 17–29. https://doi.org/10.1016/j.nlm.2013.09.017

Fischl, B., 2012. FreeSurfer. NeuroImage 62, 774–781. https://doi.org/10.1016/j.neuroimage.2012.01.021

Fliege, H., Rose, M., Arck, P., Walter, O.B., Kocalevent, R.-D., Weber, C., Klapp, B.F., 2005. The Perceived Stress Questionnaire (PSQ) Reconsidered: Validation and Reference Values From Different Clinical and Healthy Adult Samples: Psychosomatic Medicine 67, 78–88. https://doi.org/10.1097/01.psy.0000151491.80178.78

Geva, T., 2006. Magnetic Resonance Imaging: Historical Perspective. Journal of Cardiovascular Magnetic Resonance 8, 573–580. https://doi.org/10.1080/10976640600755302

Giuliani, N.R., Calhoun, V.D., Pearlson, G.D., Francis, A., Buchanan, R.W., 2005. Voxel-based morphometry versus region of interest: a comparison of two methods for analyzing gray matter differences in schizophrenia. Schizophrenia Research 74, 135–147. https://doi.org/10.1016/j.schres.2004.08.019

Goldstein, D.S., Kopin, I.J., 2007. Evolution of concepts of stress. Stress 10, 109–120. https://doi.org/10.1080/10253890701288935

Good, C.D., Johnsrude, I.S., Ashburner, J., Henson, R.N.A., Friston, K.J., Frackowiak, R.S.J., 2001. A Voxel-Based Morphometric Study of Ageing in 465 Normal Adult Human Brains. NeuroImage 14, 21–36. https://doi.org/10.1006/nimg.2001.0786

Halford, C., Jonsdottir, I.H., Eek, F., 2012. Perceived Stress, Psychological Resources and Salivary Cortisol. Bentham eBooks 67–86.

Hall, B.S., Moda, R.N., Liston, C., 2015. Glucocorticoid mechanisms of functional connectivity changes in stress-related neuropsychiatric disorders. Neurobiology of Stress 1, 174–183. https://doi.org/10.1016/j.ynstr.2014.10.008

Hannibal, K.E., Bishop, M.D., 2014. Chronic Stress, Cortisol Dysfunction, and Pain: A Psychoneuroendocrine Rationale for Stress Management in Pain Rehabilitation. Physical Therapy 94, 1816–1825. https://doi.org/10.2522/ptj.20130597

Harper, C., Kril, J., Raven, D., Jones, N., 1984. INTRACRANIAL CAVITY VOLUMES: A NEW METHOD AND ITS POTENTIAL APPLICATIONS. Neuropathol Appl Neurobiol 10, 25–32. https://doi.org/10.1111/j.1365-2990.1984.tb00337.x

Herman, J.P., Cullinan, W.E., Watson, S.J., 1994. Involvement of the Bed Nucleus of the Stria Terminalis in Tonic Regulation of Paraventricular Hypothalamic CRH and AVP mRNA Expression. J Neuroendocrinol 6, 433–442. https://doi.org/10.1111/j.1365-2826.1994.tb00604.x

Herman, J.P., Figueiredo, H., Mueller, N.K., Ulrich-Lai, Y., Ostrander, M.M., Choi, D.C., Cullinan, W.E., 2003. Central mechanisms of stress integration: hierarchical circuitry controlling hypothalamo–pituitary–adrenocortical responsiveness. Frontiers in Neuroendocrinology 24, 151–180. https://doi.org/10.1016/j.yfrne.2003.07.001

Herman, J.P., Ostrander, M.M., Mueller, N.K., Figueiredo, H., 2005. Limbic system mechanisms of stress regulation: Hypothalamo-pituitary-adrenocortical axis. Progress in Neuro-Psychopharmacology and Biological Psychiatry 29, 1201–1213. https://doi.org/10.1016/j.pnpbp.2005.08.006

Hölzel, B.K., Carmody, J., Evans, K.C., Hoge, E.A., Dusek, J.A., Morgan, L., Pitman, R.K., Lazar, S.W., 2010. Stress reduction correlates with structural changes in the amygdala. Social Cognitive and Affective Neuroscience 5, 11–17. https://doi.org/10.1093/scan/nsp034

Iqbal, T., Elahi, A., Redon, P., Vazquez, P., Wijns, W., Shahzad, A., 2021. A Review of Biophysiological and Biochemical Indicators of Stress for Connected and Preventive Healthcare. Diagnostics 11, 556. https://doi.org/10.3390/diagnostics11030556

Jänig, W., 1989. Autonomic Nervous System, in: Schmidt, R.F., Thews, G. (Eds.), Human Physiology. Springer Berlin Heidelberg, Berlin, Heidelberg, pp. 333–370. https://doi.org/10.1007/978-3-642-73831-9_16

Jenkinson, M., Smith, S.M., 2006. Pre-processing of BOLD fMRI data. Oxford University Centre for Functional MRI of the Brain (FMRIB) 1.

Joss, D., Khan, A., Lazar, S.W., Teicher, M.H., 2021. A pilot study on amygdala volumetric changes among young adults with childhood maltreatment histories after a mindfulness intervention. Behavioural Brain Research 399, 113023. https://doi.org/10.1016/j.bbr.2020.113023

Joss, D., Lazar, S.W., Teicher, M.H., 2020. Effects of a mindfulness based behavioral intervention for young adults with childhood maltreatment history on hippocampal morphometry: a pilot MRI study with voxel-based morphometry. Psychiatry Res Neuroimaging 301, 111087. https://doi.org/10.1016/j.pscychresns.2020.111087

Kassi, E., Chrousos, G., 2013. The central CLOCK system and the stress axis in health and disease. HJ 12, 172–191. https://doi.org/10.14310/horm.2002.1402

Kaul, D., Schwab, S.G., Mechawar, N., Matosin, N., 2021. How stress physically re-shapes the brain: Impact on brain cell shapes, numbers and connections in psychiatric disorders. Neuroscience & Biobehavioral Reviews 124, 193–215. https://doi.org/10.1016/j.neubiorev.2021.01.025

Keller-Wood, M.E., Dallman, M.F., 1984. Corticosteroid Inhibition of ACTH Secretion*. Endocrine Reviews 5, 1–24. https://doi.org/10.1210/edrv-5-1-1

Kim, E.Y., Miklowitz, D.J., Biuckians, A., Mullen, K., 2007. Life stress and the course of early-onset bipolar disorder. Journal of Affective Disorders 99, 37–44. https://doi.org/10.1016/j.jad.2006.08.022

Koenig, J.I., Walker, C.-D., Romeo, R.D., Lupien, S.J., 2011. Effects of stress across the lifespan. Stress 14, 475–480. https://doi.org/10.3109/10253890.2011.604879

Kogler, L., Müller, V.I., Chang, A., Eickhoff, S.B., Fox, P.T., Gur, R.C., Derntl, B., 2015. Psychosocial versus physiological stress — Meta-analyses on deactivations and activations of the neural correlates of stress reactions. NeuroImage 119, 235–251. https://doi.org/10.1016/j.neuroimage.2015.06.059

Kreibig, S.D., 2010. Autonomic nervous system activity in emotion: A review. Biological Psychology 84, 394–421. https://doi.org/10.1016/j.biopsycho.2010.03.010

Larabi, D.I., Renken, R.J., Cabral, J., Marsman, J.-B.C., Aleman, A., Ćurčić-Blake, B., 2020. Trait self-reflectiveness relates to time-varying dynamics of resting state functional connectivity and underlying structural connectomes: Role of the default mode network. NeuroImage 219, 116896. https://doi.org/10.1016/j.neuroimage.2020.116896

Lederbogen, F., Kirsch, P., Haddad, L., Streit, F., Tost, H., Schuch, P., Wüst, S., Pruessner, J.C., Rietschel, M., Deuschle, M., Meyer-Lindenberg, A., 2011. City living and urban upbringing affect neural social stress processing in humans. Nature 474, 498–501. https://doi.org/10.1038/nature10190

LeDoux, J.E., 2000. Emotion Circuits in the Brain. Annual review of neuroscience 23, 155–184. https://doi.org/10.1146/annurev.neuro.23.1.155

Lee, E.-H., 2012. Review of the Psychometric Evidence of the Perceived Stress Scale. Asian Nursing Research 6, 121–127. https://doi.org/10.1016/j.anr.2012.08.004

Lee, R.S., Sawa, A., 2014. Environmental Stressors and Epigenetic Control of the Hypothalamic-Pituitary-Adrenal Axis. Neuroendocrinology 100, 278–287. https://doi.org/10.1159/000369585

Li, H., Li, W., Wei, D., Chen, Q., Jackson, T., Zhang, Q., Qiu, J., 2014. Examining brain structures associated with perceived stress in a large sample of young adults via voxel-based morphometry. NeuroImage 92, 1–7. https://doi.org/10.1016/j.neuroimage.2014.01.044

Liang, Z.-P., Lauterbur, P.C., 2000. Principles of magnetic resonance imaging: a signal processing perspective, IEEE Press series in biomedical engineering. SPIE Optical Engineering Press ; IEEE Press, Bellingham, Wash. : New York.

Liston, C., McEwen, B.S., Casey, B.J., 2009. Psychosocial stress reversibly disrupts prefrontal processing and attentional control. PNAS 106, 912–917. https://doi.org/10.1073/pnas.0807041106

Lovibond, P.F., Lovibond, S.H., 1995. The structure of negative emotional states: Comparison of the Depression Anxiety Stress Scales (DASS) with the Beck Depression and Anxiety Inventories. Behaviour Research and Therapy 33, 335–343. https://doi.org/10.1016/0005-7967(94)00075-U

Lucassen, P.J., Heine, V.M., Muller, M.B., van der Beek, E.M., Wiegant, V.M., De Kloet, E.R., Joels, M., Fuchs, E., Swaab, D.F., Czeh, B., 2006. Stress, depression and hippocampal apoptosis. CNS Neurol Disord Drug Targets 5, 531–546. https://doi.org/10.2174/187152706778559273

Lucassen, P.J., Pruessner, J., Sousa, N., Almeida, O.F.X., Van Dam, A.M., Rajkowska, G., Swaab, D.F., Czéh, B., 2014. Neuropathology of stress. Acta Neuropathol 127, 109–135. https://doi.org/10.1007/s00401-013-1223-5

Lv, H., Wang, Z., Tong, E., Williams, L.M., Zaharchuk, G., Zeineh, M., Goldstein-Piekarski, A.N., Ball, T.M., Liao, C., Wintermark, M., 2018. Resting-State Functional MRI: Everything That Nonexperts Have Always Wanted to Know. AJNR Am J Neuroradiol ajnr;ajnr.A5527v1. https://doi.org/10.3174/ajnr.A5527

Magalhães, R., Barrière, D.A., Novais, A., Marques, F., Marques, P., Cerqueira, J., Sousa, J.C., Cachia, A., Boumezbeur, F., Bottlaender, M., Jay, T.M., Mériaux, S., Sousa, N., 2018. The dynamics of stress: a longitudinal MRI study of rat brain structure and connectome. Mol Psychiatry 23, 1998–2006. https://doi.org/10.1038/mp.2017.244

Magalhães, R., Novais, A., Barrière, D.A., Marques, P., Marques, F., Sousa, J.C., Cerqueira, J.J., Cachia, A., Jay, T.M., Bottlaender, M., Sousa, N., Mériaux, S., Boumezbeur, F., 2019. A Resting-State Functional MR Imaging and Spectroscopy Study of the Dorsal Hippocampus in the Chronic Unpredictable Stress Rat Model. J. Neurosci. 39, 3640–3650. https://doi.org/10.1523/JNEUROSCI.2192-18.2019

Magalhães, R., Picó-Pérez, M., Esteves, M., Vieira, R., Castanho, T.C., Amorim, L., Sousa, M., Coelho, A., Fernandes, H.M., Cabral, J., Moreira, P.S., Sousa, N., 2021. Habitual coffee drinkers display a distinct pattern of brain functional connectivity. Mol Psychiatry. https://doi.org/10.1038/s41380-021-01075-4

Maier, S.F., Amat, J., Baratta, M.V., Paul, E., Watkins, L.R., 2006. Behavioral control, the medial prefrontal cortex, and resilience. Dialogues Clin Neurosci 8, 397–406. https://doi.org/10.31887/DCNS.2006.8.4/smaier

Mazziotta, J.C., Toga, A.W., Evans, A., Fox, P., Lancaster, J., 1995. A Probabilistic Atlas of the Human Brain: Theory and Rationale for Its Development. NeuroImage 2, 89–101. https://doi.org/10.1006/nimg.1995.1012

McDermott, K., Ren, P., Lin, F., 2019. The mediating role of hippocampal networks on stress regulation in amnestic mild cognitive impairment. Neurobiology of Stress 10, 100162. https://doi.org/10.1016/j.ynstr.2019.100162

McEwen, B.S., Bowles, N.P., Gray, J.D., Hill, M.N., Hunter, R.G., Karatsoreos, I.N., Nasca, C., 2015. Mechanisms of stress in the brain. Nat Neurosci 18, 1353–1363. https://doi.org/10.1038/nn.4086

McEwen, B.S., Nasca, C., Gray, J.D., 2016. Stress Effects on Neuronal Structure: Hippocampus, Amygdala, and Prefrontal Cortex. Neuropsychopharmacol 41, 3–23. https://doi.org/10.1038/npp.2015.171

Menon, S.S., Krishnamurthy, K., 2019. A Comparison of Static and Dynamic Functional Connectivities for Identifying Subjects and Biological Sex Using Intrinsic Individual Brain Connectivity. Sci Rep 9, 5729. https://doi.org/10.1038/s41598-019-42090-4

Merkulov, V.M., Merkulova, T.I., Bondar, N.P., 2017. Mechanisms of brain glucocorticoid resistance in stress-induced psychopathologies. Biochemistry Moscow 82, 351–365. https://doi.org/10.1134/S0006297917030142

Mills, K.L., Tamnes, C.K., 2014. Methods and considerations for longitudinal structural brain imaging analysis across development. Developmental Cognitive Neuroscience 9, 172–190. https://doi.org/10.1016/j.dcn.2014.04.004

Mitra, R., Jadhav, S., McEwen, B.S., Vyas, A., Chattarji, S., 2005. Stress duration modulates the spatiotemporal patterns of spine formation in the basolateral amygdala. Proceedings of the National Academy of Sciences 102, 9371–9376. https://doi.org/10.1073/pnas.0504011102

Moreno, G.L., Bruss, J., Natalie, L.D., 2017. Increased perceived stress is related to decreased prefrontal cortex volumes among older adults. Journal of Clinical and Experimental Neuropsychology 313–325. https://doi.org/10.1080/13803395.2016.1225006

Morgado, P., Sousa, N., Cerqueira, J.J., 2015. The impact of stress in decision making in the context of uncertainty: Stress Influence in Decision Making. Journal of Neuroscience Research 93, 839–847. https://doi.org/10.1002/jnr.23521

Nichols, T.E., Holmes, A.P., 2002. Nonparametric permutation tests for functional neuroimaging: A primer with examples. Hum. Brain Mapp. 15, 1–25. https://doi.org/10.1002/hbm.1058

Nicolson, N.A., 2008. Measurement of Cortisol, in: Handbook of Physiological Research Methods in Health Psychology. SAGE Publications, Inc., 2455 Teller Road, Thousand Oaks California 91320 United States, pp. 37–74. https://doi.org/10.4135/9781412976244.n3

Novais, A., Monteiro, S., Roque, S., Correia-Neves, M., Sousa, N., 2017. How age, sex and genotype shape the stress response. Neurobiology of Stress 6, 44–56. https://doi.org/10.1016/j.ynstr.2016.11.004

Oliveira, M., Rodrigues, A.-J., Leão, P., Cardona, D., Pêgo, J.M., Sousa, N., 2012. The bed nucleus of stria terminalis and the amygdala as targets of antenatal glucocorticoids: implications for fear and anxiety responses. Psychopharmacology 220, 443–453. https://doi.org/10.1007/s00213-011-2494-y

Pais-Ribeiro, J.L., Honrado, A., Leal, I., 2014. Contribuição para o estudo da adaptação portuguesa das escalas de ansiedade, depressão e stress (EADS) de 21 itens de Lovibond e Lovibond. Psicologia, saúde & doenças 5, 229–239.

Pêgo, J.M., Sousa, J.C., Almeida, O., Sousa, N., 2009. Stress and the Neuroendocrinology of Anxiety Disorders, in: Stein, M.B., Steckler, T. (Eds.), Behavioral Neurobiology of Anxiety and Its Treatment, Current Topics in Behavioral Neurosciences. Springer Berlin Heidelberg, Berlin, Heidelberg, pp. 97–118. https://doi.org/10.1007/7854_2009_13

Pinto, V., Costa, J.C., Morgado, P., Mota, C., Miranda, A., Bravo, F.V., Oliveira, T.G., Cerqueira, J.J., Sousa, N., 2015. Differential impact of chronic stress along the hippocampal dorsal–ventral axis. Brain Struct Funct 220, 1205–1212. https://doi.org/10.1007/s00429-014-0713-0

Plotsky, P.M., Cunningham, E.T., Widmaier, E.P., 1989. Catecholaminergic Modulation of Corticotropin-Releasing Factor and Adrenocorticotropin Secretion. Endocrine Reviews 10, 437–458. https://doi.org/10.1210/edrv-10-4-437

Popoli, M., Yan, Z., McEwen, B.S., Sanacora, G., 2012. The stressed synapse: the impact of stress and glucocorticoids on glutamate transmission. Nat Rev Neurosci 13, 22–37. https://doi.org/10.1038/nrn3138

Prewitt, C.M.F., Herman, J.P., 1998. Anatomical interactions between the central amygdaloid nucleus and the hypothalamic paraventricular nucleus of the rat: a dual tract-tracing analysis. Journal of Chemical Neuroanatomy 15, 173–186. https://doi.org/10.1016/S0891-0618(98)00045-3

Raabe, F.J., Spengler, D., 2013. Epigenetic Risk Factors in PTSD and Depression. Front. Psychiatry 4. https://doi.org/10.3389/fpsyt.2013.00080

Radley, J., Morilak, D., Viau, V., Campeau, S., 2015. Chronic stress and brain plasticity: Mechanisms underlying adaptive and maladaptive changes and implications for stress-related CNS disorders. Neuroscience & Biobehavioral Reviews 58, 79–91. https://doi.org/10.1016/j.neubiorev.2015.06.018

Reser, J.E., 2016. Chronic stress, cortical plasticity and neuroecology. Behavioural Processes 129, 105–115. https://doi.org/10.1016/j.beproc.2016.06.010

Rorden, C., Bonilha, L., Nichols, T.E., 2007. Rank-order versus mean based statistics for neuroimaging. NeuroImage 35, 1531–1537. https://doi.org/10.1016/j.neuroimage.2006.12.043

Sapolsky, R.M., Krey, L.C., McEWEN, B.S., 1986. The Neuroendocrinology of Stress and Aging: The Glucocorticoid Cascade Hypothesis*. Endocrine Reviews 7, 284–301. https://doi.org/10.1210/edrv-7-3-284

Selye, H., 1998. A Syndrome Produced by Diverse Nocuous Agents. JNP 10, 230a–2231. https://doi.org/10.1176/jnp.10.2.230a

Selye, H., 1956. The stress of life.

Seyedi, S., Jafari, R., Talaei, A., Naseri, S., Momennezhad, M., Moghaddam, M.D., Akbari-Lalimi, H., 2020. Comparing VBM and ROI analyses for detection of gray matter abnormalities in patients

with bipolar disorder using MRI. Middle East Curr Psychiatry 27, 69. https://doi.org/10.1186/s43045-020-00076-3

Sharp, B.M., 2017. Basolateral amygdala and stress-induced hyperexcitability affect motivated behaviors and addiction. Transl Psychiatry 7, e1194–e1194. https://doi.org/10.1038/tp.2017.161

Sharp, L.K., Kimmel, L.G., Kee, R., Saltoun, C., Chang, C.-H., 2007. Assessing the Perceived Stress Scale for African American Adults with Asthma and Low Literacy. Journal of Asthma 44, 311–316. https://doi.org/10.1080/02770900701344165

Sherman, S.M., Cheng, Y.-P., Fingerman, K.L., Schnyer, D.M., 2016. Social support, stress and the aging brain. Soc Cogn Affect Neurosci 11, 1050–1058. https://doi.org/10.1093/scan/nsv071

Smith, S.M., Jenkinson, M., Woolrich, M.W., Beckmann, C.F., Behrens, T.E.J., Johansen-Berg, H., Bannister, P.R., De Luca, M., Drobnjak, I., Flitney, D.E., Niazy, R.K., Saunders, J., Vickers, J., Zhang, Y., De Stefano, N., Brady, J.M., Matthews, P.M., 2004. Advances in functional and structural MR image analysis and implementation as FSL. NeuroImage 23, S208–S219. https://doi.org/10.1016/j.neuroimage.2004.07.051

Soares, J.M., Magalhães, R., Moreira, P.S., Sousa, A., Ganz, E., Sampaio, A., Alves, V., Marques, P., Sousa, N., 2016. A Hitchhiker's Guide to Functional Magnetic Resonance Imaging. Front. Neurosci. 10. https://doi.org/10.3389/fnins.2016.00515

Soares, J.M., Marques, P., Magalhães, R., Santos, N.C., Sousa, N., 2017. The association between stress and mood across the adult lifespan on default mode network. Brain Struct Funct 222, 101–112. https://doi.org/10.1007/s00429-016-1203-3

Soares, J.M., Sampaio, A., Ferreira, L.M., Santos, N.C., Marques, F., Palha, J.A., Cerqueira, J.J., Sousa, N., 2012. Stress-induced changes in human decision-making are reversible. Transl Psychiatry 2, e131–e131. https://doi.org/10.1038/tp.2012.59

Soares, J.M., Sampaio, A., Ferreira, L.M., Santos, N.C., Marques, P., Marques, F., Palha, J.A., Cerqueira, J.J., Sousa, N., 2013a. Stress Impact on Resting State Brain Networks. PLoS ONE 8, e66500. https://doi.org/10.1371/journal.pone.0066500

Soares, J.M., Sampaio, A., Marques, P., Ferreira, L.M., Santos, N.C., Marques, F., Palha, J.A., Cerqueira, J.J., Sousa, N., 2013b. Plasticity of resting state brain networks in recovery from stress. Front. Hum. Neurosci. 7. https://doi.org/10.3389/fnhum.2013.00919

Sousa, N., 2016. The dynamics of the stress neuromatrix. Mol Psychiatry 21, 302–312. https://doi.org/10.1038/mp.2015.196

Sousa, N., Cerqueira, J.J., Almeida, O.F.X., 2008. Corticosteroid receptors and neuroplasticity. Brain Research Reviews 57, 561–570. https://doi.org/10.1016/j.brainresrev.2007.06.007

Sousa, N., Lukoyanov, N.V., Madeira, M.D., Almeida, O.F.X., Paula-Barbosa, M.M., 2000. Reorganization of the morphology of hippocampal neurites and synapses after stress-induced damage correlates with behavioral improvement. Neuroscience 97, 253–266. https://doi.org/10.1016/S0306-4522(00)00050-6

Sturmberg, J.P., Bennett, J.M., Picard, M., Seely, A.J.E., 2015. The trajectory of life. Decreasing physiological network complexity through changing fractal patterns. Front. Physiol. 6. https://doi.org/10.3389/fphys.2015.00169

Sutton, B.P., Ouyang, C., Karampinos, D.C., Miller, G.A., 2009. Current trends and challenges in MRI acquisitions to investigate brain function. International Journal of Psychophysiology 73, 33–42. https://doi.org/10.1016/j.ijpsycho.2008.12.020

Taren, A.A., Gianaros, P.J., Greco, C.M., Lindsay, E.K., Fairgrieve, A., Brown, K.W., Rosen, R.K., Ferris, J.L., Julson, E., Marsland, A.L., Bursley, J.K., Ramsburg, J., Creswell, J.D., 2015. Mindfulness meditation training alters stress-related amygdala resting state functional connectivity: a randomized controlled trial. Soc. Cogn. Affect. Neurosci. 10, 1758–1768. https://doi.org/10.1093/scan/nsv066

Trigo, M., Canudo, N., Branco, F., Silva, D., 2010. Estudo das propriedades psicométricas da Perceived Stress Scale (PSS) na população portuguesa. Psychologica 353–378. https://doi.org/10.14195/1647-8606_53_17

van Ast, V.A., Cornelisse, S., Marin, M.-F., Ackermann, S., Garfinkel, S.N., Abercrombie, H.C., 2013. Modulatory mechanisms of cortisol effects on emotional learning and memory: Novel perspectives. Psychoneuroendocrinology 38, 1874–1882. https://doi.org/10.1016/j.psyneuen.2013.06.012

Ventura-Silva, A.P., Borges, S., Sousa, N., Rodrigues, A.J., Pêgo, J.M., 2020. Amygdalar corticotropin-releasing factor mediates stress-induced anxiety. Brain Research 1729, 146622. https://doi.org/10.1016/j.brainres.2019.146622

Vohryzek, J., Deco, G., Cessac, B., Kringelbach, M.L., Cabral, J., 2020. Ghost Attractors in Spontaneous Brain Activity: Recurrent Excursions Into Functionally-Relevant BOLD Phase-Locking States. Front. Syst. Neurosci. 14, 20. https://doi.org/10.3389/fnsys.2020.00020

Weaver, I.C.G., Meaney, M.J., Szyf, M., 2006. Maternal care effects on the hippocampal transcriptome and anxiety-mediated behaviors in the offspring that are reversible in adulthood. Proceedings of the National Academy of Sciences 103, 3480–3485. https://doi.org/10.1073/pnas.0507526103

Welberg, L., 2014. A REDD line from stress to depression. Nat Rev Neurosci 15, 350–350. https://doi.org/10.1038/nrn3749

World Health Organization, 2021. Mental health [WWW Document]. URL https://www.who.int/westernpacific/health-topics/mental-health (accessed 12.4.21).

Wu, J., Geng, X., Shao, R., Wong, N.M.L., Tao, J., Chen, L., Chan, C.C.H., Lee, T.M.C., 2018. Neurodevelopmental changes in the relationship between stress perception and prefrontal-amygdala functional circuitry. NeuroImage-Clin. 20, 267–274. https://doi.org/10.1016/j.nicl.2018.07.022

Wu, J., Tong, H., Liu, Z., Tao, J., Chen, L., Chan, C.C.H., Lee, T.M.C., 2020. Neurobiological effects of perceived stress are different between adolescents and middle-aged adults. Brain Imaging and Behavior. https://doi.org/10.1007/s11682-020-00294-7

Yousaf, T., Dervenoulas, G., Politis, M., 2018. Advances in MRI Methodology, in: International Review of Neurobiology. Elsevier, pp. 31–76. https://doi.org/10.1016/bs.irn.2018.08.008

Yuan, L., Chen, F., Zeng, L.-L., Wang, L., Hu, D., 2018. Gender Identification of Human Brain Image with A Novel 3D Descriptor. IEEE/ACM Trans. Comput. Biol. and Bioinf. 15, 551–561. https://doi.org/10.1109/TCBB.2015.2448081

Yuen, E.Y., Wei, J., Liu, W., Zhong, P., Li, X., Yan, Z., 2012. Repeated Stress Causes Cognitive Impairment by Suppressing Glutamate Receptor Expression and Function in Prefrontal Cortex. Neuron 73, 962–977. https://doi.org/10.1016/j.neuron.2011.12.033

Zhang, W.-H., Zhang, J.-Y., Holmes, A., Pan, B.-X., 2021. Amygdala Circuit Substrates for Stress Adaptation and Adversity. Biological Psychiatry 89, 847–856. https://doi.org/10.1016/j.biopsych.2020.12.026

CHAPTER II

Amygdala size varies with stress perception

Inês Caetano, Liliana Amorim, José Miguel Soares, Sónia Ferreira, Ana Coelho, Joana Reis, Nadine Correia Santos, Pedro Silva Moreira, Paulo Marques, Ricardo Magalhães, Madalena Esteves, Maria Picó-Pérez, Nuno Sousa

Article published in Neurobiology of Stress, 1 May 2021

DOI: 10.1016/j.ynstr.2021.100334

Link: https://doi.org/10.1016/j.ynstr.2021.100334

Neurobiology of Stress 14 (2021) 100334

Contents lists available at ScienceDirect

Neurobiology of Stress

journal homepage: www.elsevier.com/locate/ynstr

Amygdala size varies with stress perception

Inês Caetano [a,b,c], Liliana Amorim [a,b,c,d], José Miguel Soares [a,b,c], Sónia Ferreira [a,b,c], Ana Coelho [a,b,c], Joana Reis [a,b,c], Nadine Correia Santos [a,b,c], Pedro Silva Moreira [a,b,c], Paulo Marques [a,b,c], Ricardo Magalhães [a,b,c,e,f], Madalena Esteves [a,b,c], Maria Picó-Pérez [a,b,c], Nuno Sousa [a,b,c,d,*]

[a] Life and Health Sciences Research Institute (ICVS), School of Medicine, University of Minho, 4710-057, Braga, Portugal
[b] ICVS/3B's, PT Government Associate Laboratory, 4710-057, Braga/Guimarães, Portugal
[c] Clinical Academic Center – Braga, Braga, Portugal, 4710-057, Braga/Guimarães, Portugal
[d] Association P5 Digital Medical Center (ACMP5), 4710-057, Braga, Portugal
[e] NeuroSpin, Institut des Sciences du Vivant Frédéric Joliot, Commisariat à l'Énergie Atomique et aux Énergies Alternatives, 91191, Gif-Sur-Yvette, France
[f] Université Paris-Saclay, 91191, Gif-Sur-Yvette, France

ARTICLE INFO

Keywords:
Perceived stress
Amygdala
Voxel-based morphometry
FreeSurfer
Healthy subjects

ABSTRACT

Stress is inevitably linked to life. It has many and complex facets. Notably, perception of stressful stimuli is an important factor when mounting stress responses and measuring its impact. Indeed, moved by the increasing number of stress-triggered pathologies, several groups drew on advanced neuroimaging techniques to explore stress effects on the brain. From that, several regions and circuits have been linked to stress, and a comprehensive integration of the distinct findings applied to common individuals is being pursued, but with conflicting results. Herein, we performed a volumetric regression analysis using participants' perceived stress as a variable of interest. Data shows that increased levels of perceived stress positively associate with the right amygdala and anterior hippocampal volumes.

1. Introduction

When facing a stressor, and depending on its type, duration, and individual vulnerability, a subject triggers a variable response that can be partially measured; however, it is important to note that, largely, stress is a subjective perception (Godoy et al., 2018; Novais et al., 2017). Indeed, stress, and the individual perception of stress, is a key factor in mental health. Either by the time pressure of a busy life, economic factors, professional questions (Everaerd et al., 2020), personal and social relationships, or individual susceptibility (Duman et al., 2016), stress has invaded our lives to become a common presence in modern society (Kalisch et al., 2017; Lucassen et al., 2014). In line with the increasing number of people with stress symptoms, several studies have shown an association between stress and neuropsychiatric conditions such as major depression disease (Hammen, 2005; Kendler et al., 1999; Melchior et al., 2007; Welberg, 2014), anxiety (Melchior et al., 2007), schizophrenia (Walker et al., 2008), bipolar (Kim et al., 2007) and posttraumatic stress disorder (Brewin et al., 2000). As a result, there has been a significant effort of the scientific community to build a map of brain regions impacted by stress (Sousa, 2016) as well as their functional consequences both in physiological and pathological conditions (Lucassen et al., 2014; Novais et al., 2017). Such effort has resulted in an impressive collection of data, but unfortunately with several discrepancies. In terms of cortical volumetry, some studies showed reduced volumes of the prefrontal cortex (PFC), orbitofrontal cortex (OFC), anterior cingulate cortex (ACC), superior temporal gyrus (STG) and

Abbreviations: PSS10, 10-items Perceived Stress Scale; FSL, FMRIB Software Library; VBM, Voxel-based morphometry; ROI, Region-of-interest; TFCE, Threshold-free cluster enhancement; FWE-R, Family-wise error rate; GM, Gray matter; WM, White matter; eTIV, Estimated total intracranial volume; M, Mean; SD, Standard deviation.

* Corresponding author. Life and Health Sciences Research Institute, School of Medicine, University of Minho, Campus de Gualtar, 4710-057, Braga, Portugal.
E-mail addresses: ines.caetano91@gmail.com (I. Caetano), liliana.amorim@gmail.com (L. Amorim), zmmsoares@gmail.com (J.M. Soares), soniamgaf@gmail.com (S. Ferreira), acoelho.tkd@gmail.com (A. Coelho), joana.reis21@gmail.com (J. Reis), nsantos@med.uminho.pt (N.C. Santos), pedromsmoreira@gmail.com (P.S. Moreira), paulo.c.g.marques@gmail.com (P. Marques), ricardo.lazarus@gmail.com (R. Magalhães), madalena.curva.esteves@gmail.com (M. Esteves), mariapico231@gmail.com (M. Picó-Pérez), njcsousa@med.uminho.pt (N. Sousa).

https://doi.org/10.1016/j.ynstr.2021.100334
Received 31 December 2020; Received in revised form 26 April 2021; Accepted 27 April 2021
Available online 1 May 2021

insula (Ansell et al., 2012; Moreno et al., 2017; Savic et al., 2018), whereas others failed to find such volumetric differences in the same cortical regions or even found potential signs of the opposite (Merz et al., 2019; Piccolo and Noble, 2018; Soares et al., 2012; Zhang et al., 2018). Interestingly, two opposite trends on the structure of subcortical regions implicated in the stress response are extensively reported in the literature and need to be revised. While some studies show, for example, volumetric increases in several subcortical brain regions, in particular the amygdala, (De Bellis et al., 2000; Henigsberg et al., 2019; Klaming et al., 2019; Kuo et al., 2012; Lucassen et al., 2014; Morey et al., 2016; Novais et al., 2017; Pinto et al., 2015; Schienle et al., 2011), others fail to reproduce these findings (Herringa et al., 2012; Karl et al., 2006; Kitayama et al., 2005; Koshiyama et al., 2018; Magalhães et al., 2018; Morey et al., 2012; Soares et al., 2012; Vriend et al., 2016; Zimmerman et al., 2016).

A significant part of such conflicting findings derives from methodological approaches. On one hand, there are technical issues related to image processing. In fact, particular attention to preprocessing and analysis steps is required when conducting neuroimaging studies. For instance, Katuwal et al. demonstrated that brain volume estimates were dependent on the software chosen (SPM, FSL, and FreeSurfer), leading to differences upon between-group comparisons, with some results presenting opposite directions (Katuwal et al., 2016). Similarly, Grimm et al. have shown large differences upon amygdala and hippocampal volumes that were computed through manual segmentation, using FreeSurfer, and using VBM (implemented in SPM8), highlighting the disparities across methods (Grimm et al., 2015). On the other hand, there are important issues in study design. In fact, stress is not a homogenous concept and group comparisons always suffer from the intra-group variability in measurements (namely in endocrine measurements). Interestingly, the 10-items Perceived Stress Scale instrument (PSS10) has been well validated, both for healthy and pathological populations (Fliege et al., 2005; Trigo et al., 2010), with several studies showing its psychometric qualities on the individual quantification of perceived stress levels (Lee, 2012; Soares et al., 2012). Thus, taking into account that stress perception is a central element in the present study, we opted to use the PSS10.

Herein, we have tackled such methodological issues by performing a study that explores the association of perceived stress scores using the PSS10 questionnaire and the volumes of subcortical brain regions determined with multiple techniques. By doing so, we avoid the bias of group classification and high variability between individuals in cortisol measurements, but also the bias of distinct software/pipelines for volumetric analysis.

2. Material and methods

2.1. Ethics statement

The present study was conducted in accordance with the principles expressed in the Declaration of Helsinki (59th amendment) and approved by the national and local ethics review board committees (*Comissão Nacional de Protecção de Dados*, *Comissão de Ética para a Saúde of Hospital de Braga*, and *Subcomissão de ética para as ciências da vida e da saúde* from University of Minho). The study aims were explained to all participants and all signed informed consent.

2.2. Participants and study design

The present study gathered 50 participants recruited at the School of Medicine, University of Minho, and at Faculty of Medicine, University of Porto. Primary exclusion criteria included inability to understand the informed consent or its non-acceptance, individual choice to withdraw from the study, incapacity and/or inability to attend the MRI session and/or diagnosed neuropsychiatric disorder or any other comorbidity of the central nervous system.

Structural acquisitions from all participants were collected as well as the PSS10 questionnaire. This scale reports to the previous month and is a reliable and validated self-administered instrument largely used to assess chronic psychosocial stress both in clinical and healthy adult samples (Cohen et al., 1983; Fliege et al., 2005; Liston et al., 2009; Soares et al., 2012; Trigo et al., 2010). Additionally, before the MRI acquisition, half of the participants collected saliva samples for posterior analysis of cortisol, the primary stress hormone.

To unveil associations between morphometry and psychological stress, a volumetric regression analysis with PSS10 scores as a variable of interest was conducted, using the FSL-VBM software (voxel-based method). As a complementary analysis, we also addressed our question using FreeSurfer (ROI-based analysis).

To further explore the association between cortisol and morphometry, we performed an additional volumetric regression using FreeSurfer software.

2.3. Participants characterization and cortisol measurement

The demographic, psychological and endocrine characterization of participants was made using SPSS version 23 (IBM, SPSS, Chicago, IL, USA). The normality assumption for each variable was tested and non-parametric tests used when the assumption not met.

Due to the use of age and sex as covariates in all MRI analyses, a correlation between PSS10 scores/cortisol and age/sex was performed to disclose the existence of a possible association that could affect volumetric regression results.

For cortisol measurement, saliva samples were collected in the morning, between 9 a.m. and 12 a.m., using Salivette collection devices (Sarstedt, Germany). The samples were stored at −22 °C until the biologically active, free fraction of cortisol be analysed with an immunoassay (IBL, Hamburg).

2.4. MRI data acquisition

Imaging sessions were conducted at Hospital of Braga (Braga, Portugal) on a clinical approved Siemens Magnetom Avanto 1.5 T MRI scanner (Siemens Medical Solutions, Erlangen, Germany), using a 12-channel receive-only head coil. The imaging protocol consisted of a T1 high-resolution anatomical sequence. The established clinical protocols for the 3D magnetization prepared rapid gradient echo (MPRAGE) were performed with a repetition time (TR) = 2.4/2.7 s, echo time (TE) = 3.62/2.73 ms, 160/176 sagittal slices with no gap, field-of-view (FoV) = 234/256 mm, flip angle (FA) = 7/8°, in-plane resolution = 1.0/1.2 × 1.0/1.2 mm^2 and slice thickness = 1.0/1.2 mm.

2.5. MRI data preprocessing

Before any data processing, a certified neuro-radiologist visually inspected all acquisitions and confirmed that they were not affected by critical head motion and that the participants had no brain lesions or pathologies. Preprocessing was made using fMRIPrep version 1.4.1 (Esteban et al., 2019) (RRID:SCR_016216), which is based on Nipype 1.2.0 (Gorgolewski et al., 2011, 2017) (RRID:SCR_002502).

Each anatomical T1-weighted (T1w) image was corrected for intensity non-uniformity (INU) with N4BiasFieldCorrection (Tustison et al., 2010), distributed with ANTs 2.2.0 (Avants et al., 2008) (RRID: SCR_004757), and used as T1w-reference throughout the workflow. Then, the T1w-reference was skull-stripped with a Nipype implementation of the *antsBrainExtraction.sh* workflow (from ANTs), using OASIS30ANTs as target template and segmented into cerebrospinal fluid (CSF), white matter (WM), and gray matter (GM) using *fast* (Zhang et al., 2001) (FSL 5.0.9, RRID:SCR_002823). The reconstruction of brain surfaces was made with *recon-all* (Dale et al., 1999) (FreeSurfer 6.0.1, RRID: SCR_001847), and the previously brain mask estimated was refined with a custom variation of the method to reconcile ANTs-derived and

FreeSurfer-derived segmentations of the cortical GM of Mindboggle (Klein et al., 2017) (RRID:SCR_002438). The images were non-linearly transformed into standard space ICBM 152 Nonlinear Asymmetrical template (Fonov et al., 2009) (version 2009c; RRID:SCR_008796; TemplateFlow ID: MNI152NLin2009cAsym) with *antsRegistration* (ANTs 2.2.0), using brain-extracted versions of both T1w reference and T1w template.

2.6. FSL-VBM analysis

The voxel-based morphometry analysis was performed using FSL-VBM (Douaud et al., 2007) (http://fsl.fmrib.ox.ac.uk/fsl/fslwiki/FSLVBM) which is an optimized VBM protocol (Good et al., 2001) implemented through tools from the FMRIB Software Library (Smith et al., 2004) (FSL 5.0.9, www.fmrib.ox.ac.uk/fsl). The recommended analytical pipeline was followed, however, image skull-striping, segmentation into tissue classes, and non-linearly transformation to standard space steps were not performed since they had already been computed during preprocessing. To create a left-right symmetric study-specific gray matter template, the standardized GM images obtained with the fMRIPrep were averaged and flipped along the x-axis. In order to build an unbiased template, an equal number of images acquired with each configuration was used (32 in total). At this stage, all native GM images were non-linearly registered to the study-specific template created and "modulated" to correct for local expansion and/or contraction due to the non-linear component of the spatial transformation. The Jacobian modulation does not include the affine part of the registration meaning that the images are already normalized for total cranial volume differences (corrections upon total cranial volumes are only required when modulation includes the affine part (Good et al., 2002)). Then, the modulated GM images were smoothed using an isotropic Gaussian kernel with a sigma = 3 mm (corresponding to FWHM = 7 mm). Finally, considering PSS10 scores as a variable of interest and sex, age, and MRI configuration, as between-subject covariates, a voxelwise General Linear Model (GLM) was applied using non-parametric permutation-based testing (5000 permutations), with TFCE-based thresholding, upon a subcortical mask created according to FreeSurfer subcortical automatic segmentation (Fischl et al., 2002) (bilateral regions of the thalamus, caudate, putamen, pallidum, hippocampus, amygdala, and accumbens area). Correction for multiple comparisons across space were performed with a significance of 0.05, and, after visual inspection, statistically significant clusters obtained were reported also according to FreeSurfer labeling. The voxels with higher probability in each cluster were defined as peaks and the averaged probability over all the voxels in the cluster was considered for global cluster statistics.

2.7. FreeSurfer ROI-based analysis

The morphometry ROI-based analysis was conducted for each region individually. Firstly, subcortical volumes of participants were computed, and then, the statistical analysis upon those volumes was individually conducted.

For volumes computation, the FreeSurfer derivatives of the fMRIPrep were used. The general FreeSurfer (Fischl, 2012) (http://surfer.nmr.mgh.harvard.edu) pipeline implements 31 processing steps, including motion correction, spatial normalization to Talairach standard space, intensity normalization, skull stripping, and segmentation of WM, cortical, and subcortical regions. In the fMRIPrep, the processing steps of the FreeSurfer pipeline are aggregated in 3 phases. Firstly, a subject T1w structural image is initialized and a basic reconstruction, excepting skull-stripping, is performed using the *autorecon1* (first 5 preprocessing steps of *recon-all* (Dale et al., 1999) function, excluding step 5, the skull-stripping). Secondly, a brain mask that was previously computed in the fMRIPrep workflow (using *antsBrainExtraction.sh*) is directly injected into the appropriate FreeSurfer location, in place of the skull-stripping step that was not performed before. Herein, this external brain mask is also refined using the internal mask of the FreeSurfer's *aseg.mgz* segmentation, reconciling ANTs-derived, and FreeSurfer-derived segmentation of the cortical GM of Mindboggle (Klein et al., 2017). Finally, the third phase resumes *recon-all* execution (*autorecon2* and *autorecon3*), dividing all the remaining FreeSurfer steps into sub-stages, to use resources more efficiently. For the main purpose of this work only volumes resulting from the automatic subcortical segmentation (Fischl et al., 2002) were used (bilateral thalamus, caudate, putamen, pallidum, hippocampus, amygdala, and accumbens area). To best replicate the FSL-VBM analysis, all the volumes were corrected for individual GM, and multiplied by 100 to avoid a large number of decimal digits.

For statistical analysis, multilinear regression models with each ROI volume as the dependent variable and PSS10 scores (or cortisol), age and sex as independent variables were established. The models were computed in MATLAB and the Bonferroni-Holm (1979) correction for 14 multiple comparisons were used to calculate the corrected *p*-values. When two independent terms were statistically significant in the same model, the interaction effect between those terms was explored by including the interaction factor on the model. Additional analyses on the anterior (head) and posterior (body and tail) hippocampus were conducted to explore the structural segregation of this region. For hippocampal segmentation, the FreeSurfer version 7.1.1 was used (Iglesias et al., 2015).

Linear regressions and independent-samples *t*-test were used to further explore the statistical significance of independent terms of the multilinear models obtained.

As exploratory analysis, the regression between cortical brain volumes and PSS was also conducted.

Finally, an independent sample *t*-test regarding the estimated total intracranial volume (eTIV), and a Mann-Whitney *U* test regarding GW, were made to confirm that no morphometry differences are caused due to the slight protocol disparities.

3. Results

3.1. Cohort characterization

The demographic and psychological characterization of participants, as cortisol measurements, are presented in Table 1. No correlation was found between PSS10 scores and age/sex (r (50) = 0.091/0.077, p = 0.530/0.716), nor between cortisol measurements and age/sex (r (25) = −0.055/0.242, p = 0.789/0.243). Taking into consideration the usage of age and sex as covariates in MRI analysis, the absence of a significant correlation ensures that the effects of stress in the regression are not decreased or affected by the usage of covariate variables.

Regarding the association between stress measurements, no correlation was found between PSS10 scores and cortisol levels (r (25) = 0.107, p = 0.612).

Descriptive statistics of subcortical volumes, GM, WM, and estimated total intracranial volume (eTIV) obtained through FreeSurfer are

Table 1
Demographic, psychological and endocrine characterization of participants.

	N	Mean (±SD)
DEMOGRAPHIC		
Age, years	50	24.30 ± 1.81
Male	15 (30%)	
Female	35 (70%)	
PSYCHOLOGICAL		
PSS10 scores	50	26.2 ± 7.14
ENDOCRINE		
Cortisol	25	0.32 ± 0.21
Male	7 (28%)	
Female	18 (72%)	

presented in supplementary Table A.1. When comparing results from both acquisition protocols, no differences were found in subjects' eTIV (t (48) = 1.915, p = 0.061), nor in subjects' GM (U = 359, p = 0.070).

3.2. Volumetric regression with PSS10

As shown in Fig. 1 and Table 2, when exploring the association between PSS10 and morphology through FSL-VBM, a positive statistically significant association within 3 clusters is observed. The largest, and the most significant, cluster is centered in the right amygdala (peak), including also part of the right anterior hippocampus and a small portion of the right putamen. In the left hemisphere, a more dispersed cluster essentially extends through the hippocampus (peak), also comprising a portion of the amygdala, was found. Finally, data reveals a very small cluster, composed of 3 voxels of right pallidum. In all cases, these brain regions displayed higher volumes in subjects with higher stress perception.

Results from volumetric regression with perceived stress evaluated through FreeSurfer also show a statistically significant positive association between PSS10 scores and the volume of the right amygdala. In Fig. 2, a representation of such association between stress perception and the size of the right amygdala is displayed, as well as the graphical representation of the significant model obtained, corrected for age and sex covariates. The positive associations between PSS10 and right pallidum, right hippocampus, left amygdala and right accumbens area were noted, but did not survive to multiple comparison correction (See Table 2 for more information on these regions, and supplementary Table A.2 for a detailed description of all models obtained).

When exploring the association between PSS scores and hippocampal segregation, a statistically significant association was observed only in the anterior hippocampus (see Supplementary Table A.3 for details).

The exploratory analysis across the cortical regions, revealed no statistically significant results.

3.3. Volumetric regression with cortisol

A multilinear model revealed a significant negative association between cortisol measurements and the left thalamus volumes. Moreover, a positive association with sex and left thalamus was also observed, which due to the covariate codification (females as 0 and males as 1), indicates that being a male positively contribute to having a bigger volume of left thalamus, and, in contrast, being a female contribute to having smaller left thalamus volume. (See supplementary Table A.4 for a description of all models obtained). When including in the model the interaction factor between cortisol and sex, no statistical significance for the interaction was observed (p = 0.3782), which indicates that there are no differences in the association of left thalamus volumes and cortisol levels between males and females. Further between-group analysis upon sex indicates that left thalamus volumes are higher in males (M = 1.23 ± 0.082) than in females (M = 1.15 ± 0.067), when controlling for cortisol levels and age (t (23) = 2.225, p = 0.034, d = 0.94). In Fig. A.1, graphical representations of the left thalamus model, considering cortisol/sex as the independent term and the corrected left thalamus volumes as to the dependent variable, are presented.

A similar trait was observed in the right thalamus, not surviving to multiple comparisons. Importantly, no other subcortical region has shown significance for cortisol measurements.

4. Discussion

In the present study, we explore how psychosocial stress correlates with subcortical brain morphometry, using a cohort of healthy adults. Results show a positive association between perceived stress and subcortical regions, in particular, the right amygdala, linked to emotional processing.

Exposure to stress is part of life. Importantly, each subject perceives stress differently. Assuming the concept of stress perception as a continuum (Selye, 1956), we describe here a positive association between stress perception and the volume of subcortical brain regions implicated in emotional processing. The predominant effect herein observed was in the right amygdala, with a similar tendency on the left hemisphere not surviving to multiple comparisons in FreeSurfer analysis. Importantly, besides the well-stated involvement of the amygdala in emotional processing, and its role mediating stress-responses (LeDoux, 2000), studies have shown that amygdala neuroplasticity is associated with the subject's psychological state (Taren et al., 2013). Indeed, the longitudinal VBM study of Hölzel et al. in a healthy, however, stressed cohort, revealed that after an effective stress-reduction intervention, the decrease in PSS levels matched with a reduction in the right basolateral amygdala gray matter density (Hölzel et al., 2010).

Interestingly, and despite a similar trend, the present association seems to be stronger on the right hemisphere. Highlighting the right

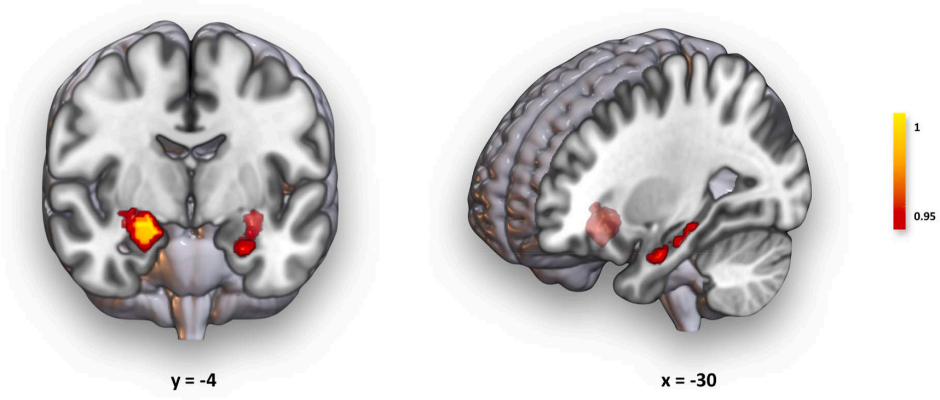

Fig. 1. Results from volumetric regression with PSS10 evaluated through FSL-VBM. A positive statistically significant association between PSS10 scores and two main subcortical clusters is observed. On the left, the biggest cluster is mainly composed of the right amygdala (peak), embracing part of the right hippocampus and a small portion of the right putamen. On the right, a smaller cluster is observed the in left hippocampus (peak) and left amygdala. Following the FSL-VBM pipeline, after brain extraction and segmentation, a study-specific GM template was created, upon which all GM images were registered. During this registration step, a compensation for the non-linear component of the transformation is introduced by the FSL-VBM protocol, which already adjusts for intracranial differences. Therefore, only age, sex, and MRI parameters were defined as covariates, and TFCE and FWE-R correction at a significance level α = 0.05 were used.

Table 2
Results from the volumetric regression analysis with PSS10 evaluated through VBM and FreeSurfer. Positive statistically significant association within PSS10 scores and subcortical regions are observed for both methods. On the left, clusters resulted from the volumetric regression analysis with perceived stress scores on FSL-VBM and respective statistics. In the middle, brain region classification according to FreeSurfer subcortical segmentation (*aseg.stats*). On the right, significant results of FreeSurfer analysis, with all regions identified in VBM-FSL clusters represented independently of its significance, plus all regions with significance on FreeSurfer before correction for multiple comparisons.

FSL-VBM								Brain Region	FreeSurfer		
Cluster index	Cluster size	Peak					*n* voxels FSL-VBM cluster		*n* voxels FreeSurfer ROI	ROI	
		t-value	*p*(FWE-corr)	coordinates (*mm*)						*p*-value	*p*(Bonf-corr)
				x	*y*	*z*					
1	310	4.39	0.007	20	−4	−12	157	54_R Amygdala	263	**<0.001**	**<0.001**
							138	53_R Hippocampus	658	**0.021**	0.248
							15	51_R Putamen	831	0.756	2.520
2	116	3.95	0.029	−30	−22	−20	99	17_L Hippocampus	634	0.093	0.838
							17	18_L Amygdala	219	**0.013**	0.163
3	3	3.15	0.049	20	−4	−6	3	52_R Pallidum	207	**0.025**	0.271
							–	58_R Accumbens-area	83	**0.033**	0.326

TFCE and FWE-R correction at a significance level of 0.05 for FSL-VBM analysis; Multilinear regression with Bonferroni-Holm correction for 14 comparisons in FreeSurfer analysis. ROI. Region of interest; R. right; L. left.

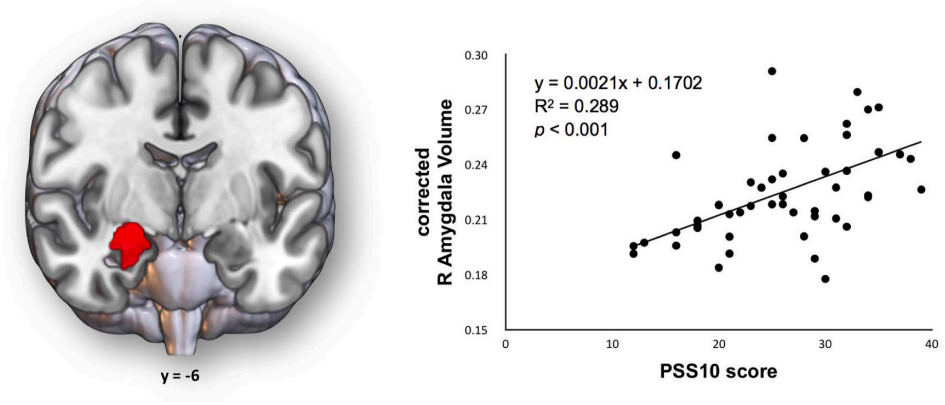

Fig. 2. Results from volumetric regression with PSS10 evaluated through FreeSurfer. A positive statistically significant association between PSS10 scores and right amygdala was observed, after correction for multiple comparisons. On the left, a representation of the *54_R Amygdala* cluster from FreeSurfer subcortical regions labelling. On the right, a graphical representation of the model with significance between PSS10 scores and right amygdala volumes corrected for GM, and age/sex covariates; the equation represents the correlation between the PSS10 scores and corrected right amygdala volumes, and not the global model *per se*. Brain volumes were computed using FreeSurfer subcortical output and corrected for individual GM to best replicate the VBM regression analysis. Multilinear regression models with ROI volumes as dependent variables and PSS10 scores, age, and sex as independent variables were established. The models were computed using the *regstats* function in MATLAB and the Bonferroni-Holm correction for 14 multiple comparisons was used to calculate the corrected p-values. Statistical significance was established for $\alpha = 0.05$.

dominance on affective and emotional processes (namely on the stress response modulation), and its contrast to the left prominence on language and motor functions (Cerqueira et al., 2008), studies have shown evidences of specific functional asymmetries. Particularly in the amygdala, variations in the affective processing are point out as a rationale for the divergences observed (Hölzel et al., 2010; Lanteaume et al., 2007; Markowitsch, 1999). Here, the fast initial, and possibly automatic, response of the right amygdala to stimuli contrasts to a further discriminative evaluation of the stressor by the left amygdala (Hölzel et al., 2010). Indeed, a clinical study revealed that right amygdala stimulation triggered negative emotions and left amygdala stimulation induced both pleasant and unpleasant emotions (Lanteaume et al., 2007). Interestingly, and in contrast, the recent study of Wu et al. has also shown a significant interaction effect of stress by age on a cluster extending to the left amygdala (Wu et al., 2020); indeed, post-hoc comparisons revealed a positive association with left amygdala volumes in adolescents, with middle-aged adults presenting a negative correlation with PSS levels, which may justify the weaker effect observed on the left hemisphere.

When focusing only on the hippocampus, our results contrast with the usual atrophy observed in stressed subjects (Cameron and Schoenfeld, 2018; Gilbertson et al., 2002; Zimmerman et al., 2016). Yet, it is important to highlight the fact that there is a functional and a structural connectivity segregation between the anterior vs posterior hippocampus (Sousa, 2016) and also that previous studies assessing the impact of stress, namely in rodents have shown a clear volumetric differential response with atrophy in dorsal hippocampus and hypertrophy in the ventral component (more related to the anterior hippocampus in humans) (Pinto et al., 2015). Interestingly, our findings also show distinct profiles across hemispheres. On the right hemisphere, volumetric changes are noted on the anterior hippocampus, a region known for its role in mediating emotional and affective processes (Strange et al., 2014). This is a novel finding, as in a similar study, Li et al. have shown a positive association not with the anterior hippocampus but, between the anterior parahippocampal gyrus and PSS (Li et al., 2014). Actually, this slight disparity upon results should be carefully interpreted, taking

particular attention to the methodological differences between studies. Most importantly, a distinguished preprocessing pipeline and morphometry analysis (using SPM8; https://www.fil.ion.ucl.ac.uk/spm/software/spm8/), represent variables that if ignored could lead to a misinterpretation of results (Popescu et al., 2016). In fact, Rajagopalan and Pioro have reported that analyses in distinct software (FSL, SPM, and FreeSurfer) lead to disparate VBM results, which enhances the importance of performing complementary analysis in the same study (Rajagopalan and Pioro, 2015). Indeed, the present study illustrates this fact, as the findings on the anterior hippocampus on the right, and posterior hippocampus on the left, are only observed with FSL-VBM analysis, but not with FreeSurfer.

A final note to highlight the findings in the putamen and nucleus accumbens in our FSL-VBM, but not FreeSurfer, analysis. The putamen is involved in distinct brain functions - such as learning, cognitive functioning, or reward (Ghandili and Munakomi, 2020) - previous reports from our group have already shown hypertrophy in sensorimotor corticostriatal circuits, which is accompanied by a shift to habit-behavior strategies (Soares et al., 2012). The nucleus accumbens gray matter increases have been linked to anxiety (Kühn et al., 2011; Lee et al., 2020), being also identified as a biomarker for treatment-responders (Burkhouse et al., 2020). Nonetheless, the residual effect observed in all these regions, that were not confirmed in our FreeSurfer analysis, preclude any conclusion on relevant associations between the volumes of these brain regions and perceived stress scores.

A considerable sex difference in sample size is a limitation in our study. However, we have tackled this limitation by doing corrections for sex through the use of a covariate in all the analyses. Another question that can be pointed out as a limitation in our study is the predominant use of PSS10, a subjective instrument that measures the individual perception of stress and not an objective quantification of stress itself. In fact, studies have struggled in showing consistent associations between cortisol and psychosocial stressors (Chida and Steptoe, 2009; Halford et al., 2012), contrasting to the well-established PSS instrument (Fliege et al., 2005; Soares et al., 2012; Trigo et al., 2010). Therefore, and bearing in mind that distress only exists when recognized by the subject (Goldstein and Kopin, 2007), we consider that this metric is of great physiological (and even clinical) relevance. Indeed, the current data confirms that the way subjects integrate stress is associated with brain morphometry, regardless of the true amount of exposure or kind of stressor. On the other hand, the additional analysis conducted on a subgroup of our participants endorses the fact that endocrine measures, namely cortisol, do not associate equally with the volume of subcortical brain regions. Our results show a negative association between cortisol and left thalamus volumes, which contrast to previous observations in an older cohort (Lau et al., 2017), and emphasizes the volumetric sex differences that have been previously reported by others (Koolschijn and Crone, 2013; Menzler et al., 2011). Indeed, using a single measurement of salivary cortisol, we are addressing an acute endocrine response that contrasts with the chronic, one-month evaluation of psychological stress measured by with PSS10 questionnaire. However, in future work, we do not exclude the possibility to combine psychological questionnaires with physiological measures, to further explore the relationship between perceived and objective stress measures, as suggested by Lee (2012). In fact, Lazarides et al. argue that the failure in demonstrating this link arises from limitations in measurements approaches and, most importantly, on the reliance of between-subject comparisons, rather than within-subject associations (Lazarides et al., 2020).

In conclusion, herein we explored the association of psychosocial stress in subcortical brain regions volumes, using a non-pathological population. We performed a volumetric regression analysis where perceived stress scores were used as a variable of interest and we demonstrate that increased levels of perceived stress positively associate with the right amygdala and anterior hippocampal volumes.

CRediT authorship contribution statement

Inês Caetano: Conceptualization, Formal analysis, Validation, Writing – original draft, Visualization, contributed to the study design, Formal analysis, interpreted the results, discussed the manuscript, wrote the first draft of the manuscript, performed data presentation. **Liliana Amorim:** Investigation, Data curation, performed participant's recruitment, neuropsychological assessment, Formal analysis, manuscript discussion. **José Miguel Soares:** Investigation, Data curation, performed participant's recruitment, MRI acquisitions. **Sónia Ferreira:** Formal analysis, Formal analysis, interpretation of results. **Ana Coelho:** Software, Visualization, Formal analysis, presentation of results. **Joana Reis:** Formal analysis, Formal analysis. **Nadine Correia Santos:** Funding acquisition, provided the resources for study development. **Pedro Silva Moreira:** Methodology, Formal analysis, Methodology, Formal analysis. **Paulo Marques:** Investigation, performed the MRI acquisitions. **Ricardo Magalhães:** Investigation, Visualization, performed the MRI acquisitions, contributed to the presentation of results. **Madalena Esteves:** Software, Formal analysis, Validation, Formal analysis. **Maria Picó-Pérez:** Software, Formal analysis, Validation, performed the data pre-processing, Formal analysis, manuscript discussion. **Nuno Sousa:** Conceptualization, Validation, Writing – review & editing, Supervision, Funding acquisition, conceived the study design, provided the resources for study development, reviewed the acquired data, interpreted the results, performed manuscript discussion, reviewed the final manuscript.

Declaration of competing interest

The authors declared that they had no conflicts of interest concerning their authorship or the publication of this article.

Acknowledgements

This work was supported by National funds, through the Foundation for Science and Technology (FCT) [projects UIDB/50026/2020, UIDP/50026/2020]; and the Norte Portugal Regional Operational Programme (NORTE 2020), under the PORTUGAL 2020 Partnership Agreement, through the European Regional Development Fund (ERDF) [projects NORTE-01-0145-FEDER-000013, NORTE-01-0145-FEDER-000023]. IC, LA and AC were supported by fellowship grants through the FCT (grants number SFRH/BD/133006/2017, SFRH/BD/101398/2014, NORTE-08-5369-FSE-000041) from the Health Science program.

Appendix A. Supplementary data

Supplementary data to this article can be found online at https://doi.org/10.1016/j.ynstr.2021.100334.

References

Ansell, E.B., Rando, K., Tuit, K., Guarnaccia, J., Sinha, R., 2012. Cumulative adversity and smaller gray matter volume in medial prefrontal, anterior cingulate, and insula regions. Biol. Psychiatr. 72, 57–64. https://doi.org/10.1016/j.biopsych.2011.11.022.

Avants, B., Epstein, C., Grossman, M., Gee, J., 2008. Symmetric diffeomorphic image registration with cross-correlation: evaluating automated labeling of elderly and neurodegenerative brain. Med. Image Anal. 12, 26–41. https://doi.org/10.1016/j.media.2007.06.004.

Brewin, C.R., Andrews, B., Valentine, J.D., 2000. Meta-analysis of risk factors for posttraumatic stress disorder in trauma-exposed adults. J. Consult. Clin. Psychol. 68, 748–766. https://doi.org/10.1037/0022-006X.68.5.748.

Burkhouse, K.L., Jimmy, Jagan, Defelice, N., Klumpp, H., Ajilore, O., Hosseini, B., Fitzgerald, K.D., Monk, C.S., Phan, K.L., 2020. Nucleus accumbens volume as a predictor of anxiety symptom improvement following CBT and SSRI treatment in two independent samples. Neuropsychopharmacology 45, 561–569. https://doi.org/10.1038/s41386-019-0575-5.

Cameron, H.A., Schoenfeld, T.J., 2018. Behavioral and structural adaptations to stress. Front. Neuroendocrinol. 49, 106–113. https://doi.org/10.1016/j.yfrne.2018.02.002.

Cerqueira, J.J., Almeida, O.F.X., Sousa, N., 2008. The stressed prefrontal cortex. Left? Right! Brain, Behavior, and Immunity 22, 630–638. https://doi.org/10.1016/j.bbi.2008.01.005.
Chida, Y., Steptoe, A., 2009. Cortisol awakening response and psychosocial factors: a systematic review and meta-analysis. Biol. Psychol. 80, 265–278. https://doi.org/10.1016/j.biopsycho.2008.10.004.
Cohen, S., Kamarck, T., Mermelstein, R., 1983. A global measure of perceived stress. J. Health Soc. Behav. 24, 385. https://doi.org/10.2307/2136404.
Dale, A.M., Fischl, B., Sereno, M.I., 1999. Cortical Surface-Based Analysis 16. https://doi.org/10.1006/nimg.1998.0395.
De Bellis, M.D., Casey, B.J., Dahl, R.E., Birmaher, B., Williamson, D.E., Thomas, K.M., Axelson, D.A., Frustaci, K., Boring, A.M., Hall, J., Ryan, N.D., 2000. A pilot study of amygdala volumes in pediatric generalized anxiety disorder. Biol. Psychiatr. 48, 51–57. https://doi.org/10.1016/S0006-3223(00)00835-0.
Douaud, G., Smith, S., Jenkinson, M., Behrens, T., Johansen-Berg, H., Vickers, J., James, S., Voets, N., Watkins, K., Matthews, P.M., James, A., 2007. Anatomically related grey and white matter abnormalities in adolescent-onset schizophrenia. Brain 130, 2375–2386. https://doi.org/10.1093/brain/awm184.
Duman, R.S., Aghajanian, G.K., Sanacora, G., Krystal, J.H., 2016. Synaptic plasticity and depression: new insights from stress and rapid-acting antidepressants. Nat. Med. 22, 238–249. https://doi.org/10.1038/nm.4050.
Esteban, O., Markiewicz, C.J., Blair, R.W., Moodie, C.A., Isik, A.I., Erramuzpe, A., Kent, J. D., Goncalves, M., DuPre, E., Snyder, M., Oya, H., Ghosh, S.S., Wright, J., Durnez, J., Poldrack, R.A., Gorgolewski, K.J., 2019. fMRIPrep: a robust preprocessing pipeline for functional MRI. Nat. Methods 16, 111–116. https://doi.org/10.1038/s41592-018-0235-4.
Everaerd, D.S., Henckens, M.J.A.G., Bloemendaal, M., Bovy, L., Kaldewaij, R., Maas, F.M. W.M., Mulders, P.C.R., Niermann, H.C.M., van de Pavert, I., Przezdzik, I., Fernández, G., Klumpers, F., de Voogd, L.D., 2020. Good vibrations: an observational study of real-life stress induced by a stage performance. Psychoneuroendocrinology 114, 104593. https://doi.org/10.1016/j.psyneuen.2020.104593.
Fischl, B., 2012. FreeSurfer. NeuroImage 62, 774–781. https://doi.org/10.1016/j.neuroimage.2012.01.021.
Fischl, B., Salat, D.H., Busa, E., Albert, M., Dieterich, M., Haselgrove, C., van der Kouwe, A., Killiany, R., Kennedy, D., Klaveness, S., Montillo, A., Makris, N., Rosen, B., Dale, A.M., 2002. Whole brain segmentation. Neuron 33, 341–355. https://doi.org/10.1016/S0896-6273(02)00569-X.
Fliege, H., Rose, M., Arck, P., Walter, O.B., Kocalevent, R.-D., Weber, C., Klapp, B.F., 2005. The perceived stress questionnaire (PSQ) reconsidered: validation and reference values from different clinical and healthy adult samples. Psychosom. Med. 67, 78–88. https://doi.org/10.1097/01.psy.0000151491.80178.78.
Fonov, V., Evans, A., McKinstry, R., Almli, C., Collins, D., 2009. Unbiased nonlinear average age-appropriate brain templates from birth to adulthood. Neuroimage 47, S102. https://doi.org/10.1016/S1053-8119(09)70884-5.
Ghandili, M., Munakomi, S., 2020. Neuroanatomy, Putamen. StatPearls Publishing.
Gilbertson, M.W., Shenton, M.E., Ciszewski, A., Kasai, K., Lasko, N.B., Orr, S.P., Pitman, R.K., 2002. Smaller hippocampal volume predicts pathologic vulnerability to psychological trauma. Nat. Neurosci. 5, 1242–1247. https://doi.org/10.1038/nn958.
Godoy, L.D., Rossignoli, M.T., Delfino-Pereira, P., Garcia-Cairasco, N., de Lima Umeoka, E.H., 2018. A comprehensive overview on stress neurobiology: basic concepts and clinical implications. Front. Behav. Neurosci. 12, 127. https://doi.org/10.3389/fnbeh.2018.00127.
Goldstein, D.S., Kopin, I.J., 2007. Evolution of concepts of stress. Stress 10, 109–120. https://doi.org/10.1080/10253890701288935.
Good, C.D., Johnsrude, I.S., Ashburner, J., Henson, R.N.A., Friston, K.J., Frackowiak, R.S. J., 2001. A voxel-based morphometric study of ageing in 465 normal adult human brains. Neuroimage 14, 21–36. https://doi.org/10.1006/nimg.2001.0786.
Good, C.D., Scahill, R.I., Fox, N.C., Ashburner, J., Friston, K.J., Chan, D., Crum, W.R., Rossor, M.N., Frackowiak, R.S.J., 2002. Automatic differentiation of anatomical patterns in the human brain: validation with studies of degenerative dementias. Neuroimage 17, 29–46. https://doi.org/10.1006/nimg.2002.1202.
Gorgolewski, K., Burns, C.D., Madison, C., Clark, D., Halchenko, Y.O., Waskom, M.L., Ghosh, S.S., 2011. Nipype: a flexible, lightweight and extensible neuroimaging data processing framework in Python. Front. Neuroinf. 5 https://doi.org/10.3389/fninf.2011.00013.
Gorgolewski, K.J., Esteban, O., Ellis, D.G., Notter, M.P., Ziegler, E., Johnson, H., Hamalainen, C., Yvernault, B., Burns, C., Manhães-Savio, A., Jarecka, D., Markiewicz, C.J., Salo, T., Clark, Daniel, Waskom, M., Wong, J., Modat, M., Dewey, B.E., Clark, M.G., Dayan, M., Loney, F., Madison, C., Gramfort, A., Keshavan, A., Berleant, S., Pinsard, B., Goncalves, M., Clark, Dav, Cipollini, B., Varoquaux, G., Wassermann, D., Rokem, A., Halchenko, Y.O., Forbes, J., Moloney, B., Malone, I.B., Hanke, M., Mordom, D., Buchanan, C., Pauli, W.M., Huntenburg, J.M., Horea, C., Schwartz, Y., Tungaraza, R., Iqbal, S., Kleesiek, J., Sikka, S., Frohlich, C., Kent, J., Perez-Guevara, M., Watanabe, A., Welch, D., Cumba, C., Ginsburg, D., Eshaghi, A., Kastman, E., Bougacha, S., Blair, R., Acland, B., Gillman, A., Schaefer, A., Nichols, B.N., Giavasis, S., Erickson, D., Correa, C., Ghayoor, A., Küttner, R., Haselgrove, C., Zhou, D., Craddock, R.C., Haehn, D., Lampe, L., Millman, J., Lai, J., Renfro, M., Liu, S., Stadler, J., Glatard, T., Kahn, A.E., Kong, X.-Z., Triplett, W., Park, A., McDermottroe, C., Hallquist, M., Poldrack, R., Perkins, L.N., Noel, M., Gerhard, S., Salvatore, J., Mertz, F., Broderick, W., Inati, S., Hinds, O., Brett, M., Durnez, J., Tambini, A., Rothmei, S., Andberg, S.K., Cooper, G., Marina, A., Mattfeld, A., Urchs, S., Sharp, P., Matsubara, K., Geisler, D., Cheung, B., Floren, A., Nickson, T., Pannetier, N., Weinstein, A., Dubois, M., Arias, J., Tarbert, C., Schlamp, K., Jordan, K., Liem, F., Saase, V., Harms, R., Khanuja, R., Podranski, K., Flandin, G., Papadopoulos Orfanos, D., Schwabacher, I., McNamee, D., Falkiewicz, M., Pellman, J., Linkersdörfer, J., Varada, J., Pérez-García, F., Davison, A., Shachnev, D., Ghosh, S., 2017. Nipype: a Flexible, Lightweight and Extensible Neuroimaging Data Processing Framework in Python. 0.13. 1 (Version 0.13. 1). Zenodo. Zenodo. Nipype: A Flexible, Lightweight And Extensible Neuroimaging Data Processing Framework In Python. 0.13.1.
Grimm, O., Pohlack, S., Cacciaglia, R., Winkelmann, T., Plichta, M.M., Demirakca, T., Flor, H., 2015. Amygdalar and hippocampal volume: a comparison between manual segmentation, Freesurfer and VBM. J. Neurosci. Methods 253, 254–261. https://doi.org/10.1016/j.jneumeth.2015.05.024.
Halford, C., Jonsdottir, I.H., Eek, F., 2012. Perceived stress, psychological resources and salivary cortisol. Bentham eBooks 67–86.
Hammen, C., 2005. Stress and depression. Annu. Rev. Clin. Psychol. 1, 293–319. https://doi.org/10.1146/annurev.clinpsy.1.102803.143938.
Henigsberg, N., Kalember, P., Petrović, Z.K., Šečić, A., 2019. Neuroimaging research in posttraumatic stress disorder – focus on amygdala, hippocampus and prefrontal cortex. Prog. Neuro Psychopharmacol. Biol. Psychiatr. 90, 37–42. https://doi.org/10.1016/j.pnpbp.2018.11.003.
Herringa, R., Phillips, M., Almeida, J., Insana, S., Germain, A., 2012. Post-traumatic stress symptoms correlate with smaller subgenual cingulate, caudate, and insula volumes in unmedicated combat veterans. Psychiatr. Res. Neuroimaging 203, 139–145. https://doi.org/10.1016/j.pscychresns.2012.02.005.
Holm, S., 1979. A simple sequentially rejective multiple test procedure. Scand. J. Stat. 6, 65–70.
Hölzel, B.K., Carmody, J., Evans, K.C., Hoge, E.A., Dusek, J.A., Morgan, L., Pitman, R.K., Lazar, S.W., 2010. Stress reduction correlates with structural changes in the amygdala. Soc. Cognit. Affect Neurosci. 5, 11–17. https://doi.org/10.1093/scan/nsp034.
Iglesias, J.E., Augustinack, J.C., Nguyen, K., Player, C.M., Player, A., Wright, M., Roy, N., Frosch, M.P., McKee, A.C., Wald, L.L., Fischl, B., Van Leemput, K., 2015. A computational atlas of the hippocampal formation using ex vivo , ultra-high resolution MRI: application to adaptive segmentation of in vivo MRI. Neuroimage 115, 117–137. https://doi.org/10.1016/j.neuroimage.2015.04.042.
Kalisch, R., Baker, D.G., Basten, U., Boks, M.P., Bonanno, G.A., Brummelman, E., Chmitorz, A., Fernàndez, G., Fiebach, C.J., Galatzer-Levy, I., Geuze, E., Groppa, S., Helmreich, I., Hendler, T., Hermans, E.J., Jovanovic, T., Kubiak, T., Lieb, K., Lutz, B., Müller, M.B., Murray, R.J., Nievergelt, C.M., Reif, A., Roelofs, K., Rutten, B.P.F., Sander, D., Schick, A., Tüscher, O., Diest, I.V., Harmelen, van, A.-L., Veer, I.M., Vermetten, E., Vinkers, C.H., Wager, T.D., Walter, H., Wessa, M., Wibral, M., Kleim, B., 2017. The resilience framework as a strategy to combat stress-related disorders. Nat. Human Behav. 1, 784–790. https://doi.org/10.1038/s41562-017-0200-8.
Karl, A., Schaefer, M., Malta, L., Dorfel, D., Rohleder, N., Werner, A., 2006. A meta-analysis of structural brain abnormalities in PTSD. Neurosci. Biobehav. Rev. 30, 1004–1031. https://doi.org/10.1016/j.neubiorev.2006.03.004.
Katuwal, G.J., Baum, S.A., Cahill, N.D., Dougherty, C.C., Evans, E., Evans, D.W., Moore, G.J., Michael, A.M., 2016. Inter-method discrepancies in brain volume estimation may drive inconsistent findings in autism. Front. Neurosci. 10 https://doi.org/10.3389/fnins.2016.00439.
Kendler, K.S., Karkowski, L.M., Prescott, C.A., 1999. Causal relationship between stressful life events and the onset of major depression. Aust. J. Pharm. 156, 837–841. https://doi.org/10.1176/ajp.156.6.837.
Kim, E.Y., Miklowitz, D.J., Biuckians, A., Mullen, K., 2007. Life stress and the course of early-onset bipolar disorder. J. Affect. Disord. 99, 37–44. https://doi.org/10.1016/j.jad.2006.08.022.
Kitayama, N., Vaccarino, V., Kutner, M., Weiss, P., Bremner, J.D., 2005. Magnetic resonance imaging (MRI) measurement of hippocampal volume in posttraumatic stress disorder: a meta-analysis. J. Affect. Disord. 88, 79–86. https://doi.org/10.1016/j.jad.2005.05.014.
Klaming, R., Spadoni, A.D., Veltman, D.J., Simmons, A.N., 2019. Expansion of hippocampal and amygdala shape in posttraumatic stress and early life stress. Neuroimage: Clinical 24, 101982. https://doi.org/10.1016/j.nicl.2019.101982.
Klein, A., Ghosh, S.S., Bao, F.S., Giard, J., Häme, Y., Stavsky, E., Lee, N., Rossa, B., Reuter, M., Chaibub Neto, E., Keshavan, A., 2017. Mindboggling morphometry of human brains. PLoS Comput. Biol. 13, e1005350 https://doi.org/10.1371/journal.pcbi.1005350.
Koolschijn, P.C.M.P., Crone, E.A., 2013. Sex differences and structural brain maturation from childhood to early adulthood. Dev. Cogn. Neurosci. 5, 106–118. https://doi.org/10.1016/j.dcn.2013.02.003.
Koshiyama, D., Fukunaga, M., Okada, N., Yamashita, F., Yamamori, H., Yasuda, Y., Fujimoto, M., Ohi, K., Fujino, H., Watanabe, Y., Kasai, K., Hashimoto, R., 2018. Role of subcortical structures on cognitive and social function in schizophrenia. Sci. Rep. 8, 1183. https://doi.org/10.1038/s41598-017-18950-2.
Kühn, S., Schubert, F., Gallinat, J., 2011. Structural correlates of trait anxiety: reduced thickness in medial orbitofrontal cortex accompanied by volume increase in nucleus accumbens. J. Affect. Disord. 134, 315–319. https://doi.org/10.1016/j.jad.2011.06.003.
Kuo, J.R., Kaloupek, D.G., Woodward, S.H., 2012. Amygdala volume in combat-exposed veterans with and without posttraumatic stress disorder: a cross-sectional study. Arch. Gen. Psychiatr. 69, 1080. https://doi.org/10.1001/archgenpsychiatry.2012.73.
Lanteaume, L., Khalfa, S., Regis, J., Marquis, P., Chauvel, P., Bartolomei, F., 2007. Emotion induction after direct intracerebral stimulations of human amygdala. Cerebr. Cortex 17, 1307–1313. https://doi.org/10.1093/cercor/bhl041.
Lau, W.K.W., Leung, M.K., Law, A.C.K., Lee, T.M.C., 2017. Moderating effects of cortisol on neural-cognitive association in cognitively normal elderly subjects. Front. Aging Neurosci. 9, 163. https://doi.org/10.3389/fnagi.2017.00163.

Lazarides, C., Ward, E.B., Buss, C., Chen, W.-P., Voelkle, M.C., Gillen, D.L., Wadhwa, P. D., Entringer, S., 2020. Psychological stress and cortisol during pregnancy: an ecological momentary assessment (EMA)-Based within- and between-person analysis. Psychoneuroendocrinology 121, 104848. https://doi.org/10.1016/j.psyneuen.2020.104848.

LeDoux, J.E., 2000. Emotion circuits in the brain. Annu. Rev. Neurosci. 23, 155–184. https://doi.org/10.1146/annurev.neuro.23.1.155.

Lee, E.-H., 2012. Review of the psychometric evidence of the perceived stress scale. Asian Nurs. Res. 6, 121–127. https://doi.org/10.1016/j.anr.2012.08.004.

Lee, K.H., Yoo, J.H., Lee, J., Kim, S.H., Han, J.Y., Hong, S.-B., Shin, J., Cho, S.-C., Kim, J.-W., Brent, D.A., 2020. The indirect effect of peer problems on adolescent depression through nucleus accumbens volume alteration. Sci. Rep. 10, 12870. https://doi.org/10.1038/s41598-020-69769-3.

Li, H., Li, W., Wei, D., Chen, Q., Jackson, T., Zhang, Q., Qiu, J., 2014. Examining brain structures associated with perceived stress in a large sample of young adults via voxel-based morphometry. Neuroimage 92, 1–7. https://doi.org/10.1016/j.neuroimage.2014.01.044.

Liston, C., McEwen, B.S., Casey, B.J., 2009. Psychosocial stress reversibly disrupts prefrontal processing and attentional control. Proc. Natl. Acad. Sci. Unit. States Am. 106, 912–917. https://doi.org/10.1073/pnas.0807041106.

Lucassen, P.J., Pruessner, J., Sousa, N., Almeida, O.F.X., Van Dam, A.M., Rajkowska, G., Swaab, D.F., Czéh, B., 2014. Neuropathology of stress. Acta Neuropathol. 127, 109–135. https://doi.org/10.1007/s00401-013-1223-5.

Magalhães, R., Barrière, D.A., Novais, A., Marques, F., Marques, P., Cerqueira, J., Sousa, J.C., Cachia, A., Boumezbeur, F., Bottlaender, M., Jay, T.M., Mériaux, S., Sousa, N., 2018. The dynamics of stress: a longitudinal MRI study of rat brain structure and connectome. Mol. Psychiatr. 23, 1998–2006. https://doi.org/10.1038/mp.2017.244.

Markowitsch, H.J., 1999. Differential contribution of right and left amygdala to affective information processing. Behav. Neurol. 11, 233–244. https://doi.org/10.1155/1999/180434.

Melchior, M., Caspi, A., Milne, B.J., Danese, A., Poulton, R., Moffitt, T.E., 2007. Work stress precipitates depression and anxiety in young, working women and men. Psychol. Med. 37, 1119–1129. https://doi.org/10.1017/S0033291707000414.

Menzler, K., Belke, M., Wehrmann, E., Krakow, K., Lengler, U., Jansen, A., Hamer, H.M., Oertel, W.H., Rosenow, F., Knake, S., 2011. Men and women are different: diffusion tensor imaging reveals sexual dimorphism in the microstructure of the thalamus, corpus callosum and cingulum. Neuroimage 54, 2557–2562. https://doi.org/10.1016/j.neuroimage.2010.11.029.

Merz, E.C., Desai, P.M., Maskus, E.A., Melvin, S.A., Rehman, R., Torres, S.D., Meyer, J., He, X., Noble, K.G., 2019. Socioeconomic disparities in chronic physiologic stress are associated with brain structure in children. Biol. Psychiatr. 86, 921–929. https://doi.org/10.1016/j.biopsych.2019.05.024.

Moreno, G.L., Bruss, J., Natalie, L.D., 2017. Increased perceived stress is related to decreased prefrontal cortex volumes among older adults. J. Clin. Exp. Neuropsychol. 313–325. https://doi.org/10.1080/13803395.2016.1225006.

Morey, R.A., Gold, A.L., LaBar, K.S., Beall, S.K., Brown, V.M., Haswell, C.C., Nasser, J.D., Wagner, H.R., McCarthy, G., Mid-Atlantic MIRECC Workgroup, for the, 2012. Amygdala volume changes in posttraumatic stress disorder in a large case-controlled veterans group. Arch. Gen. Psychiatr. 69, 1169. https://doi.org/10.1001/archgenpsychiatry.2012.50.

Morey, R.A., Haswell, C.C., Hooper, S.R., De Bellis, M.D., 2016. Amygdala, Hippocampus, and ventral medial prefrontal cortex volumes differ in maltreated youth with and without chronic posttraumatic stress disorder. Neuropsychopharmacology 41, 791–801. https://doi.org/10.1038/npp.2015.205.

Novais, A., Monteiro, S., Roque, S., Correia-Neves, M., Sousa, N., 2017. How age, sex and genotype shape the stress response. Neurobiol. Stress 6, 44–56. https://doi.org/10.1016/j.ynstr.2016.11.004.

Piccolo, L.R., Noble, K.G., 2018. Perceived stress is associated with smaller hippocampal volume in adolescence. Psychophysiology 55, e13025. https://doi.org/10.1111/psyp.13025.

Pinto, V., Costa, J.C., Morgado, P., Mota, C., Miranda, A., Bravo, F.V., Oliveira, T.G., Cerqueira, J.J., Sousa, N., 2015. Differential impact of chronic stress along the hippocampal dorsal–ventral axis. Brain Struct. Funct. 220, 1205–1212. https://doi.org/10.1007/s00429-014-0713-0.

Popescu, V., Schoonheim, M.M., Versteeg, A., Chaturvedi, N., Jonker, M., Xavier de Menezes, R., Gallindo Garre, F., Uitdehaag, B.M.J., Barkhof, F., Vrenken, H., 2016. Grey matter atrophy in multiple sclerosis: clinical interpretation depends on choice of analysis method. PloS One 11, e0143942. https://doi.org/10.1371/journal.pone.0143942.

Rajagopalan, V., Pioro, E.P., 2015. Disparate voxel based morphometry (VBM) results between SPM and FSL softwares in ALS patients with frontotemporal dementia: which VBM results to consider? BMC Neurol. 15, 32. https://doi.org/10.1186/s12883-015-0274-8.

Savic, I., Perski, A., Osika, W., 2018. MRI shows that exhaustion syndrome due to chronic occupational stress is associated with partially reversible cerebral changes. Cerebr. Cortex 28, 894–906. https://doi.org/10.1093/cercor/bhw413.

Schienle, A., Ebner, F., Schäfer, A., 2011. Localized gray matter volume abnormalities in generalized anxiety disorder. Eur. Arch. Psychiatr. Clin. Neurosci. 261, 303–307. https://doi.org/10.1007/s00406-010-0147-5.

Selye, H., 1956. The Stress of Life.

Smith, S.M., Jenkinson, M., Woolrich, M.W., Beckmann, C.F., Behrens, T.E.J., Johansen-Berg, H., Bannister, P.R., De Luca, M., Drobnjak, I., Flitney, D.E., Niazy, R.K., Saunders, J., Vickers, J., Zhang, Y., De Stefano, N., Brady, J.M., Matthews, P.M., 2004. Advances in functional and structural MR image analysis and implementation as FSL. Neuroimage 23, S208–S219. https://doi.org/10.1016/j.neuroimage.2004.07.051.

Soares, J.M., Sampaio, A., Ferreira, L.M., Santos, N.C., Marques, F., Palha, J.A., Cerqueira, J.J., Sousa, N., 2012. Stress-induced changes in human decision-making are reversible. Transl. Psychiatry 2. https://doi.org/10.1038/tp.2012.59 e131–e131.

Sousa, N., 2016. The dynamics of the stress neuromatrix. Mol. Psychiatr. 21, 302–312. https://doi.org/10.1038/mp.2015.196.

Strange, B.A., Witter, M.P., Lein, E.S., Moser, E.I., 2014. Functional organization of the hippocampal longitudinal axis. Nat. Rev. Neurosci. 15, 655–669. https://doi.org/10.1038/nrn3785.

Taren, A.A., Creswell, J.D., Gianaros, P.J., 2013. Dispositional mindfulness Co-varies with smaller amygdala and caudate volumes in community adults. PloS One 8, e64574. https://doi.org/10.1371/journal.pone.0064574.

Trigo, M., Canudo, N., Branco, F., Silva, D., 2010. Estudo das propriedades psicométricas da Perceived Stress Scale (PSS) na população portuguesa. Psychologica 353–378. https://doi.org/10.14195/1647-8606_53_17.

Tustison, N.J., Avants, B.B., Cook, P.A., Zheng, Yuanjie, Egan, A., Yushkevich, P.A., Gee, J.C., 2010. N4ITK: improved N3 bias correction. IEEE Trans. Med. Imag. 29, 1310–1320. https://doi.org/10.1109/TMI.2010.2046908.

Vriend, C., Boedhoe, P.S., Rutten, S., Berendse, H.W., van der Werf, Y.D., van den Heuvel, O.A., 2016. A smaller amygdala is associated with anxiety in Parkinson's disease: a combined FreeSurfer—VBM study. J. Neurol. Neurosurg. Psychiatry 87, 493–500. https://doi.org/10.1136/jnnp-2015-310383.

Walker, E., Mittal, V., Tessner, K., 2008. Stress and the hypothalamic pituitary adrenal Axis in the developmental course of schizophrenia. Annu. Rev. Clin. Psychol. 4, 189–216. https://doi.org/10.1146/annurev.clinpsy.4.022007.141248.

Welberg, L., 2014. A REDD line from stress to depression. Nat. Rev. Neurosci. 15 https://doi.org/10.1038/nrn3749, 350–350.

Wu, J., Tong, H., Liu, Z., Tao, J., Chen, L., Chan, C.C.H., Lee, T.M.C., 2020. Neurobiological effects of perceived stress are different between adolescents and middle-aged adults. Brain Imag. Behav. https://doi.org/10.1007/s11682-020-00294-7.

Zhang, X., Zhang, J., Wang, L., Zhang, W., 2018. Altered gray matter volume and its correlation with PTSD severity in Chinese earthquake survivors. Front. Psychiatr. 9, 9. https://doi.org/10.3389/fpsyt.2018.00629.

Zhang, Y., Brady, M., Smith, S., 2001. Segmentation of brain MR images through a hidden Markov random field model and the expectation-maximization algorithm. IEEE Trans. Med. Imag. 20, 45–57. https://doi.org/10.1109/42.906424.

Zimmerman, M.E., Ezzati, A., Katz, M.J., Lipton, M.L., Brickman, A.M., Sliwinski, M.J., Lipton, R.B., 2016. Perceived stress is differentially related to hippocampal subfield volumes among older adults. PloS One 11, e0154530. https://doi.org/10.1371/journal.pone.0154530.

1. Supplementary material

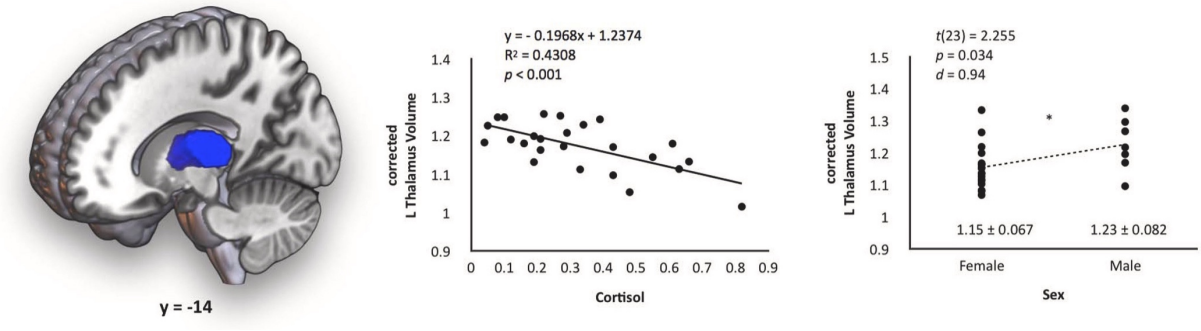

Fig. A.1. Representation of the multilinear model resulted from left thalamus regression with cortisol. A statistically significant association between left thalamus volumes and both cortisol (negative) and sex (positive) independent terms was observed, even after correction for multiple comparisons. Note that the direction of the sex association is only related to the way sex covariate was codified (females as 0 and males as 1). Therefore, the positive association between left thalamus volumes and sex indicates that being a male positively contribute to having a bigger volume of left thalamus, and, in contrast, being a female contribute to having smaller left thalamus volume. On left, representation of the *10_L Thalamus* cluster from FreeSurfer subcortical regions labeling. In the middle, graphical representation of the model with cortisol measurements as the independent variable and left thalamus volumes, corrected for age and sex covariates, as dependent variable; the equation represents the correlation between cortisol measurements and corrected thalamus volumes, where statistical significance is observed. On the right, a graphical representation of the model with sex as the independent factor and left thalamus volumes, corrected for age and cortisol measurements, as the dependent variable; herein an independent-sample t-test indicates that left thalamus volumes are significantly higher for males than for females (on graph, mean volumes ± standard deviation for each level are presented).
Brain volumes were computed using FreeSurfer subcortical output and corrected for individual GM. To avoid a large number of decimal digits, corrected volumes were multiplied by 100. Multilinear regression models with ROI volumes as dependent variable and cortisol measurements, age, and sex as independent terms were established. The models were computed using the *regstats* function in *MATLAB* and the Bonferroni-Holm correction for 14 multiple comparisons was used to calculate the corrected *p*-values. Statistical significance was established for $\alpha = 0.05$.

Table A.1. Descriptive statistics of subcortical volumes obtain through FreeSurfer. Brain volumes were computed using FreeSurfer subcortical output (*aseg.stats*), and corrected for individual GM to best replicate the FSL-VBM pipeline. To avoid using further decimal digits, corrected volumes were multiplied by 100.

	Volumes (mm^3)		**Volumes/GM**	
Subcortical ROI	Mean	Standard Deviation	Mean	Standard Deviation
10_L Thalamus-Proper	7759	904	1.173	0.073
49_R Thalamus-Proper	7413	797	1.121	0.061
11_L Caudate	3725	490	0.564	0.059
50_R Caudate	3842	506	0.582	0.057
12_L Putamen	5015	501	0.760	0.061
51_R Putamen	5017	527	0.760	0.061
13_L Pallidum	1985	236	0.301	0.028
52_R Pallidum	1924	241	0.291	0.027
17_L Hippocampus	3978	475	0.602	0.046
53_R Hippocampus	4048	466	0.613	0.048
18_L Amygdala	1404	208	0.212	0.023
54_R Amygdala	1497	258	0.226	0.029
26_L Accumbens-area	625	91	0.095	0.014
58_R Accumbens-area	572	82	0.087	0.012
General Volumes				
eTIV	1.59×10^6	1.51×10^5		
GM	6.61×10^5	5.50×10^4		
WM	4.68×10^5	5.89×10^4		

VBM. Voxel-based-morphometry; ROI. Region-of-interest; eTIV. Estimated Intracranial Volume; GM. Gray matter; WM. White matter; R. Right; L. Left.

Table A.2. Results from FreeSurfer subcortical volumetric regression with PSS. A statistically significant positive association between PSS and right amygdala volume is observed, even when correcting for multiple comparisons. Positive associations between PSS and right pallidum, right hippocampus, left amygdala and right accumbens-area did not survive multiple comparison correction.
Brain volumes were computed using FreeSurfer subcortical output (*aseg.stats*) and corrected for individual GM to best replicate the FSL-VBM regression analysis. To avoid using further decimal digits, corrected volumes were multiplied by 100. Multilinear regression models with ROI volumes as dependent variables and PSS, age, and sex as independent variables were established. The models were computed using the function *regstats* in *MATLAB* and the Bonferroni-Holm correction for 14 multiple comparisons was used to calculate the corrected *p*-values. For easy interpretation, *p*- and corrected *p*-values statistically significant are presented in bold, as the respective ROI description and effect size when significance is observed in PSS independent term. Statistical significance was established for $\alpha = 0.05$.

	MULTILINEAR REGRESSION										
	PSS			Age			Sex			Model Effect size	
ROI	*p*-value	Corrected *p*-value	Slope (β)	*p*-value	Corrected *p*-value	Slope (β)	*p*-value	Corrected *p*-value	Slope (β)	R^2	Adjusted R^2
Subcortical											
10_L Thalamus-Proper	0.181	1.432	0.0020	0.728	2.006	0.0020	**0.049**	0.680	0.0230	0.113	0.054
49_R Thalamus-Proper	0.630	2.520	0.0006	0.470	2.822	0.0035	0.120	1.558	0.0152	0.071	0.010
11_L Caudate	0.965	1.604	0.0001	0.549	2.822	0.0029	0.888	1.369	0.0014	0.008	0.056
50_R Caudate	0.283	1.697	0.0012	0.641	2.743	0.0020	0.518	4.207	0.0056	0.032	0.033
12_L Putamen	0.381	1.907	0.0011	0.174	1.389	0.0068	0.590	3.686	0.0052	0.064	0.003
51_R Putamen	0.756	2.520	0.0004	0.120	1.436	0.0078	0.666	3.538	0.0043	0.063	0.001
13_L Pallidum	0.802	2.267	0.0001	0.105	1.366	0.0036	0.467	4.386	0.0031	0.075	0.014
52_R Pallidum	**0.025**	0.271	0.0012	0.143	1.417	0.0030	0.168	2.021	0.0056	**0.180**	**0.126**
17_L Hippocampus	0.093	0.838	0.0015	0.933	1.457	0.0003	0.679	2.706	0.0029	0.071	0.009
53_R Hippocampus	**0.021**	0.248	0.0021	0.126	1.436	0.0053	0.409	4.498	0.0057	**0.184**	**0.130**
18_L Amygdala	**0.013**	0.163	0.0011	0.343	2.401	0.0017	0.684	2.038	0.0014	**0.156**	**0.100**
54_R Amygdala	**< 0.001**	**< 0.001**	0.0022	0.142	1.417	0.0027	0.527	4.140	0.0023	**0.382**	**0.341**
26_L Accumbens-area	0.179	1.432	0.0003	**0.026**	0.363	0.0023	0.439	4.498	0.0015	0.130	0.072
58_R Accumbens-area	**0.033**	0.326	0.0004	0.669	2.565	0.0003	0.676	3.331	0.0007	**0.111**	**0.051**

VBM. Voxel-based-morphometry; ROI. Region-of-interest; R. Right; L. Left.

Table A.3. Results from FreeSurfer hippocampal subfields association with PSS. A statistically significant positive association between PSS and right anterior hippocampus is observed. No statistically significant association is observed between the right posterior hippocampus and PSS scores.
After the FreeSurfer segmentation (*aseg.stats*), the hippocampal segmentation was made (*hipposubfields.rh.T1.v21.stats*) and the subfields grouped into anterior hippocampus (head) and posterior hippocampus (body and tail). Individual correction for GM volumes was made, and corrected volumes were multiplied by 100 to avoid using further decimal digits. Multilinear regression models with ROI volumes as dependent variables and PSS, age, and sex as independent variables were established. The models were computed using the function *regstats* in *MATLAB* and the Bonferroni-Holm correction for 2 multiple comparisons was used to calculate the corrected *p*-values. For easy interpretation, *p*- and corrected *p*-values statistically significant are presented in bold, as the respective region and effect size, when significance is observed in PSS independent term. Statistical significance was established for $\alpha = 0.05$.

	MULTILINEAR REGRESSION										
	PSS			**Age**			**Sex**			**Model Effect size**	
ROI	***p*-value**	**Corrected *p*-value**	**Slope (β)**	***p*-value**	**Corrected *p*-value**	**Slope (β)**	***p*-value**	**Corrected *p*-value**	**Slope (β)**	**R^2**	**Adjusted R^2**
R Hippocampus											
Anterior	**0.012**	**0.023**	0.0011	0.075	0.075	0.0031	0.379	0.757	-0.0060	**0.219**	**0.166**
Posterior	0.287	0.287	0.0004	**0.025**	**0.049**	0.0038	0.422	0.757	-0.0052	0.147	0.090

VBM. Voxel-based-morphometry; ROI. Region-of-interest; R. Right; L. Left.

Table A.4. Models resulted from the volumetric regression with cortisol measurements. Multilinear regression models with ROI volumes as dependent variable and cortisol measurements, age, and sex as independent variables were established. A statistically significant negative association between cortisol and left thalamus is observed, as well as a significant positive association between sex and the left thalamus volumes. Note that the direction of the sex association is only related to the way sex covariate was codified (females as 0 and males as 1). Therefore, the positive association between left thalamus volumes and sex indicates that being a male positively contribute for having a bigger volume of left thalamus, and, in contrast, being a female contribute for having smaller left thalamus volume. A similar trait in the right thalamus did not survive to multiple comparisons, such as the associations between age and bilateral putamen, and between sex and right pallidum. The negative value of the adjusted R^2 of left caudate, bilateral hippocampus, and bilateral amygdala indicates that the multilinear models are not appropriate for the data.
Brain volumes were computed using FreeSurfer subcortical output (*aseg.stats*) and corrected for individual GM and multiplied by 100. The models were computed using the function *regstats* in *MATLAB* and the Bonferroni-Holm correction for 14 multiple comparisons was used to calculate the corrected *p*-values. For easy interpretation, *p*- and corrected *p*-values statistically significant are presented in bold, as the respective ROI description and model's effect sizes when significance is observed in cortisol independent term. Statistical significance was established for $\alpha = 0.05$.

	MULTILINEAR REGRESSION										
	Cortisol			**Age**			**Sex**			**Model Effect size**	
ROI	***p*-value**	**Corrected *p*-value**	**Slope (β)**	***p*-value**	**Corrected *p*-value**	**Slope (β)**	***p*-value**	**Corrected *p*-value**	**Slope (β)**	**R^2**	**Adjusted R^2 ***
Subcortical											
10_L Thalamus-Proper	**0.0016**	**0.0221**	-0.1961	0.4494	2.6963	-0.0065	**< 0.0001**	**0.0005**	0.1347	**0.599**	**0.542**
49_R Thalamus-Proper	**0.0065**	0.0844	-0.1770	0.9404	1.1632	-0.0007	**0.0102**	0.1320	0.0790	0.388	0.301
11_L Caudate	0.9227	1.8367	-0.0068	0.5740	2.0783	0.0062	0.8614	3.3306	-0.0058	0.017	-0.123
50_R Caudate	0.1672	1.8395	-0.0777	0.5196	2.5157	0.0055	0.5066	2.5330	-0.0176	0.156	0.030
12_L Putamen	0.1814	1.7403	-0.0857	**0.0488**	0.6346	0.0204	0.2957	2.0699	0.0318	0.307	0.208
51_R Putamen	0.3259	1.9552	-0.0648	**0.0246**	0.3445	0.0245	0.3449	2.0699	0.0297	0.326	0.229
13_L Pallidum	0.2092	1.5046	-0.0298	0.2419	2.0660	0.0044	0.1220	1.2197	0.0177	0.242	0.134
52_R Pallidum	0.1740	1.8395	-0.0363	0.5816	1.7220	0.0023	**0.0172**	0.2063	0.0319	0.306	0.207
17_L Hippocampus	0.8942	4.2712	-0.0068	0.2296	2.0660	0.0096	0.8915	2.5843	0.0034	0.081	-0.056
53_R Hippocampus	0.9183	2.7069	-0.0056	0.1945	1.9449	0.0112	0.9739	1.7831	-0.0009	0.088	-0.049
18_L Amygdala	0.8542	4.2712	-0.0051	0.1226	1.4708	0.0070	0.8327	3.3306	-0.0028	0.119	-0.006
54_R Amygdala	0.9023	3.5767	-0.0043	0.5031	2.6963	0.0037	0.2502	2.0013	0.0194	0.119	-0.007
26_L Accumbens-area	0.0860	1.0323	-0.0196	0.3043	2.1299	0.0018	0.1076	1.1835	0.0087	0.264	0.159
58_R Accumbens-area	0.1881	1.6330	-0.0144	0.1550	1.7053	-0.0025	0.1786	1.6071	0.0070	0.152	0.031

*VBM. Voxel-based-morphometry; ROI. Region-of-interest; R. Right; L. Left; * A negative R^2 statistic indicates that the model is not appropriate for the data.*

CHAPTER III

Association of amygdala size with stress perception: findings of a transversal study across the lifespan

Inês Caetano, Liliana Amorim, Teresa Costa Castanho, Ana Coelho, Sónia Ferreira, Carlos Portugal-Nunes, José Miguel Soares, Nuno Gonçalves, Rui Sousa, Joana Reis, Catarina Lima, Paulo Marques, Pedro Silva Moreira, Ana João Rodrigues, Nadine Correia Santos, Pedro Morgado, Madalena Esteves, Ricardo Magalhães, Maria Picó-Pérez, Nuno Sousa

Manuscript submitted for publication

Association of amygdala size with stress perception: findings of a transversal study across the lifespan.

Inês Caetano[a,b,c], Liliana Amorim[a,b,c,d], Teresa Costa Castanho[a,b,c,d], Ana Coelho[a,b,c], Sónia Ferreira[a,b,c], Carlos Portugal-Nunes[a,b,c,e], José Miguel Soares[a,b,c], Nuno Gonçalves[a,b,c], Rui Sousa[a,b,c,f], Joana Reis[a,b,c], Catarina Lima[a,b,c], Paulo Marques[a,b,c], Pedro Silva Moreira[a,b,c], Ana João Rodrigues[a,b,c], Nadine Correia Santos[a,b,c], Pedro Morgado[a,b,c], Madalena Esteves[a,b,c], Ricardo Magalhães[a,b,c], Maria Picó-Pérez[a,b,c], Nuno Sousa[a,b,c,d]

[a]Life and Health Sciences Research Institute (ICVS), School of Medicine, University of Minho, 4710-057 Braga, Portugal; [b]ICVS/3B's, PT Government Associate Laboratory, 4710-057 Braga/Guimarães, Portugal; [c]Clinical Academic Center – Braga (2CA), 4710-243 Braga, Portugal; [d]Association P5 Digital Medical Center (ACMP5), 4710-057 Braga, Portugal; [e]CECAV - Veterinary and Animal Science Research Centre, Quinta de Prados, 5000-801 Vila Real, Portugal; [f]Departamento de Psiquiatria e Saúde Mental, Centro Hospitalar Tondela-Viseu, 3500-228 Viseu, Portugal.

1. Abstract

As modern civilizations advance, daily routines are getting increasingly stressful. Interestingly, associations between stress perception and amygdala volume, a brain region implicated in emotional behavior, have been observed both in adult and older cohorts. Life stress, on the other hand, has become pervasive and is no longer restricted to a specific age group or life stage. As a result, it is vital to consider stress as a continuum across the lifespan. In this study, we investigated the relationship between perceived stress and amygdala size in 272 non-pathological participants with a broad age range. Participants were submitted to a structural magnetic resonance imaging (MRI) to extract amygdala volume, and we used the scores of the Perceived Stress Scale (PSS) as the independent variable in volumetric regressions. We found that perceived stress is positively associated with the right amygdala volume throughout life.

Keywords: Psychophysiology, Perceived stress, Amygdala, Volumetry, Healthy subjects, Stress appraisal, MRI

2. Introduction

Several changes have marked human history. From the first small communities in which our ancestors lived to the modern societies of the present times, an entirely new way to live, work and interact with others has emerged (Ritchie & Roser, 2018). This shift triggered new challenges for mental health (Lederbogen et al., 2018; Ritchie & Roser, 2018; Szabo, 2018). While the increased tendency of urbanization has beneficial protective effects, such as access to healthcare and resources, on the other hand, the highly demanded social interactions, the social fragmentation, the economics, and the professional aspects are critical risk factors for psychological wellbeing (Everaerd et al., 2020; Fett, Lemmers-Jansen, & Krabbendam, 2019; Gong, Palmer, Gallacher, Marsden, & Fone, 2016). In fact, the increased awareness of the relevance of this topic has led to the discovery of the impact that psychosocial stress has on the brain (Cerqueira, Almeida, & Sousa, 2008; Koenig, Walker, Romeo, & Lupien, 2011; Lucassen et al., 2014; Magalhães et al., 2018; Novais, Monteiro, Roque, Correia-Neves, & Sousa, 2017; Soares et al., 2012; Soares, Sampaio, Ferreira, et al., 2013; Sousa, 2016), but also of new resilience strategies to successfully cope with stress (Gotink, Meijboom, Vernooij, Smits, & Hunink, 2016; Gotink et al., 2018; Kalisch et al., 2017). Interestingly, particular life stages seem to be more associated with specific stressors, meaning that, besides individual susceptibility (Novais et al., 2017; Sousa, 2016), the subject's response is conditioned by the stage of life in which the stressor occurs (Koenig et al., 2011). Indeed, there is an inherent link between stress and age (Aldwin, 2010; Kalisch et al., 2017; Lucassen et al., 2014; Sousa, 2016).

The way stress changes throughout life is intrinsically related to how stress is defined (Aldwin, 2010). The stressor, varying in type, time, recurrence, and intensity (Sousa, 2016), triggers a variable response on the subject that can be partially measured (Caetano et al., 2021). Notably, a stressor encompasses real quantifiable components, like duration, and subjective dimensions, as the individual quantification of stress intensity (Sousa, 2016). Importantly, this subjective perception of stress (Godoy, Rossignoli, Delfino-Pereira, Garcia-Cairasco, & de Lima Umeoka, 2018; Novais et al., 2017) is closely related to mental health, with studies showing a consistent association between chronic psychosocial stress and the Perceived Stress Scale (PSS) (Cohen, Kamarck, & Mermelstein, 1983; Fliege et al., 2005; Liston, McEwen, & Casey, 2009; Soares et al., 2012; Trigo, Canudo, Branco, & Silva, 2010). On the contrary, endocrine parameters, such as cortisol levels, besides being involved in several biological processes, usually reflect a response to acute events, conditioning its use as surrogate markers of longitudinal processes (Caetano et al., 2021; Canbolat, Erbay, Şenol, Uçar, & Yıldız, 2021; Chida & Steptoe, 2009;

Halford, Jonsdottir, & Eek, 2012; Kronenberg et al., 2009). Indeed, it is this difference in temporal dynamics that makes the PSS of great physiological relevance, namely when considering the number of studies showing that the way subjects integrate stress correlates with brain morphometry (Caetano et al., 2021; Goldstein & Kopin, 2007; Hölzel et al., 2010; Li et al., 2014).

There are also relevant clinical aspects that justify examining the impact of prolonged stress on brain morphometry. Chronic stress is a significant precursor for the development of pathological conditions such as anxiety (Melchior et al., 2007; Pêgo, Sousa, Almeida, & Sousa, 2009; Shin & Liberzon, 2010), major depression (Hammen, 2005; Kendler, Karkowski, & Prescott, 1999; Melchior et al., 2007; Welberg, 2014), schizophrenia (Betensky et al., 2008; Gispen-de Wied, 2000; Walker, Mittal, & Tessner, 2008), bipolar (Carvalho, Firth, & Vieta, 2020; Kim, Miklowitz, Biuckians, & Mullen, 2007), and post-traumatic stress disorders (Brewin, Andrews, & Valentine, 2000; Bryant, 2019; Davidson, Hughes, Blazer, & George, 1991). Despite having common precipitating factors, each pathology has distinct morphological variations in specific regions (De Bellis et al., 2000; Herringa, Phillips, Almeida, Insana, & Germain, 2012; Morey et al., 2012; Schienle, Ebner, & Schäfer, 2011) which are known to be conditioned by the patient's age and stage of disease (McKinnon, Yucel, Nazarov, & MacQueen, 2009; Schuhmacher et al., 2012). Therefore, unveiling how the brain is affected prior to disease is the best of value, particularly if considering the way the brain changes across the lifespan (Potvin, Dieumegarde, & Duchesne, 2017; Potvin, Mouiha, Dieumegarde, & Duchesne, 2016; Sousa, 2016; van der Plas, Boes, Wemmie, Tranel, & Nopoulos, 2010; Zhao et al., 2019).

In a previous study, we have shown how subcortical regions are associated with stress perception (Caetano et al., 2021). Although our findings were in line with those reported by others (Hölzel et al., 2010; Lanteaume et al., 2007; Taren, Creswell, & Gianaros, 2013), we only looked at a specific age range (young adults) in which a positive association between the right amygdala volume and perceived stress was found. Herein, using a cohort of different ages, we aimed to uphold our previous conclusions across the lifespan.

3. Material and Methods

3.1. Ethics Statement

This study was conducted in accordance with the principles expressed in the Declaration of Helsinki (59th amendment) and was approved by the national and local ethics review board committees (*Comissão Nacional de Protecção de Dados*, *Comissão de Ética para a Saúde of Hospital de Braga*, and *Subcomissão de ética para as ciências da vida e da saúde* from University of Minho).

The aims of the study were explained to all participants, which signed informed consent. Additionally, parents of participants under the age of 18 years also signed informed consent.

3.2. Participants and study design

This study enrolled 272 participants. Being a healthy individual and having the capability to perform an MRI session were the primary inclusion criteria. The exclusion criteria consisted of the non-acceptance or inability to understand the informed consent, the individual choice to withdraw from the study, the presence of any comorbidity from the central nervous system, or the diagnose of any neuropsychiatric disorder.

The protocol of this study consisted of a single-moment evaluation. Participants were characterized in terms of age and sex, and completed the 10-item Perceived Stress Scale (PSS10) (Trigo et al., 2010). Reporting to the previous month, the PSS10 is a well-validated self-administered Likert instrument used to quantify prolonged psychosocial stress (Cohen et al., 1983; Fliege et al., 2005; Liston et al., 2009; Soares et al., 2012). Moreover, subjects underwent a structural MRI acquisition.

The anatomical images of participants were segmented using FreeSurfer (region of interest [ROI]-based analysis). Then, volumetric regressions between PSS10 scores and amygdala volume were performed to explore the association between amygdala size and psychological stress.

3.3. Participants characterization

Participants' demographic and psychological characterization was made using SPSS version 23 (IBM, SPSS, Chicago, IL, USA). Normality was tested for each variable, and non-parametric tests were used when the assumption was not met. To better characterize the cohort, between-group comparisons (factor sex) and correlations between PSS10 scores and the continuous variables (age, total gray matter [GM],

and estimated total intracranial volume [eTIV]) were made. The statistical significance was established for $\alpha = 0.05$.

3.4. MRI data acquisition

MRI acquisitions were made at the Hospital of Braga (Braga, Portugal), using a clinical approved Siemens Magnetom Avanto 1.5 T scanner (Siemens Medical Solutions, Erlangen, Germany), with a 12-channel receive-only head coil. The anatomical acquisition consisted of one high-resolution T1-weighted (T1w) Magnetization-Prepared Rapid Acquisition with Gradient Echo (MPRAGE) sequence, with voxel size = 1 mm × 1 mm × 1 mm, repetition time (TR) = 2.73 s, echo time (TE) = 3.48 ms, flip angle = 7°, field of view (FoV) = 234 mm × 234 mm and 176 slices with no gap.

After the acquisition, all images were inspected by a certified neuro-radiologist to confirm that the scans were not critically affected by head motion and that participants had no pathologies or brain lesions.

3.5. MRI data preprocessing

Preprocessing was performed using *fMRIPrep* 1.4.1 (Esteban et al., 2018, 2021) (RRID:SCR_016216), which is based on *Nipype* 1.2.0 (Esteban et al., 2020; Gorgolewski et al., 2011) (RRID:SCR_002502).

The T1w image was corrected for intensity non-uniformity (INU) with N4BiasFieldCorrection (Tustison et al., 2010), distributed with ANTs 2.2.0 (Avants, Epstein, Grossman, & Gee, 2008) (RRID:SCR_004757), and used as T1w-reference throughout the workflow. The T1w-reference was then skull-stripped with a *Nipype* implementation of the antsBrainExtraction.sh workflow (from ANTs), using OASIS30ANTs as target template. Brain tissue segmentation of cerebrospinal fluid (CSF), white matter (WM) and GM was performed on the brain-extracted T1w using fast (FSL 5.0.9, RRID:SCR_002823) (Y. Zhang, Brady, & Smith, 2001). Brain surfaces were reconstructed using recon-all (FreeSurfer 6.0.1, RRID:SCR_001847) (Dale, Fischl, & Sereno, 1999), and the brain mask estimated previously was refined with a custom variation of the method to reconcile ANTs-derived and FreeSurfer-derived segmentations of the cortical gray-matter of Mindboggle (RRID:SCR_002438) (Klein et al., 2017). Volume-based spatial normalization to two standard spaces (MNI152NLin2009cAsym, MNI152NLin6Asym) was performed through nonlinear registration with antsRegistration (ANTs 2.2.0), using brain-extracted versions of both T1w reference and the T1w template. The following templates were selected for spatial normalization: *ICBM 152 Nonlinear Asymmetrical template version 2009c* [(Fonov, Evans, McKinstry, Almli, & Collins, 2009),

RRID:SCR_008796; TemplateFlow ID: MNI152NLin2009cAsym], *FSL's MNI ICBM 152 non-linear 6th Generation Asymmetric Average Brain Stereotaxic Registration Model* [(Evans, Janke, Collins, & Baillet, 2012), RRID:SCR_002823; TemplateFlow ID: MNI152NLin6Asym].

3.6. ROI segmentation and volume estimation

Right and left amygdala volumes were obtained using the automatic subcortical segmentation (Fischl et al., 2002). In addition, all other subcortical and cortical regions (Desikan et al., 2006) were extracted as part of the cohort volumetric brain characterization. Subjects' individual total GM was also collected to correct for individual head size and brain atrophy. All the volumes were computed during *fMRIPrep* preprocessing steps and made automatically available in the Freesurfer derivative folder.

The FreeSurfer pipeline (Fischl, 2012) (http://surfer.nmr.mgh.harvard.edu) follows 31 processing steps that include motion correction, Talairach standard space normalization, intensity normalization, skull stripping, and tissue segmentation of WM, cortical, and subcortical regions. In the execution of *fMRIPrep*, FreeSurfer processing steps are aggregated in 3 phases. First, a T1w structural image is initialized, and a basic reconstruction is performed using the *autorecon1* (first 5 preprocessing steps of *recon-all* (Dale et al., 1999), excluding the skull-stripping step 5). Then, a brain mask computed before in the *fMRIPrep* pipeline (using *antsBrainExtraction.sh*) is moved to a specific FreeSurfer directory to replace the mask of the skull-stripping step that was not performed. This brain mask is refined using the FreeSurfer's internal segmentation mask *aseg.mgz*, reconciling ANTs-derived and FreeSurfer-derived segmentation of the cortical GM of Mindboggle (Klein et al., 2017). Lastly, the *recon-all* execution (*autorecon2* and *autorecon3*) is resumed, with FreeSurfer workflow being divided into sub-stages to increase the efficient use of resources.

3.7. Volumetric regression

Due to the differences in magnitudes, all the variables were standardized. Then, a multilinear regression model with right or left amygdala volume as the dependent variable, and perceived stress (measured by PSS10), age, sex, and individual total GM as independent variables was defined. Herein, age, sex, and total GM were used as non-explanatory variables.

The volumetric regressions were conducted in SPSS version 23 (IBM, SPSS, Chicago, IL, USA). Additional correlations between amygdala volume and independent terms were performed to further explore the significant model obtained.

The assumptions for the multiple linear regression models were tested and met. The statistical significance was established for α = 0.05, and the obtained *p*-values were corrected for 2 multiple comparisons (right and left amygdala models) using the Bonferroni-Holm correction (Holm, 1979).

4. Results

4.1. Cohort Characterization

The distribution of the population and respective socio-demographic, psychological, and volumetric brain characterization (left and right amygdala, total GM, and eTIV) is presented in Table 1. In addition, descriptive statistics of all cortical and subcortical regions can be consulted in Supplementary Table A1 as a characterization of a general Portuguese population.

A between-group comparison indicated that no age differences were found between sex (U = 7955.0, p = 0.094). A Mann-Whitney test indicated higher perceived stress scores in females than in males (U = 7451.5, p = 0.014, r = 0.149). Regarding brain volumes, independent-samples *t*-tests indicated that total GM and eTIV were significantly higher for males than females (t(270) = 4.924, p < 0.001, d = 0.61, and t(270) = 10.069, p < 0.001, d = 1.26, respectively).

A negative association between PSS10 score and age was found (r(272) = -0.276, p < 0.001). Between PSS10 and individual total GM, a positive significant correlation was observed (r(272) = 0.153, p = 0.011). No association was verified among PSS10 scores and eTIV (r(272) = 0.038, p = 0.038).

Table 1. Participants characterization. Demographic, psychological and brain morphological characterization of the population included in this study.

	Demographic		**Psychological**	**Brain Volume (mm^3)**			
	N (%)	Age (years)	Perceived Stress (PSS10)	Left amygdala	Right amygdala	Total GM	eTIV
Global population	272 (100%)						
min		15	1	$8.50x10^2$	$9.46x10^2$	$4.39x10^5$	$1.14x10^6$
max		84	39	$2.14x10^3$	$2.62x10^3$	$8.35x10^5$	$1.99x10^6$
Mean ± SD		38.3 ± 20.85	16.5 ± 7.85	$1.36x10^3 \pm 2.17x10^2$	$1.45x10^3 \pm 2.35x10^2$	$6.30x10^5 \pm 7.74x10^4$	$1.57x10^6 \pm 1.65x10^5$
Male	115 (42.3%)						
min		15	2	$1.01x10^3$	$1.04x10^3$	$5.05x10^5$	$1.24x10^6$
max		80	35	$2.14x10^3$	$2.62x10^3$	$8.38x10^5$	$1.99x10^6$
Mean ± SD		41.7 ± 21.49	15.1 ± 7.29	$1.46x10^3 \pm 2.11x10^2$	$1.56x10^3 \pm 2.55x10^2$	$6.57x10^5 \pm 8.28x10^4$	$1.67x10^6 \pm 1.58x10^5$
Female	157 (57.7%)						
min		15	1	$8.50x10^2$	$9.46x10^2$	$4.39x10^5$	$1.14x10^6$
max		84	39	$1.93x10^3$	$2.06x10^3$	$7.37x10^5$	$1.80x10^6$
Mean ± SD		35.9 ± 20.09	17.5 ± 8.10	$1.29x10^3 \pm 1.94x10^2$	$1.37x10^3 \pm 1.81x10^2$	$6.10x10^5 \pm 6.69x10^4$	$1.49x10^6 \pm 1.23 \times 10^5$

eTIV. Estimated Intracranial Volume; GM. Gray matter; SD. Standard Deviation.

4.2. Volumetric regression with PSS10

Multilinear regressions were computed to predict amygdala volume based on participants' PSS10, total GM, age, and sex (one model for the right amygdala and another for the left). The two models obtained were statistically significant; however, perceived stress (measured by PSS10) was only a significant predictor of the right amygdala volume (positive association).

Regarding covariates, total GM and age were positively associated with right and left amygdala volumes. On the contrary, sex only achieved statistical significance in the left amygdala model (males have a larger left amygdala than females).

In Table 2, the results of the global models and the individual effects of each variable corrected for all the other independent terms included in the regression are presented. A graphical representation of the right amygdala regression model and the partial regression plot for PSS10 scores are shown in Figure 1. The partial regression plots for the non-exploratory variables (age and total GM) are presented in Supplementary Figure A1.

Table 2. Multilinear models resulted from amygdala volumetric regressions. Both regressions resulted in statistically significant models; however, perceived stress only shows significance as a predictor of the right amygdala. Besides perceived stress, total GM and age are also significant predictors of the right amygdala size. On the left hemisphere, total GM, age, and sex are significant predictors of the left amygdala volume. The *fMRIprep* FreeSurfer derivatives were used to extract amygdala and total GM volumes. Due to differences in magnitudes, all the variables were demeaned and standardized before model computation. In SPSS, the models were established using amygdala sizes as the dependent variable and PSS10, total GM, age, and sex as independent terms. The obtained p-values were then corrected for 2 multiple comparisons using the Bonferroni-Holm correction. The statistical significance was established for $\alpha = 0.05$.

	Global Model		**Independent terms**					
				PSS10	**GM**	**Age**	**Sex**	**Constant**
Right Amygdala	F (4,267)	53.540	F (4,267)	6.128	96.399	28.404	3.614	
	R squared	0.445	Partial Eta Squared	0.022	0.265	0.096	0.013	
	Adjusted R squared	0.437	Slope(β)	0.118	0.851	0.451	0.111	-3.810×10^{-11}
	Partial Eta Squared	0.445	Std. Error	0.048	0.087	0.085	0.058	0.046
	p-value	**<0.001**	p-value	**0.014**	**<0.001**	**<0.001**	0.058	
			corrected p-value	**0.028**	**<0.001**	**<0.001**	0.058	
Left Amygdala	F (4,267)	71.276	F (4,267)	0.747	93.189	5.380	5.600	
	R squared	0.516	Partial Eta Squared	0.003	0.259	0.020	0.021	
	Adjusted R squared	0.509	Slope (β)	0.039	0.781	0.183	0.128	-2.723×10^{-11}
	Partial Eta Squared	0.516	Std. Error	0.045	0.081	0.079	0.054	0.042
	p-value	**<0.001**	p-value	0.388	**<0.001**	**0.021**	**0.019**	
			corrected p-value	0.388	**<0.001**	**0.021**	**0.038**	

GM. Gray matter; PSS10. 10-item Perceived Stress Scale.

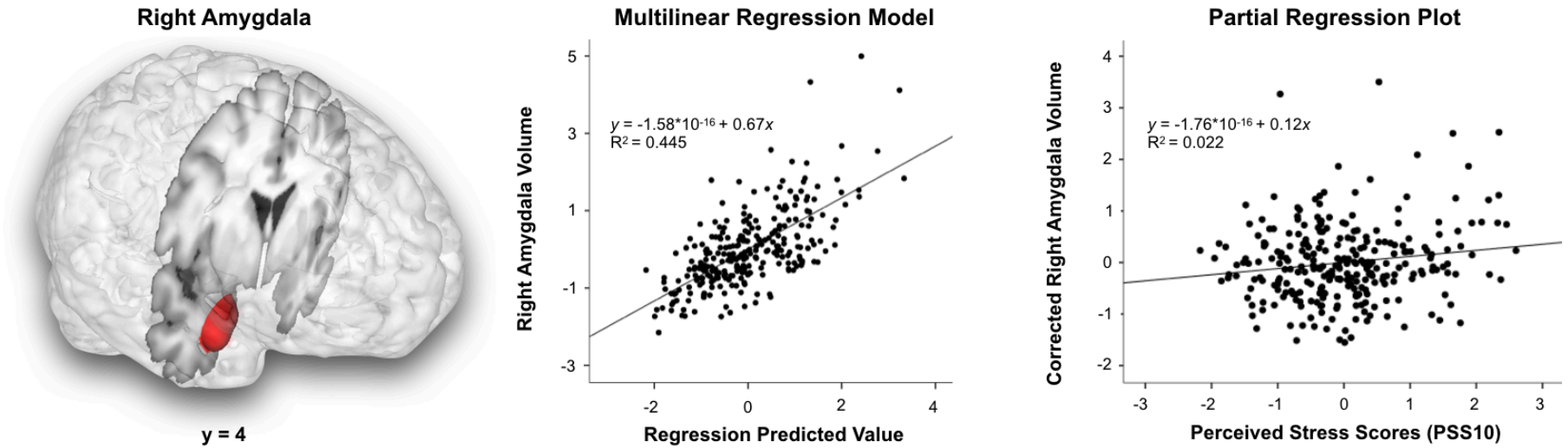

Fig.1. Results from volumetric regression of the right amygdala and PSS10 scores. A statistically significant model was obtained, with perceived stress showing significance as a predictor of the right amygdala volume.

On the left, representation of the right amygdala cluster from FreeSurfer. A graphical representation of the multilinear model obtained is presented in the middle; herein, the equation represents the correlation between the right amygdala volumes and the expected predicted values according to the model, not the model's global equation. Finally, on the right, the partial regression of the right amygdala volumes corrected for total GM, age, and sex, and perceived stress scores (PSS10) is presented, plus the correlation between those variables.

Amygdala volumes were computed using the *fMRIprep FreeSurfer* derivatives. Then, all the variables were demeaned and standardized. Next, a multilinear model was computed using SPSS, with right amygdala volume as the dependent variable and PSS10, total GM, age, and sex as independent terms. The Bonferroni-Holm correction for 2 multiple comparisons (left and right amygdala models) was used to compute the corrected p-values, and the statistical significance was established for $\alpha = 0.05$. Finally, the graphical representations, as the linear correlation between y and x values, were made using SPSS.

5. Discussion

This study uses a representative cohort of a general population to explore the relationship between amygdala size and perceived stress. Results show a positive association between the size of the right amygdala and PSS10 scores throughout the lifespan.

Associations between subjects' perception of stress and the volume of emotional regions like the amygdala have been shown in specific ages (e.g., young adults (Caetano et al., 2021) and aged individuals (Gerritsen et al., 2015)). Herein, using a healthy cohort with a broad range of ages, we show that the positive association of the subject's psychological state and right amygdala volume is present across the lifespan. Indeed, our results highlight amygdala neuroplasticity, reinforcing its involvement in stress-response and emotional processing, as suggested by others (Hölzel et al., 2010; Kaul, Schwab, Mechawar, & Matosin, 2021; Sublette et al., 2016; Taren et al., 2013).

In line with a previous study (Caetano et al., 2021), we did not observe any effect on the left amygdala. Thus, and again, the right hemisphere's prominence on emotional and affective functions, as well as the left dominance on language and motor function (Cerqueira et al., 2008; Duboc, Dufourcq, Blader, & Roussigné, 2015), appears to be the most reasonable explanation for the findings observed. Indeed, a reduction in subjects' perceived stress was previously associated with a shrinkage only on the right amygdala (Hölzel et al., 2010). Similarly, another study showed that right amygdala stimulation induced negative emotions, contrasting with the pleasant and unpleasant feelings caused by left amygdala stimulation (Lanteaume et al., 2007). Interestingly, however, there are studies associating stress perception with the left, and not right, hemisphere. For example, Wu et al. reported a positive and a negative association with left amygdala size in 26 adolescents and 26 middle-aged adults, respectively (Wu et al., 2020). In line with this, Sublette et al. demonstrated a negative association between the left amygdala and recent stressful life events in 60 healthy adults (Sublette et al., 2016).

When looking for case-control studies, the discrepancies are even more enhanced. For example, Butterworth et al. observed that 19 adults with financial hardship, when compared to controls, had smaller hippocampal and amygdalar volumes in both hemispheres (Butterworth, Cherbuin, Sachdev, & Anstey, 2012). Contrarily, Cacciaglia demonstrated that 18 healthy trauma-exposed individuals had higher left amygdala volume than non-exposed controls (Cacciaglia et al., 2017). Indeed, as noted by Kaul et al., both stressor type and timing of occurrence conditionate the amygdala's response (Kaul et

al., 2021). Therefore, to unravel the amygdala's role in disease development, it is essential to first fully understand its early response to stressful stimuli (Kaul et al., 2021). As a consequence, the conductance of sizeable non-pathological studies is required.

As far as we know, this is the first study using a significant representation of a general non-pathological population to unravel the linkage between perceived stress and amygdala size. Importantly, our cohort's psychosocial and demographic characteristics are similar to other representative populations (Brougham, Zail, Mendoza, & Miller, 2009; Eshel, Kimhi, Lahad, & Leykin, 2016; Matud, 2004; Teles, Valle, Rodríguez, Piñeiro, & Regueiro, 2020). Indeed, by including younger, middle-aged, and older participants, we obtained a more faithful representation of the global healthy populace, from which conclusions can now be extrapolated. However, studying lifespan with a single acquisition per subject is also a limitation. We tackled this constraint by including age as a covariate but, we denote that this is a cross-sectional study and not a longitudinal one. In light of this, special care should be taken when categorizing PSS10 as an amygdala size predictor. Mathematically, a predictor is an independent term that is meant to offer information on the dependent variable without inferring any causality. Indeed, due to this study's design, no cause-and-effect relationship can be assumed (Caruana, Roman, Hernández- Sánchez, & Solli, 2015; Taris & Kompier, 2014).

As future work, a longitudinal morphometric study could help to disclose the causal link between perceived stress and amygdala size, as further detail amygdala plasticity over time (Caetano et al., 2021; Caruana et al., 2015; Hölzel et al., 2010; Taris & Kompier, 2014). Interestingly, alterations in amygdala connectivity and functioning have also been reported (Chang & Yu, 2018; Eckstrand et al., 2021; Lederbogen et al., 2018; Liston et al., 2009; Soares, Sampaio, Ferreira, et al., 2013; Soares, Sampaio, Marques, et al., 2013; Vaisvaser et al., 2013; X. Zhang et al., 2018). Therefore, future studies might expand on our findings by exploring amygdala function and its association with perceived stress.

In conclusion, herein, we investigated the relationship between psychosocial stress and amygdala volume in a sizeable cohort with a broad range of ages. We conducted volumetric regressions using PSS10 as the independent term and amygdala size as the dependent variable, and we found that perceived stress is favorably associated with the right amygdala volume throughout life.

6. Acknowledgments

This work was funded by the Foundation for Science and Technology (FCT) [projects UIDB/50026/2020, UIDP/50026/2020, PTDC/MED-NEU/29071/2017 and POCI-01-0145-FEDER-016428]; by BIAL Foundation [grants PT/FB/BL-2016-206, BIAL Foundation 30-16]; Fundação Calouste Gulbenkian [contract grant P-139977]; and the European Commission (FP7) [contract HEALTH-F2-2010-259772].

Fellowship grants supported IC, LA, and AC through the FCT [grants number SFRH/BD/133006/2017, SFRH/BD/101398/2014, NORTE-08-5369-FSE-000041] from the Health Science program.

7. Data Accessibility statement

All the scripts and software used to generate the analysis presented in this work are freely available on the web pages of each official developer (see methods and references). The global preprocessed brain volumes for all sub-cortical and cortical regions are presented in the Supplementary material.

8. Conflict of interest statement

The authors declared that they had no conflicts of interest concerning their authorship or the publication of this article.

9. CRediT author statement

Inês Caetano: Conceptualization, Formal analysis, Validation, Writing - Original Draft, Visualization; contributed to the study design, organized the raw data, performed the data preprocessing, quality check and analysis, interpreted the results, discussed the manuscript, wrote the first draft of the manuscript, and performed data presentation. **Liliana Amorim:** Investigation, Data Curation, Validation; performed participant's recruitment and psychological assessment, discussed statistical analysis, and participated in the manuscript discussion. **Teresa Costa Castanho:** Investigation, Data Curation, Validation; performed participant's recruitment and psychological assessment, organized and validated psychological assessment. **Ana Coelho:** Software, Investigation, Data Curation; performed MRI

acquisitions and maintained research data. **Sónia Ferreira:** Investigation, Data Curation; performed MRI acquisitions and maintained research data. **Carlos Portugal-Nunes:** Investigation, Data Curation; performed MRI acquisitions and maintained research data. **José Miguel Soares:** Investigation, Data Curation; performed participant recruitment and MRI acquisitions. **Nuno Gonçalves:** Investigation; performed participant's recruitment and psychological assessment. **Rui Sousa:** Investigation; performed participant's recruitment and psychological evaluation. **Joana Reis:** Investigation; performed MRI acquisitions. **Catarina Lima:** Validation; contributed for segmentation quality check. **Paulo Marques:** Investigation; performed MRI acquisitions. **Pedro Silva Moreira**: Investigation, Data Curation; performed MRI acquisitions. **Ana João Rodrigues:** Investigation, Resources, Funding acquisition; performed participant's recruitment, psychological assessment and contributed with funds and resources for study development. **Nadine C Santos:** Resources, Funding acquisition; provided the resources and funds for study development. **Pedro Morgado:** Investigation, Resources, Funding acquisition; performed participant's recruitment, psychological assessment and contributed with funds and resources for study development. **Madalena Esteves:** Software, Formal analysis, Validation; contributed for volumetric analysis and discussion. **Ricardo Magalhães:** Software, Investigation, Data Curation; performed MRI acquisitions, maintained research data and contributed for analysis. **Maria Picó-Pérez:** Software, Formal analysis, Methodology, Validation; performed the data preprocessing, contributed to data analysis and discussion. **Nuno Sousa:** Conceptualization, Validation, Writing - Review & Editing, Supervision, Resources, Funding acquisition; conceived the study design, provided resources and funds for the study development, reviewed the acquired data, interpreted the results, performed manuscript discussion, and reviewed the final manuscript.

10. References

Aldwin, C. (2010). *Stress and Coping across the Lifespan*. Oxford University Press. doi: 10.1093/oxfordhb/9780195375343.013.0002

Avants, B., Epstein, C., Grossman, M., & Gee, J. (2008). Symmetric diffeomorphic image registration with cross-correlation: Evaluating automated labeling of elderly and neurodegenerative brain. *Medical Image Analysis*, *12*(1), 26–41. doi: 10.1016/j.media.2007.06.004

Betensky, J. D., Robinson, D. G., Gunduz-Bruce, H., Sevy, S., Lencz, T., Kane, J. M., ... Szeszko, P. R. (2008). Patterns of stress in schizophrenia. *Psychiatry Research*, *160*(1), 38–46. doi: 10.1016/j.psychres.2007.06.001

Brewin, C. R., Andrews, B., & Valentine, J. D. (2000). Meta-analysis of risk factors for posttraumatic stress disorder in trauma-exposed adults. *Journal of Consulting and Clinical Psychology*, *68*(5), 748–766. doi: 10.1037/0022-006X.68.5.748

Brougham, R. R., Zail, C. M., Mendoza, C. M., & Miller, J. R. (2009). Stress, Sex Differences, and Coping Strategies Among College Students. *Current Psychology*, *28*(2), 85–97. doi: 10.1007/s12144-009-9047-0

Bryant, R. A. (2019). Post-traumatic stress disorder: A state-of-the-art review of evidence and challenges. *World Psychiatry*, *18*(3), 259–269. doi: 10.1002/wps.20656

Butterworth, P., Cherbuin, N., Sachdev, P., & Anstey, K. J. (2012). The association between financial hardship and amygdala and hippocampal volumes: Results from the PATH through life project. *Social Cognitive and Affective Neuroscience*, *7*(5), 548–556. doi: 10.1093/scan/nsr027

Cacciaglia, R., Nees, F., Grimm, O., Ridder, S., Pohlack, S. T., Diener, S. J., ... Flor, H. (2017). Trauma exposure relates to heightened stress, altered amygdala morphology and deficient extinction learning: Implications for psychopathology. *Psychoneuroendocrinology*, *76*, 19–28. doi: 10.1016/j.psyneuen.2016.11.012

Caetano, I., Amorim, L., Soares, J. M., Ferreira, S., Coelho, A., Reis, J., ... Sousa, N. (2021). Amygdala size varies with stress perception. *Neurobiology of Stress*, *14*, 100334. doi: 10.1016/j.ynstr.2021.100334

Canbolat, M., Erbay, M. F., Şenol, D., Uçar, C., & Yıldız, S. (2021). Is amygdala size correlated with stress? *Folia Morphol.*, *80*(3), 6. doi: 10.5603/FM.a2020.0095

Caruana, E., Roman, M., Hernández- Sánchez, J., & Solli, P. (2015). Longitudinal studies. *Journal of Thoracic Disease*, *7*(11), E537–E540. doi: 10.3978/j.issn.2072-1439.2015.10.63

Carvalho, A. F., Firth, J., & Vieta, E. (2020). Bipolar Disorder. *New England Journal of Medicine*, *383*(1), 58–66. doi: 10.1056/NEJMra1906193

Cerqueira, J. J., Almeida, O. F. X., & Sousa, N. (2008). The stressed prefrontal cortex. Left? Right! *Brain, Behavior, and Immunity*, *22*(5), 630–638. doi: 10.1016/j.bbi.2008.01.005

Chang, J., & Yu, R. (2018). Alternations in functional connectivity of amygdalar subregions under acute social stress. *Neurobiology of Stress*, *9*, 264–270. doi: 10.1016/j.ynstr.2018.06.001

Chida, Y., & Steptoe, A. (2009). Cortisol awakening response and psychosocial factors: A systematic review and meta-analysis. *Biological Psychology*, *80*(3), 265–278. doi: 10.1016/j.biopsycho.2008.10.004

Cohen, S., Kamarck, T., & Mermelstein, R. (1983). A Global Measure of Perceived Stress. *Journal of Health and Social Behavior*, *24*(4), 385. doi: 10.2307/2136404

Dale, A. M., Fischl, B., & Sereno, M. I. (1999). Cortical Surface-Based Analysis: I. Segmentation and Surface Reconstruction. *NeuroImage*, *9*(2), 179–194. doi: 10.1006/nimg.1998.0395

Davidson, J. R. T., Hughes, D., Blazer, D. G., & George, L. K. (1991). Post-traumatic stress disorder in the community: An epidemiological study. *Psychological Medicine*, *21*(3), 713–721. doi: 10.1017/S0033291700022352

De Bellis, M. D., Casey, B. J., Dahl, R. E., Birmaher, B., Williamson, D. E., Thomas, K. M., ... Ryan, N. D. (2000). A pilot study of amygdala volumes in pediatric generalized anxiety disorder. *Biological Psychiatry*, *48*(1), 51–57. doi: 10.1016/S0006-3223(00)00835-0

Desikan, R. S., Ségonne, F., Fischl, B., Quinn, B. T., Dickerson, B. C., Blacker, D., ... Killiany, R. J. (2006). An automated labeling system for subdividing the human cerebral cortex on MRI scans into gyral based regions of interest. *NeuroImage*, *31*(3), 968–980. doi: 10.1016/j.neuroimage.2006.01.021

Duboc, V., Dufourcq, P., Blader, P., & Roussigné, M. (2015). Asymmetry of the Brain: Development and Implications. *Annual Review of Genetics*, *49*(1), 647–672. doi: 10.1146/annurev-genet-112414-055322

Eckstrand, K. L., Forbes, E. E., Bertocci, M. A., Chase, H. W., Greenberg, T., Lockovich, J., ... Phillips, M. L. (2021). Trauma Affects Prospective Relationships Between Reward-Related Ventral Striatal and Amygdala Activation and 1-Year Future Hypo/ Mania Trajectories. *Biological Psychiatry*, *89*(9), 868–877. doi: 10.1016/j.biopsych.2020.11.017

Eshel, Y., Kimhi, S., Lahad, M., & Leykin, D. (2016). Individual, Community, and National Resiliencies and Age: Are Older People Less Resilient than Younger Individuals? *The American Journal of Geriatric Psychiatry*, *24*(8), 644–647. doi: 10.1016/j.jagp.2016.03.002

Esteban, O., Markiewicz, C. J., Blair, R. W., Moodie, C. A., Isik, A. I., Erramuzpe, A., ... Gorgolewski, K. J. (2018). fMRIPrep: A robust preprocessing pipeline for functional MRI. *Nature Methods*, *16*(1), 111–116. doi: 10.1038/s41592-018-0235-4

Esteban, O., Markiewicz, C. J., Burns, C., Goncalves, M., Jarecka, D., Ziegler, E., ... Ghosh, S. (2020). *Nipype (software)*. Zenodo. doi: 10.5281/zenodo.4035081

Esteban, O., Markiewicz, C. J., Goncalves, M., DuPre, E., Kent, J. D., Salo, T., ... Gorgolewski, K. J. (2021). *FMRIPrep (software)*. Zenodo. doi: 10.5281/zenodo.5569959

Evans, A. C., Janke, A. L., Collins, D. L., & Baillet, S. (2012). Brain templates and atlases. *NeuroImage*, *62*(2), 911–922. doi: 10.1016/j.neuroimage.2012.01.024

Everaerd, D. S., Henckens, M. J. A. G., Bloemendaal, M., Bovy, L., Kaldewaij, R., Maas, F. M. W. M., ... de Voogd, L. D. (2020). Good vibrations: An observational study of real-life stress induced by a stage performance. *Psychoneuroendocrinology*, *114*, 104593. doi: 10.1016/j.psyneuen.2020.104593

Fett, A.-K. J., Lemmers-Jansen, I. L. J., & Krabbendam, L. (2019). Psychosis and urbanicity: A review of the recent literature from epidemiology to neurourbanism. *Current Opinion in Psychiatry*, *32*(3), 232–241. doi: 10.1097/YCO.0000000000000486

Fischl, B. (2012). FreeSurfer. *NeuroImage*, *62*(2), 774–781. doi: 10.1016/j.neuroimage.2012.01.021

Fischl, B., Salat, D. H., Busa, E., Albert, M., Dieterich, M., Haselgrove, C., ... Dale, A. M. (2002). Whole Brain Segmentation. *Neuron*, *33*(3), 341–355. doi: 10.1016/S0896-6273(02)00569-X

Fliege, H., Rose, M., Arck, P., Walter, O. B., Kocalevent, R.-D., Weber, C., & Klapp, B. F. (2005). The Perceived Stress Questionnaire (PSQ) Reconsidered: Validation and Reference Values From Different Clinical and Healthy Adult Samples: *Psychosomatic Medicine*, *67*(1), 78–88. doi: 10.1097/01.psy.0000151491.80178.78

Fonov, V., Evans, A., McKinstry, R., Almli, C., & Collins, D. (2009). Unbiased nonlinear average age-appropriate brain templates from birth to adulthood. *NeuroImage*, *47*, S102. doi: 10.1016/S1053-8119(09)70884-5

Gerritsen, L., Kalpouzos, G., Westman, E., Simmons, A., Wahlund, L.-O., Bäckman, L., ... Wang, H.-X. (2015). The influence of negative life events on hippocampal and amygdala volumes in old age: A life-course perspective. *Psychological Medicine*, *45*(6), 1219–1228. doi: 10.1017/S0033291714002293

Gispen-de Wied, C. C. (2000). Stress in schizophrenia: An integrative view. *European Journal of Pharmacology*, *405*(1–3), 375–384. doi: 10.1016/S0014-2999(00)00567-7

Godoy, L. D., Rossignoli, M. T., Delfino-Pereira, P., Garcia-Cairasco, N., & de Lima Umeoka, E. H. (2018). A Comprehensive Overview on Stress Neurobiology: Basic Concepts and Clinical Implications. *Frontiers in Behavioral Neuroscience*, *12*, 127. doi: 10.3389/fnbeh.2018.00127

Goldstein, D. S., & Kopin, I. J. (2007). Evolution of concepts of stress. *Stress*, *10*(2), 109–120. doi: 10.1080/10253890701288935

Gong, Y., Palmer, S., Gallacher, J., Marsden, T., & Fone, D. (2016). A systematic review of the relationship between objective measurements of the urban environment and psychological distress. *Environment International*, *96*, 48–57. doi: 10.1016/j.envint.2016.08.019

Gorgolewski, K., Burns, C. D., Madison, C., Clark, D., Halchenko, Y. O., Waskom, M. L., & Ghosh, S. S. (2011). Nipype: A Flexible, Lightweight and Extensible Neuroimaging Data Processing Framework in Python. *Frontiers in Neuroinformatics*, *5*. doi: 10.3389/fninf.2011.00013

Gotink, R. A., Meijboom, R., Vernooij, M. W., Smits, M., & Hunink, M. G. M. (2016). 8-week Mindfulness Based Stress Reduction induces brain changes similar to traditional long-term meditation practice – A systematic review. *Brain and Cognition*, *108*, 32–41. doi: 10.1016/j.bandc.2016.07.001

Gotink, R. A., Vernooij, M. W., Ikram, M. A., Niessen, W. J., Krestin, G. P., Hofman, A., ... Hunink, M. G. M. (2018). Meditation and yoga practice are associated with smaller right amygdala volume: The Rotterdam study. *Brain Imaging and Behavior*, *12*(6), 1631–1639. doi: 10.1007/s11682-018-9826-z

Halford, C., Jonsdottir, I. H., & Eek, F. (2012). Perceived Stress, Psychological Resources and Salivary Cortisol. *Bentham EBooks*, 67–86.

Hammen, C. (2005). Stress and Depression. *Annual Review of Clinical Psychology*, *1*(1), 293–319. doi: 10.1146/annurev.clinpsy.1.102803.143938

Herringa, R., Phillips, M., Almeida, J., Insana, S., & Germain, A. (2012). Post-traumatic stress symptoms correlate with smaller subgenual cingulate, caudate, and insula volumes in unmedicated combat veterans. *Psychiatry Research: Neuroimaging*, *203*(2–3), 139–145. doi: 10.1016/j.pscychresns.2012.02.005

Holm, S. (1979). A Simple Sequentially Rejective Multiple Test Procedure. *Scandinavian Journal of Statistics*, *6*(2), 65–70.

Hölzel, B. K., Carmody, J., Evans, K. C., Hoge, E. A., Dusek, J. A., Morgan, L., ... Lazar, S. W. (2010). Stress reduction correlates with structural changes in the amygdala. *Social Cognitive and Affective Neuroscience*, *5*(1), 11–17. doi: 10.1093/scan/nsp034

Kalisch, R., Baker, D. G., Basten, U., Boks, M. P., Bonanno, G. A., Brummelman, E., ... Kleim, B. (2017). The resilience framework as a strategy to combat stress-related disorders. *Nature Human Behaviour*, *1*(11), 784–790. doi: 10.1038/s41562-017-0200-8

Kaul, D., Schwab, S. G., Mechawar, N., & Matosin, N. (2021). How stress physically re-shapes the brain: Impact on brain cell shapes, numbers and connections in psychiatric disorders. *Neuroscience & Biobehavioral Reviews*, *124*, 193–215. doi: 10.1016/j.neubiorev.2021.01.025

Kendler, K. S., Karkowski, L. M., & Prescott, C. A. (1999). Causal Relationship Between Stressful Life Events and the Onset of Major Depression. *American Journal of Psychiatry*, *156*(6), 837–841. doi: 10.1176/ajp.156.6.837

Kim, E. Y., Miklowitz, D. J., Biuckians, A., & Mullen, K. (2007). Life stress and the course of early-onset bipolar disorder. *Journal of Affective Disorders*, *99*(1–3), 37–44. doi: 10.1016/j.jad.2006.08.022

Klein, A., Ghosh, S. S., Bao, F. S., Giard, J., Häme, Y., Stavsky, E., ... Keshavan, A. (2017). Mindboggling morphometry of human brains. *PLOS Computational Biology*, *13*(2), e1005350. doi: 10.1371/journal.pcbi.1005350

Koenig, J. I., Walker, C.-D., Romeo, R. D., & Lupien, S. J. (2011). Effects of stress across the lifespan. *Stress*, *14*(5), 475–480. doi: 10.3109/10253890.2011.604879

Kronenberg, G., Tebartz van Elst, L., Regen, F., Deuschle, M., Heuser, I., & Colla, M. (2009). Reduced amygdala volume in newly admitted psychiatric in-patients with unipolar major depression. *Journal of Psychiatric Research*, *43*(13), 1112–1117. doi: 10.1016/j.jpsychires.2009.03.007

Lanteaume, L., Khalfa, S., Regis, J., Marquis, P., Chauvel, P., & Bartolomei, F. (2007). Emotion Induction After Direct Intracerebral Stimulations of Human Amygdala. *Cerebral Cortex*, *17*(6), 1307–1313. doi: 10.1093/cercor/bhl041

Lederbogen, F., Ulshoefer, E., Peifer, A., Fehlner, P., Bilek, E., Streit, F., ... Meyer-Lindenberg, A. (2018). No association between cardiometabolic risk and neural reactivity to acute psychosocial stress. *Neuroimage-Clinical*, *20*, 1115–1122. doi: 10.1016/j.nicl.2018.10.018

Li, H., Li, W., Wei, D., Chen, Q., Jackson, T., Zhang, Q., & Qiu, J. (2014). Examining brain structures associated with perceived stress in a large sample of young adults via voxel-based morphometry. *NeuroImage*, *92*, 1–7. doi: 10.1016/j.neuroimage.2014.01.044

Liston, C., McEwen, B. S., & Casey, B. J. (2009). Psychosocial stress reversibly disrupts prefrontal processing and attentional control. *Proceedings of the National Academy of Sciences*, *106*(3), 912–917. doi: 10.1073/pnas.0807041106

Lucassen, P. J., Pruessner, J., Sousa, N., Almeida, O. F. X., Van Dam, A. M., Rajkowska, G., ... Czéh, B. (2014). Neuropathology of stress. *Acta Neuropathologica*, *127*(1), 109–135. doi: 10.1007/s00401-013-1223-5

Magalhães, R., Barrière, D. A., Novais, A., Marques, F., Marques, P., Cerqueira, J., ... Sousa, N. (2018). The dynamics of stress: A longitudinal MRI study of rat brain structure and connectome. *Molecular Psychiatry*, *23*(10), 1998–2006. doi: 10.1038/mp.2017.244

Matud, M. P. (2004). Gender differences in stress and coping styles. *Personality and Individual Differences*, *37*(7), 1401–1415. doi: 10.1016/j.paid.2004.01.010

McKinnon, M. C., Yucel, K., Nazarov, A., & MacQueen, G. M. (2009). A meta-analysis examining clinical predictors of hippocampal volume in patients with major depressive disorder. *J Psychiatry Neurosci*, 14.

Melchior, M., Caspi, A., Milne, B. J., Danese, A., Poulton, R., & Moffitt, T. E. (2007). Work stress precipitates depression and anxiety in young, working women and men. *Psychological Medicine*, *37*(8), 1119–1129. doi: 10.1017/S0033291707000414

Morey, R. A., Gold, A. L., LaBar, K. S., Beall, S. K., Brown, V. M., Haswell, C. C., ... Mid-Atlantic MIRECC Workgroup, for the. (2012). Amygdala Volume Changes in Posttraumatic Stress Disorder in a Large Case-Controlled Veterans Group. *Archives of General Psychiatry*, *69*(11), 1169. doi: 10.1001/archgenpsychiatry.2012.50

Novais, A., Monteiro, S., Roque, S., Correia-Neves, M., & Sousa, N. (2017). How age, sex and genotype shape the stress response. *Neurobiology of Stress*, *6*, 44–56. doi: 10.1016/j.ynstr.2016.11.004

Pêgo, J. M., Sousa, J. C., Almeida, O., & Sousa, N. (2009). Stress and the Neuroendocrinology of Anxiety Disorders. In M. B. Stein & T. Steckler (Eds.), *Behavioral Neurobiology of Anxiety and Its Treatment* (pp. 97–118). Berlin, Heidelberg: Springer Berlin Heidelberg. doi: 10.1007/7854_2009_13

Potvin, O., Dieumegarde, L., & Duchesne, S. (2017). Normative morphometric data for cerebral cortical areas over the lifetime of the adult human brain. *NeuroImage*, *156*, 315–339. doi: 10.1016/j.neuroimage.2017.05.019

Potvin, O., Mouiha, A., Dieumegarde, L., & Duchesne, S. (2016). Normative data for subcortical regional volumes over the lifetime of the adult human brain. *NeuroImage*, *137*, 9–20. doi: 10.1016/j.neuroimage.2016.05.016

Ritchie, H., & Roser, M. (2018). Urbanization. *Our World in Data*. Retrieved from https://ourworldindata.org/urbanization

Schienle, A., Ebner, F., & Schäfer, A. (2011). Localized gray matter volume abnormalities in generalized anxiety disorder. *European Archives of Psychiatry and Clinical Neuroscience*, *261*(4), 303–307. doi: 10.1007/s00406-010-0147-5

Schuhmacher, A., Mössner, R., Jessen, F., Scheef, L., Block, W., Belloche, A. C., ... Zobel, A. (2012). Association of amygdala volumes with cortisol secretion in unipolar depressed patients. *Psychiatry Research: Neuroimaging*, *202*(2), 96–103. doi: 10.1016/j.pscychresns.2011.09.007

Shin, L. M., & Liberzon, I. (2010). The Neurocircuitry of Fear, Stress, and Anxiety Disorders. *Neuropsychopharmacology*, *35*(1), 169–191. doi: 10.1038/npp.2009.83

Soares, J. M., Sampaio, A., Ferreira, L. M., Santos, N. C., Marques, F., Palha, J. A., ... Sousa, N. (2012). Stress-induced changes in human decision-making are reversible. *Translational Psychiatry*, *2*(7), e131–e131. doi: 10.1038/tp.2012.59

Soares, J. M., Sampaio, A., Ferreira, L. M., Santos, N. C., Marques, P., Marques, F., ... Sousa, N. (2013). Stress Impact on Resting State Brain Networks. *PLoS ONE*, *8*(6), e66500. doi: 10.1371/journal.pone.0066500

Soares, J. M., Sampaio, A., Marques, P., Ferreira, L. M., Santos, N. C., Marques, F., ... Sousa, N. (2013). Plasticity of resting state brain networks in recovery from stress. *Frontiers in Human Neuroscience*, *7*. doi: 10.3389/fnhum.2013.00919

Sousa, N. (2016). The dynamics of the stress neuromatrix. *Molecular Psychiatry*, *21*(3), 302–312. doi: 10.1038/mp.2015.196

Sublette, M. E., Galfalvy, H. C., Oquendo, M. A., Bart, C. P., Schneck, N., Arango, V., & Mann, J. J. (2016). Relationship of recent stress to amygdala volume in depressed and healthy adults. *Journal of Affective Disorders*, *203*, 136–142. doi: 10.1016/j.jad.2016.05.036

Szabo, C. P. (2018). Urbanization and mental health: A developing world perspective. *Current Opinion in Psychiatry*, *31*(3), 256–257. doi: 10.1097/YCO.0000000000000414

Taren, A. A., Creswell, J. D., & Gianaros, P. J. (2013). Dispositional Mindfulness Co-Varies with Smaller Amygdala and Caudate Volumes in Community Adults. *PLoS ONE*, *8*(5), e64574. doi: 10.1371/journal.pone.0064574

Taris, T. W., & Kompier, M. A. J. (2014). Cause and effect: Optimizing the designs of longitudinal studies in occupational health psychology. *Work & Stress*, *28*(1), 1–8. doi: 10.1080/02678373.2014.878494

Teles, R., Valle, A., Rodríguez, S., Piñeiro, I., & Regueiro, B. (2020). Perceived Stress and Indicators of Burnout in Teachers at Portuguese Higher Education Institutions (HEI). *International Journal of Environmental Research and Public Health*, *17*(9), 3248. doi: 10.3390/ijerph17093248

Trigo, M., Canudo, N., Branco, F., & Silva, D. (2010). Estudo das propriedades psicométricas da Perceived Stress Scale (PSS) na população portuguesa. *Psychologica*, (53), 353–378. doi: 10.14195/1647-8606_53_17

Tustison, N. J., Avants, B. B., Cook, P. A., Yuanjie Zheng, Egan, A., Yushkevich, P. A., & Gee, J. C. (2010). N4ITK: Improved N3 Bias Correction. *IEEE Transactions on Medical Imaging*, *29*(6), 1310–1320. doi: 10.1109/TMI.2010.2046908

Vaisvaser, S., Lin, T., Admon, R., Podlipsky, I., Greenman, Y., Stern, N., ... Hendler, T. (2013). Neural traces of stress: Cortisol related sustained enhancement of amygdala-hippocampal functional connectivity. *Frontiers in Human Neuroscience*, *7*. doi: 10.3389/fnhum.2013.00313

van der Plas, E. A. A., Boes, A. D., Wemmie, J. A., Tranel, D., & Nopoulos, P. (2010). Amygdala volume correlates positively with fearfulness in normal healthy girls. *Social Cognitive and Affective Neuroscience*, *5*(4), 424–431. doi: 10.1093/scan/nsq009

Walker, E., Mittal, V., & Tessner, K. (2008). Stress and the Hypothalamic Pituitary Adrenal Axis in the Developmental Course of Schizophrenia. *Annual Review of Clinical Psychology*, *4*(1), 189–216. doi: 10.1146/annurev.clinpsy.4.022007.141248

Welberg, L. (2014). A REDD line from stress to depression. *Nature Reviews Neuroscience*, *15*(6), 350–350. doi: 10.1038/nrn3749

Wu, J., Tong, H., Liu, Z., Tao, J., Chen, L., Chan, C. C. H., & Lee, T. M. C. (2020). Neurobiological effects of perceived stress are different between adolescents and middle-aged adults. *Brain Imaging and Behavior*. doi: 10.1007/s11682-020-00294-7

Zhang, X., Ge, T. tong, Yin, G., Cui, R., Zhao, G., & Yang, W. (2018). Stress-Induced Functional Alterations in Amygdala: Implications for Neuropsychiatric Diseases. *Frontiers in Neuroscience*, *12*, 367. doi: 10.3389/fnins.2018.00367

Zhang, Y., Brady, M., & Smith, S. (2001). Segmentation of brain MR images through a hidden Markov random field model and the expectation-maximization algorithm. *IEEE Transactions on Medical Imaging*, *20*(1), 45–57. doi: 10.1109/42.906424

Zhao, L., Matloff, W., Ning, K., Kim, H., Dinov, I. D., & Toga, A. W. (2019). Age-Related Differences in Brain Morphology and the Modifiers in Middle-Aged and Older Adults. *Cerebral Cortex*, 29(10), 4169–4193. doi: 10.1093/cercor/bhy300

11. Supplementary Material

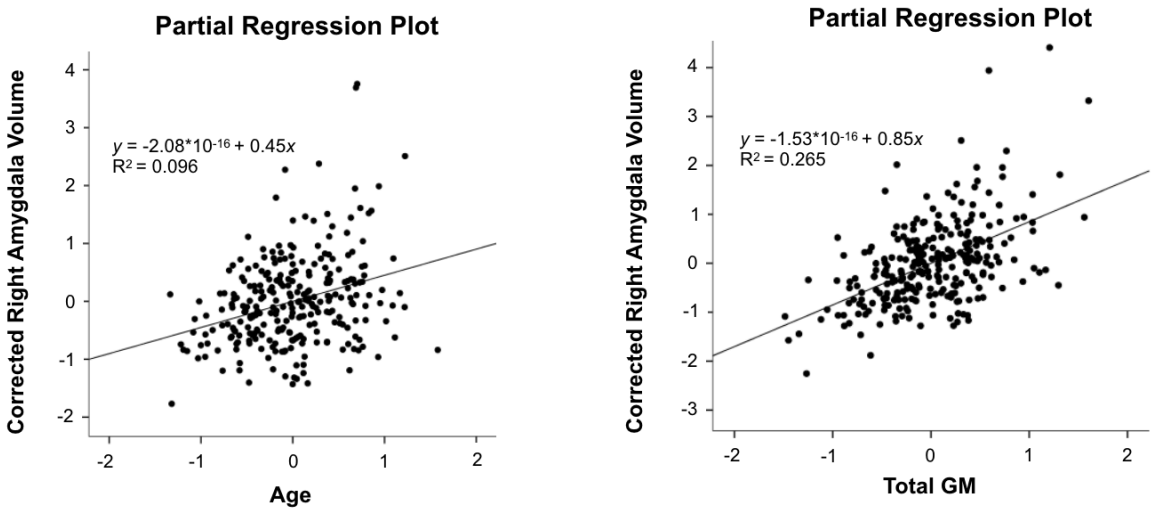

Supplementary Figure A1. Partial regression plots of age and total GM resulted from volumetric regression of the right amygdala volumes and PSS10 scores. A statistically significant model was obtained, with perceived stress, age, and total GM independent terms showing significance as predictors of the right amygdala volumes.

On the left, a graphical representation of the partial regression between age and corrected right amygdala volumes is presented, plus the correlation between those variables. On the right, the same visual depiction is applied to right amygdala volumes and total GM.

Amygdala volumes were computed using the *fMRIprep FreeSurfer* derivatives. Then, all the variables were demeaned and standardized. Next, a multilinear model was computed using SPSS, with right amygdala volume as the dependent variable and PSS10, total GM, age, and sex as independent terms. The Bonferroni-Holm correction for 2 multiple comparisons (left and right amygdala models) was used to compute the corrected p-values, and the statistical significance was established for $\alpha = 0.05$. Finally, the graphical representations, as the linear correlation between y and x values, were made using SPSS.

Supplementary Table A.1. Descriptive statistics of cortical, subcortical, and global brain volumes (in mm³). Volumes presented below are representative of a Portuguese population and were computed using the *fMRIprep* FreeSurfer derivatives.

	Left Hemisphere		Right Hemisphere	
	Mean	Standard Deviation	Mean	Standard Deviation
Cortical ROI				
Banks of the Superior Temporal Sulcus	2396	491	2187	402
Caudal Anterior-Cingulate Cortex	1822	444	1990	493
Caudal Middle Frontal Gyrus	6299	1239	6119	1221
Cuneus Cortex	2964	521	3303	644
Entorhinal Cortex	2006	354	1986	376
Fusiform Gyrus	9352	1258	9194	1336
Inferior Parietal Cortex	11903	2232	14379	2598
Inferior Temporal Gyrus	11244	1844	10951	1719
Isthmus–Cingulate Cortex	2535	421	2393	423
Lateral Occipital Cortex	11359	1764	11783	1861
Lateral Orbital Frontal Cortex	7838	1066	7469	1065
Lingual Gyrus	6426	1055	6953	1117
Medial Orbital Frontal Cortex	5136	720	5385	711
Middle Temporal Gyrus	11121	1954	11848	1971
Parahippocampal Gyrus	2072	286	1934	273
Paracentral Lobule	3421	468	3839	552
Pars Opercularis	4721	890	3892	744
Pars Orbitalis	2392	396	2771	479
Pars Triangularis	3635	748	4146	840
Pericalcarine Cortex	2214	444	2505	496
Postcentral Gyrus	9265	1452	8987	1415
Posterior-Cingulate Cortex	3148	558	3223	531
Precentral Gyrus	13221	1804	13131	1777
Precuneus Cortex	9410	1469	9859	1589
Rostral Anterior Cingulate Cortex	2598	538	1929	426
Rostral Middle Frontal Gyrus	15284	2814	15570	2854
Superior Frontal Gyrus	22426	3561	21621	3453
Superior Parietal Cortex	12601	2075	12276	2020
Superior Temporal Gyrus	12209	1949	11337	1819
Supramarginal Gyrus	11255	2162	10052	1834
Frontal Pole	924	163	1085	181
Temporal Pole	2387	342	2492	339
Transverse Temporal Cortex	1120	234	885	169
Insula	7158	899	7193	1011
Subcortical ROI				
Thalamus Proper	7329	1031	7121	970
Caudate	3594	493	3719	508
Putamen	4909	661	4911	641
Pallidum	1956	259	1879	244
Hippocampus	3782	436	3870	444
Amygdala	1363	217	1451	235
Accumbens	594	120	533	110

Global Volumes	**Mean**	**Standard Deviation**
eTIV	1.57x10^6	1.65x10^5
GM	6.30x10^5	7.74x10^4
WM	4.60x10^5	5.91x10^4

ROI. Region-of-interest; eTIV. Estimated Intracranial Volume; GM. Gray matter; WM. White matter.

Graphical Abstract

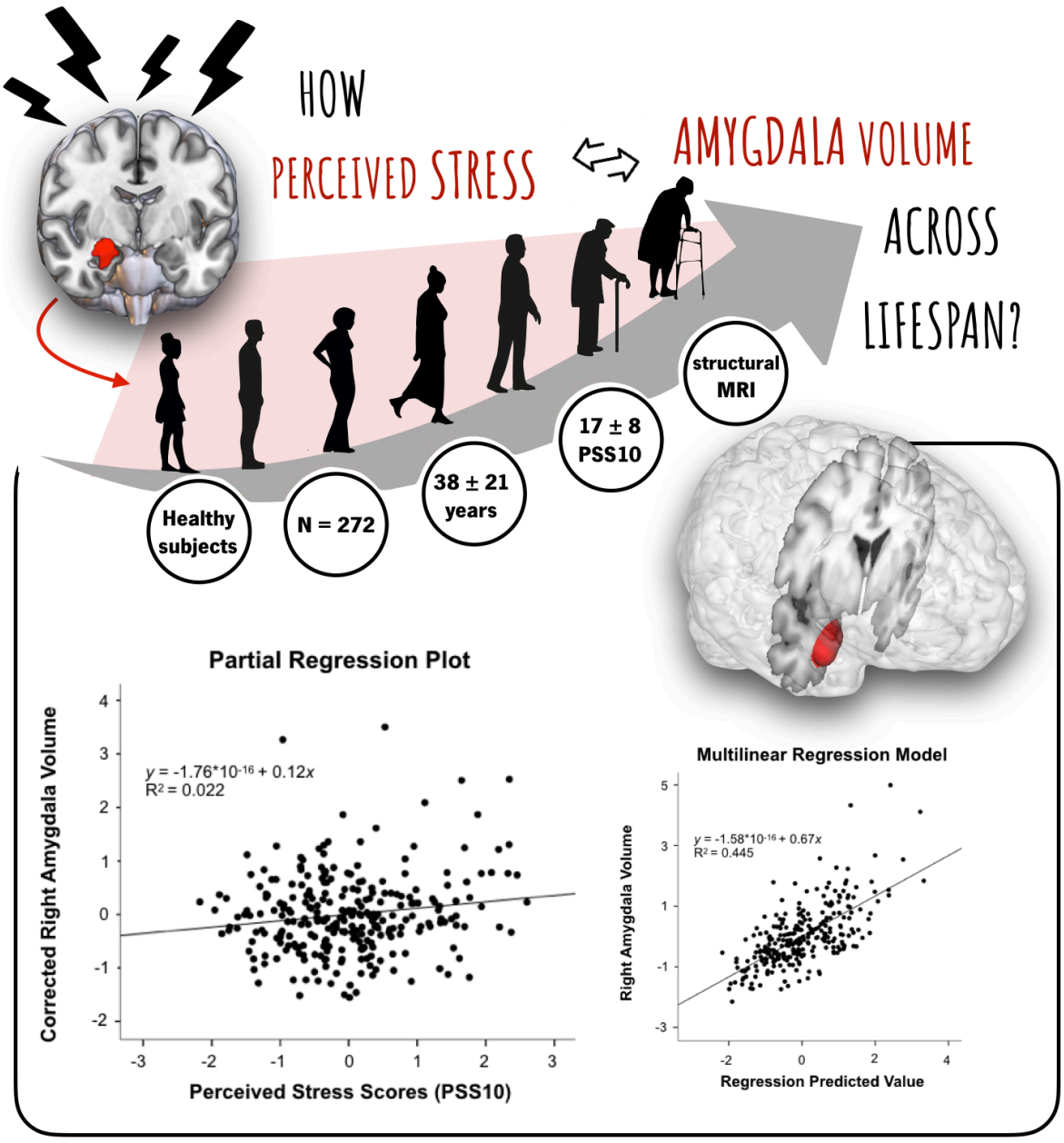

Graphical abstract text:

Previous studies shown associations between stress perception and amygdala volume in narrow age ranged cohorts. Life stress, on the other hand, has become pervasive and is no longer restricted to a specific age group or life stage. Herein, using a sizeable non-pathological cohort, we show that perceived stress is positively associated with the right amygdala volume across lifespan.

CHAPTER IV

Perceived stress disrupts counterbalanced activity between amygdala and cortex

Inês Caetano, Sónia Ferreira, Ana Coelho, Liliana Amorim, Teresa Costa Castanho, Carlos Portugal-Nunes, José Miguel Soares, Nuno Gonçalves, Rui Sousa, Joana Reis, Catarina Lima, Paulo Marques, Pedro Silva Moreira, Ana João Rodrigues, Nadine Correia Santos, Pedro Morgado, Ricardo Magalhães, Maria Picó-Pérez, Joana Cabral, Nuno Sousa

Manuscript in submission

Perceived stress disrupts counterbalanced activity between amygdala and cortex

Inês Caetano[a,b,c], Sónia Ferreira[a,b,c], Ana Coelho[a,b,c], Liliana Amorim[a,b,c,d], Teresa Costa Castanho[a,b,c,d], Carlos Portugal-Nunes[a,b,c,e], José Miguel Soares[a,b,c], Nuno Gonçalves[a,b,c], Rui Sousa[a,b,c,f], Joana Reis[a,b,c], Catarina Lima[a,b,c], Paulo Marques[a,b,c], Pedro Silva Moreira[a,b,c], Ana João Rodrigues[a,b,c], Nadine Correia Santos[a,b,c], Pedro Morgado[a,b,c], Ricardo Magalhães[a,b,c], Maria Picó-Pérez[a,b,c], Joana Cabral[a,b,c], Nuno Sousa[a,b,c,d]

[a]Life and Health Sciences Research Institute (ICVS), School of Medicine, University of Minho, 4710-057 Braga, Portugal; [b]ICVS/3B's, PT Government Associate Laboratory, 4710-057 Braga/Guimarães, Portugal; [c]Clinical Academic Center – Braga (2CA), 4710-243 Braga, Portugal; [d]Association P5 Digital Medical Center (ACMP5), 4710-057 Braga, Portugal; [e]CECAV - Veterinary and Animal Science Research Centre, Quinta de Prados, 5000-801 Vila Real, Portugal; [f]Departamento de Psiquiatria e Saúde Mental, Centro Hospitalar Tondela-Viseu, 3500-228 Viseu, Portugal.

1. Abstract

The significant link between stress and psychiatric disorders has prompted research on stress's impact on the brain. Interestingly, previous studies on healthy subjects have demonstrated an association between perceived stress and amygdala volume. To better understand what this association entails at a functional level, herein we explore the association of perceived stress with disseminated functional connectivity between brain areas. Using resting-state fMRI from 252 healthy subjects spanning a broad age range, we performed both a seed-based amygdala connectivity analysis and a whole-brain data-driven approach to detect altered patterns of phase interactions between brain areas. Results show that increased perceived stress is directly associated with increased amygdala connectivity with frontal cortical regions, which is driven by a reduced occurrence of an activity pattern where the signals in the amygdala and the hippocampus evolve in opposite directions with respect to the rest of the brain. Overall, these results not only reinforce the pathological effect of in-phase synchronicity between subcortical and cortical brain areas, but also demonstrate the protective effect of counterbalanced (i.e., phase-shifted) activity between brain subsystems, which are otherwise missed with correlation-based functional connectivity analysis.

Keywords: Perceived stress, Amygdala, Seed-Based, LEiDA, Healthy subjects, Aging

2. Introduction

Daily routines are getting increasingly stressful as modern society advances (Everaerd et al., 2020; Fett et al., 2019; Gong et al., 2016). Consequently, a new way of living, working, and interacting with others has emerged, with mental health concerns growing as a result of this transition (Lederbogen et al., 2018; Ritchie and Roser, 2018; Szabo, 2018).

The way stress influences the brain has been examined at several levels, including molecular, cellular, and network levels (Cerqueira et al., 2007; Magalhães et al., 2018; Popoli et al., 2012; Sousa et al., 2000; Yuen et al., 2012). Notwithstanding, it was the development of advanced neuroimaging techniques that potentiated our knowledge of brain morphology, connectivity, and function (Koenig et al., 2011; Kogler et al., 2015; Lucassen et al., 2014; Magalhães et al., 2019, 2018; Novais et al., 2017; Soares et al., 2016, 2013a; Sousa, 2016). Moreover, emergent algorithms for functional Magnetic Resonance Imaging (fMRI) data analysis have expanded the potential of neuroimaging studies to investigate the pathophysiology of brain disorders (Cabral et al., 2017; Esteban et al., 2018; Lv et al., 2018; Soares et al., 2016). In particular, different clinical and pre-clinical psychiatric symptoms have recently been associated with disrupted phase-locking patterns in fMRI signals between brain regions captured with Leading Eigenvector Dynamics Analysis (LEiDA) (Alonso Martínez et al., 2020; Figueroa et al., 2019; Larabi et al., 2020; Wong et al., 2021). This reinforces the emerging hypothesis that optimal functional brain interactions may not necessarily be related to synchronized co-activations (as captured with correlation-based analysis), but instead to delayed interactions leading to counterbalanced activations and de-activations between different brain subsystems (Arnold Anteraper et al., 2014; Chen et al., 2020; Johnson et al., 2018; Williams, 2016).

It is well-established that chronic stress is a significant risk factor for the emergence of diseases such as post-traumatic stress disorder (Brewin et al., 2000; Bryant, 2019; Davidson et al., 1991), anxiety (Melchior et al., 2007; Pêgo et al., 2009; Shin and Liberzon, 2010), major depression (Hammen, 2005; Kendler et al., 1999; Melchior et al., 2007; Welberg, 2014), bipolar disorder (Carvalho et al., 2020; Kim et al., 2007) and schizophrenia (Betensky et al., 2008; Gispen-de Wied, 2000; Walker et al., 2008). However, due to the unique characteristics of each pathology, discovering how the brain is altered before

the illness is highly beneficial to the understanding of stress neurobiology and even crucial if considering mental preventive interventions (Avvenuti et al., 2020; Bergdahl et al., 2005; Kaul et al., 2021; Taren et al., 2015).

Interestingly, when analyzing the relationship between perceived stress and brain morphology, a positive association between amygdala volume and perceived stress is observed (Caetano et al., 2021; Hölzel et al., 2010). However, the way perceived stress affects brain function is still unclear, particularly if considering the small sample size of non-pathological studies in the literature (Archer et al., 2018; Jovanovic et al., 2011; Lebares et al., 2019; Soares et al., 2013b, 2013c, 2012; Taren et al., 2017; Wu et al., 2018).

Herein, we used a large cohort of resting-state fMRI data from healthy subjects of several ages to gain a deeper insight into the impact of perceived stress on the functional interactions between brain areas. Based on the morphological results of our previous study (Caetano et al., 2021), we started by evaluating the association of perceived stress with amygdala seed-based connectivity. Subsequently, we explored the disseminated effect of perceived stress on dynamic connectivity at a whole-brain level. We hypothesized that differences in perceived stress would be reflected in amygdala connectivity, as well as in the expression of functional connectivity patterns involving emotional processing regions.

3. Material and methods

3.1. Ethics Statement

This study followed the criteria outlined in the Declaration of Helsinki (59th amendment) and was approved by the national and local ethics review board committees (*Comissão Nacional de Protecção de Dados*, C*omissão de Ética para a Saúde of Hospital de Braga*, and *Subcomissão de ética para as ciências da vida e da saúde* from University of Minho). All participants were informed about the study's goals and signed informed consent. Informed consent was also signed by the parents of participants under the age of 18.

3.2. Participants and study design

This work gathered 252 participants. Being a healthy individual and having the capability to undergo an MRI session were the primary inclusion criteria. Non-acceptance or inability to understand informed consent, individual choice to withdraw from the study, presence of any comorbidity from the central nervous system, or diagnosis of any neuropsychiatric illness were all exclusion criteria.

The protocol of this study consisted of a single evaluation. First, participants were characterized in terms of age, sex, and psychosocial stress. For the psychological assessment, participants were required to fill out the 10-items perceived stress scale (PSS10) questionnaire to quantify chronic psychosocial stress in the last month. After this, participants were submitted to an MRI session, performing an anatomical acquisition and a resting-state fMRI.

The anatomical images were used to preprocess fMRI data. The resting-state scans were used to explore the association of perceived stress with static and dynamic brain connectivity. For the static connectivity, a seed-based approach was followed. For the dynamic connectivity, a whole-brain data-driven analysis was conducted.

3.3. Participant characterization

Participants' demographic and psychological characterization was made using SPSS version 23 (IBM, SPSS, Chicago, IL, USA). Each variable was checked for normality, and non-parametric tests were applied where the assumption was not met. Sex factor was used in between-groups comparisons. A correlation between PSS10 scores and age was also made. The statistical significance was established for $\alpha = 0.05$.

3.4. MRI data acquisition

The MRI acquisitions were made at the Hospital of Braga (Braga, Portugal), using a clinical approved Siemens Magnetom Avanto 1.5 T MRI scanner (Siemens Medical Solutions, Erlangen, Germany), with a 12-channel receive-only head coil. After the acquisition, all images were examined by a licensed neuro-radiologist to ensure that the scans were not adversely influenced by head motion and to confirm that participants did not have any pathologies or brain lesions.

3.4.1. Structural MRI

Anatomical acquisition consisted of one high-resolution T1-weighted Magnetization-Prepared Rapid Acquisition with Gradient Echo sequence (MPRAGE), with the following parameterization: voxel size = 1 × 1 mm^2, slice thickness = 1 mm repetition time (TR) = 2.73 s, echo time (TE) = 3.48 ms, flip angle (FA) = 7◦, field of view (FoV) = 256 mm, and 176 sagittal slices with no gap.

3.4.2. Resting-state functional MRI

Before the acquisition, participants were told to remain motionless with closed eyes, not to fall asleep, and not to think about anything specific. The fMRI acquisition consisted of a Blood Oxygenation Dependent Level (BOLD) sensitive echo-planar imaging (EPI), with the following parameterization: voxel size = 3.5 × 3.5 mm^2, slice thickness = 3.5 mm, TR = 2 s, TE = 30 ms, FA = 90°, FoV = 1344 mm, 30 axial slices, slice gap = 0.48 mm, and 180 volumes.

3.5. MRI data preprocessing

Results included in this manuscript come from preprocessing performed using *fMRIPrep* 1.4.1 (Esteban et al., 2021, 2018) (RRID:SCR_016216), which is based on *Nipype* 1.2.0 (Esteban et al., 2020; Gorgolewski et al., 2011) (RRID:SCR_002502).

3.5.1. Anatomical data preprocessing

The T1-weighted (T1w) image was corrected for intensity non-uniformity (INU) with N4BiasFieldCorrection (Tustison et al., 2010), distributed with ANTs 2.2.0 (Avants et al., 2008) (RRID:SCR_004757), and used as T1w-reference throughout the workflow. The T1w-reference was then skull-stripped with a *Nipype* implementation of the antsBrainExtraction.sh workflow (from ANTs), using OASIS30ANTs as target template. Brain tissue segmentation of cerebrospinal fluid (CSF), white matter (WM) and gray matter (GM) was performed on the brain-extracted T1w using fast (FSL 5.0.9, RRID:SCR_002823) (Zhang et al., 2001). Brain surfaces were reconstructed using recon-all (FreeSurfer 6.0.1, RRID:SCR_001847) (Dale et al., 1999), and the brain mask estimated previously was refined with a custom variation of the method to reconcile ANTs-derived and FreeSurfer-derived segmentations of the cortical gray-matter of Mindboggle (RRID:SCR_002438) (Klein et al., 2017)(Klein et al., 2017). Volume-based spatial normalization to two standard spaces (MNI152NLin2009cAsym, MNI152NLin6Asym) was performed through nonlinear registration with antsRegistration (ANTs 2.2.0), using brain-extracted versions of both T1w reference and

the T1w template. The following templates were selected for spatial normalization: *ICBM 152 Nonlinear Asymmetrical template version 2009c* [(Fonov et al., 2009), RRID:SCR_008796; TemplateFlow ID: MNI152NLin2009cAsym], *FSL's MNI ICBM 152 non-linear 6th Generation Asymmetric Average Brain Stereotaxic Registration Model* [(Evans et al., 2012), RRID:SCR_002823; TemplateFlow ID: MNI152NLin6Asym].

3.5.2. Resting-state data preprocessing

Before preprocessing, the first 5 volumes of each fMRI acquisition were discarded. For each subject, the following preprocessing steps were performed: First, a reference volume and its skull-stripped version were generated using a custom methodology of *fMRIPrep*. The BOLD reference was then co-registered to the T1w reference using *bbregister* (FreeSurfer) which implements boundary-based registration (Greve and Fischl, 2009). Co-registration was configured with nine degrees of freedom to account for distortions remaining in the BOLD reference. Head-motion parameters with respect to the BOLD reference (transformation matrices, and six corresponding rotation and translation parameters) were estimated before any spatiotemporal filtering using *mcflirt* (FSL 5.0.9, (Jenkinson et al., 2002)). BOLD runs were slice-time corrected using *3dTshift* from AFNI 20160207 ((Cox and Hyde, 1997), RRID:SCR_005927). The BOLD time-series (slice-time corrected) were resampled onto their original, native space by applying a single, composite transform to correct for head-motion and susceptibility distortions, and finally resampled into *MNI152NLin2009cAsym* space. Several confounding time-series were calculated based on the preprocessed BOLD: framewise displacement (FD), DVARS (rate of change of BOLD signal across the entire brain at each frame of data), and three region-wise global signals. FD and DVARS are calculated for each functional run, both using their implementations in *Nipype* (following the definitions by (Power et al., 2014)). The three global signals were extracted within the CSF, the WM, and the whole-brain masks. Additionally, a set of physiological regressors were extracted to allow for component-based noise correction (CompCor, (Behzadi et al., 2007)). Principal components were estimated after high-pass filtering the preprocessed BOLD time-series (using a discrete cosine filter with 128s cut-off) for the anatomical variant (aCompCor). A mask covering the subcortical regions was obtained by heavily eroding the brain mask, which ensures it does not include cortical GM regions. For aCompCor, components were calculated within the intersection of the aforementioned mask and the union of CSF and WM masks calculated in T1w space, after their projection to the native space of each functional run (using the inverse BOLD-to-T1w transformation). Components were calculated separately within the WM and CSF masks. For each CompCor decomposition, the k components with the largest singular values were retained, such

that the retained components' time series were sufficient to explain 50 percent of variance across the nuisance mask (CSF, WM, combined, or temporal). The remaining components were dropped from consideration. The mean CSF and WM signals, as well as the first 6 aCompCor components, the FD and the DVARS were regressed as confounds from the BOLD data using *fsl/regfilt*. Movement was considered excessive with a mean FD > 0.5 mm (Power et al., 2012), but none of the subjects exceeded this threshold and thus no subjects had to be excluded because of this. Finally, *fsl/maths* was used to spatially smooth (with a FWHM kernel of 6mm) and band-pass filter (between 0.01 and 0.08 Hz) the resulting time-series.

3.6. Amygdala Seed-Based connectivity

Seed-based connectivity analyses were performed using FSL (FMRIB Software Library, version 6.0, Analysis Group, FMRIB, UK) (Jenkinson et al., 2012; Smith et al., 2004; Woolrich et al., 2009). Individual seed connectivity maps were considered the variable of interest, perceived stress (measured by PSS10 scores) as the independent term, and age and sex as covariates. Due to the differences in magnitudes, all the variables were standardized prior to analysis.

The left and right amygdala masks were created using the Automated Anatomical Labeling (AAL) atlas (Rolls et al., 2015; Tzourio-Mazoyer et al., 2002). The mask of the right amygdala was centered in [32, 0, -30] (coordinates in mm) and composed of 248 voxels. With a voxel size of 220, the left amygdala mask was centered in [-24, -2, -28]. The mean time series of each seed region were extracted for each participant and cross-correlated with all other brain voxels' time series. The association with perceived stress (measured by PSS10) was estimated using the FSL *randomise* function, a non-parametric permutation method, considering 5000 permutations and α = 0.05 after threshold-free cluster enhancement (TFCE) and family-wise error rate (FWE-R) correction (Winkler et al., 2014). The statistically significant clusters obtained were labeled with the AAL2 (Rolls et al., 2015). The BrainNet Viewer software was used for visualization of results (Xia et al., 2013).

3.7. Dynamic functional connectivity

The dynamic functional connectivity analysis was made using the Leading Eigenvector Dynamics Analysis (LEiDA) method, which captures recurrent patterns of phase-locking between brain areas (Cabral et al., 2017; Vohryzek et al., 2020). Importantly, it allows estimating the probability of occurrence of each phase-

locking pattern in each fMRI scan, providing a quantitative measure to compare with perceived stress (measured by PSS10 scores).

The mean fMRI signal for each of the N=94 non-cerebellar brain regions of the AAL2 atlas was extracted for each subject and the signal phase computed using the Hilbert transform. After removing the first and last time points, at each of the T=178 time points, an instantaneous NxN functional connectivity matrix was computed as the cosine of the phase difference between each pair of brain regions, and the 1xN leading eigenvector (i.e., associated to the largest magnitude eigenvalue) was saved for each time point, generating a NxT matrix capturing the dominant pattern of phase interactions for each timepoint.

Previous works have shown that these patterns can be clustered into a reduced set of phase-locking patterns, where the subsets of brain areas shifting in phase from the rest of the brain reveal known resting-state networks from the literature (Lord et al., 2019; Vohryzek et al., 2020). Since the number of patterns defined is not a fixed number and only affects the sensitivity of the method, we ran the algorithm from k = 2 to k = 20, with k representing the number of patterns to cluster the data into (using the cosine distance and 500 iterations per k). For each of the 252 participants s, the probability of occurrence P(s,c,k) was calculated for each pattern c obtained for each k (with c=1,..,k). For the statistical analysis, we used a partial correlation to measure the association between each pattern probability and PSS10 scores while controlling for age and sex factors. Notably, the significance was established for α = 0.05, and the obtained *p*-values were corrected for the number of clusters tested (e.g., for k = 16, considering 16 independent multiple comparisons, the *p*-value was divided by 16).

4. Results

4.1. Cohort Characterization

The participants' socio-demographic, psychological, and volumetric brain characterization (left and right amygdala, total GM, and eTIV) are presented in Table 1. Additionally, the descriptive statistics of all cortical and subcortical regions can be consulted in Supplementary Table A1.

Table 1. Demographic and psychological characterization of participants. Demographic, psychological and brain morphometry characterization of the population included in this study.

	Demographic		**Psychological**	**Brain Volume (mm^3)**			
	N (%)	Age (years)	Perceived Stress (PSS10)	Right amygdala	Left amygdala	Total GM	eTIV
Global population	252 (100%)						
min		15	1	$9.46x10^2$	$8.50x10^2$	$4.39x10^5$	$1.14x10^6$
max		84	34	$2.62x10^3$	$2.14x10^3$	$8.35x10^5$	$1.99x10^6$
Mean ± SD		39.2 ± 21.20	15.4 ± 6.82	$1.43x10^3 \pm 2.21x10^2$	$1.35x10^3 \pm 2.10x10^2$	$6.27x10^5 \pm 7.77x10^4$	$1.56x10^6 \pm 1.65x10^5$
Male	109 (43.3%)						
min		15	2	$1.04x10^3$	$1.01x10^3$	$5.05x10^5$	$1.24x10^6$
max		80	29	$2.62x10^3$	$2.14x10^3$	$8.35x10^5$	$1.99x10^6$
Mean ± SD		42.6 ± 21.72	14.3 ± 6.44	$1.55x10^3 \pm 2.42x10^2$	$1.45x10^3 \pm 2.08x10^2$	$6.53x10^5 \pm 8.25x10^4$	$1.66x10^6 \pm 1.58x10^5$
Female	143 (56.7%)						
min		15	1	$9.46x10^2$	$8.50x10^2$	$4.39x10^5$	$1.14x10^6$
max		84	34	$1.73x10^3$	$1.69x10^3$	$7.37x10^5$	$1.80x10^6$
Mean ± SD		36.7 ± 20.51	16.3 ± 7.00	$1.35x10^3 \pm 1.57x10^2$	$1.28x10^3 \pm 1.76x10^2$	$6.07x10^5 \pm 6.76x10^4$	$1.49x10^6 \pm 1.23x10^5$

eTIV. Estimated Intracranial Volume; GM. Gray matter; SD. Standard Deviation.

A Mann-Whitney *U* test indicated that no age differences were found between sex (U = 6940.5, p = 0.136).

An independent sample *t*-test indicated higher perceived stress scores in females than in males (t (250) = -2.212, p = 0.028, d = 0.28). A negative association between PSS10 scores and age was also found (r (252) = -0.226, p < 0.001).

Regarding brain volumes, both total GM and eTIV were significantly higher for males than females *(*U = 5491, p < 0.001, r = 0.25; and t (250) = 9.691, p < 0.001, d = 1.25 respectively).

4.2. Static Seed-Based connectivity

A positive association between PSS10 scores and right amygdala seed-based connectivity was observed within 17 clusters. As illustrated in Figure 1, the cluster with the highest connectivity strength is peaked in the right Superior Frontal Gyrus (SFG) (cluster 1), also embracing part of the right Middle Frontal Gyrus (MFG). A cluster centered in the right MFG (2) and another in the right SFG (3) revealed almost the same strength of association. Interestingly, the next cluster presenting enhanced connectivity is on the right superior parietal lobule, specifically on the right precuneus (4). Next, centered in the MFG, cluster number 5 is the only one placed entirely on the left hemisphere. We also found clusters peaked in the anterior and middle right cingulate (clusters 7 and 14), a region known for its involvement in emotional processing and behavior regulation. Importantly, we observed that several other clusters of the SFG and MFG tend to synchronize with the right amygdala when perceived stress is increased (clusters 8, 10, 12 in SFG and clusters 9 and 15 [only 4 voxels] in the MFG). Importantly, cluster 10 (SFG) and cluster 9 (MFG), although with considerable voxel size (313 and 188, respectively), did not reveal heightened association with the right amygdala seed-region, as expected due to their size. Clusters 6 and 11 are peaked in the Inferior Frontal Gyrus (IFG), on the pars opercularis and pars triangularis, respectively. Finally, with the most negligible strength of association and lowest voxels size, clusters 16 (6 voxels) and 17 (2 voxels) are also centered in the IFG (pars triangularis and pars orbitalis). A more detailed description of all the clusters in which connectivity with the right amygdala is positively associated with stress is presented in Table 2.

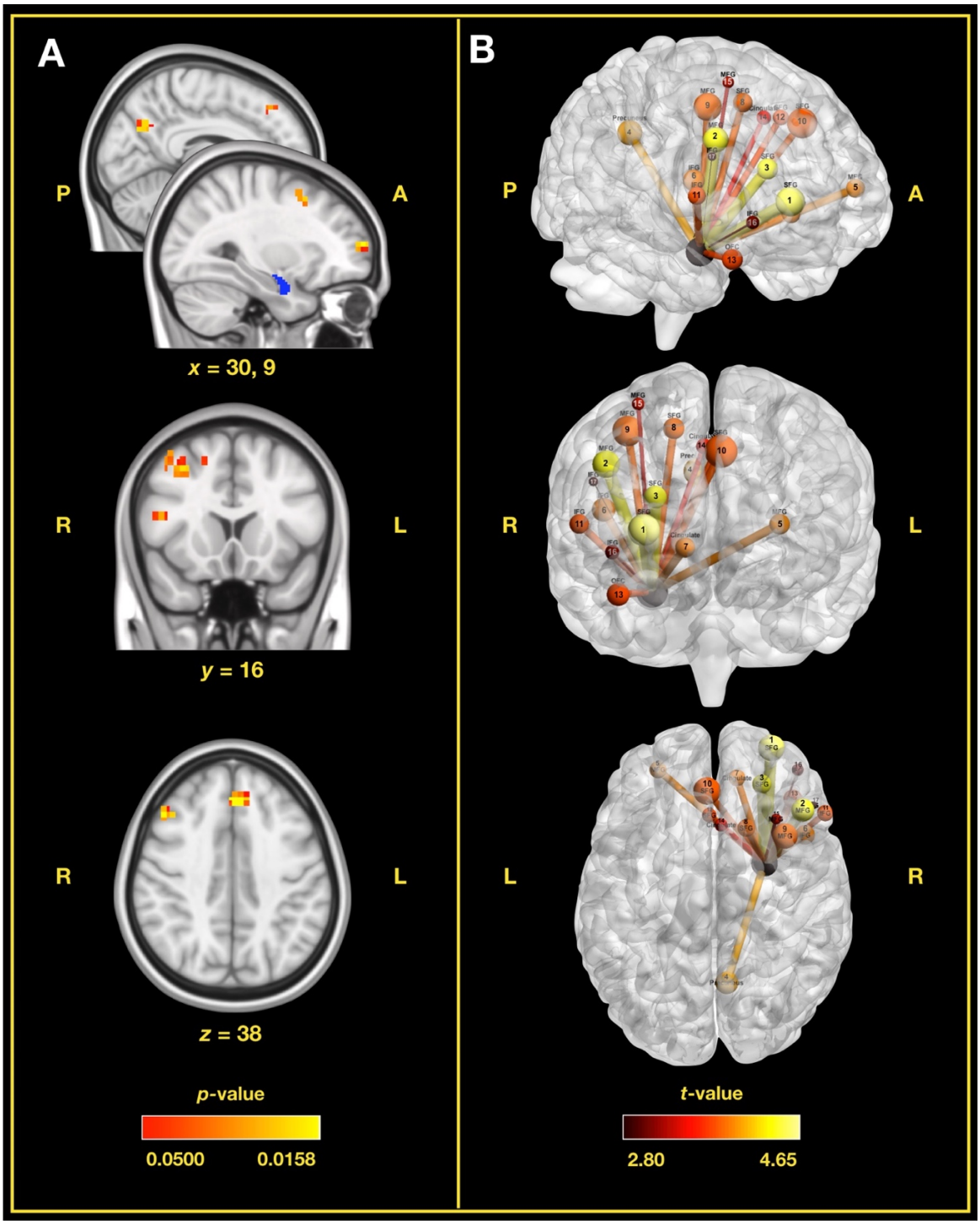

Figure 1. Results from the static connectivity: Positive association of right amygdala seed-based connectivity with PSS10 scores. A positive association between PSS10 scores and right amygdala seed-based connectivity was observed within 17 clusters. **A) Representation of the most significant clusters obtained**. Each voxel is colored by its statistical significance, and the right amygdala seed region is colored in blue. **B) 3D representation of all clusters obtained, as well as its connection with right amygdala.** Each cluster is represented by a sphere colored by the strength of the connectivity (stronger connection in yellow). Spheres sizes were defined as an approximation of clusters sizes, using a pre-defined range interval.
Seed-Based connectivity analysis were made using FSL, with individual seed connectivity maps as the variable of interest, PSS10 scores as the independent term, and age and sex as covariates. The statistical significance was considered for *p*-values < 0.05, after threshold-free cluster enhancement (TFCE) and family-wise error rate (FWE-R) correction.

Table 2. Clusters resulted from the regression analysis between the right amygdala seed-based connectivity and PSS10 scores. A positive association between perceived stress scores and amygdala connectivity was observed in 17 clusters.

The seed-based connectivity analysis was performed using FSL. The individual maps of the seed (right amygdala) connectivity were used as the variable of interest, PSS10 as the independent term, and age and sex as covariates. Due to the differences in magnitudes, all the variables were standardized prior to analysis. The association was estimated using the FSL *randomise* function, considering 5000 permutations and α = 0.05 after threshold-free cluster enhancement (TFCE) and family-wise error rate (FWE-R) correction. The results are presented by order of significance and the brain regions were labeled according to the automated anatomical atlas 2 (AAL2).

Cluster Index	Cluster size	Peak					AAL2 description	Brain Region Label
		t-value	*p*-value*	coordinates (*mm*)				
				x	*y*	*z*		
1	257	4.643	0.016	42	62	-4	67% (4) Frontal Sup 2 R 33% (6) Frontal Mid 2 R	SFG (dorsolateral) R MFG R
2	98	4.471	0.016	48	24	38	92% (6) Frontal Mid 2 R 8% (10) Frontal Inf Tri R	MFG R IFG (triangular part) R
3	36	4.417	0.025	24	36	20	71% (4) Frontal Sup 2 R 29% (6) Frontal Mid 2 R	SFG (dorsolateral) R MFG R
4	97	4.027	0.025	10	-70	28	87% (72) Precuneus R 11% (38) Cingulate Mid R	Precuneus R Middle Cingulate & Paracingulate Gyri R
5	22	3.932	0.043	-26	50	8	70% (5) Frontal Mid 2 L 30% (3) Frontal Sup 2 L	MFG L SFG (dorsolateral) L
6	42	3.891	0.030	48	16	14	100% (8) Frontal Inf Oper R	IFG (opercular part) R
7	20	3.861	0.041	14	44	2	45% (36 Cingulate Ant R 40% (22) Frontal Med Orb R 15% (20) Frontal Sup Medial R	Anterior Cingulate & Paracingulate Gyri R SFG (medial orbital) R SFG (medial) R
8	26	3.800	0.042	16	20	46	100% (4) Frontal Sup 2 R	SFG (dorsolateral) R
9	188	3.791	0.023	32	14	48	99% (6) Frontal Mid 2 R	MFG R
10	313	3.787	0.018	-2	32	38	73% (19) Frontal Sup Medial L 21% (20) Frontal Sup Medial R	SFG (medial) L SFG (medial) R
11	18	3.750	0.038	58	24	2	100% (10) Frontal Inf Tri R	IFG (triangular part) R
12	11	3.706	0.046	-2	22	42	82% (19) Frontal Sup Medial L 18% (15) Supp Motor Area L	SFG (medial) L Supplementary Motor Area L
13	36	3.686	0.032	42	28	-22	81% (30) OFCpost R 11% (32) OFClat R 8% (28) OFCant R	POG R LOG R AOG R
14	8	3.513	0.048	6	18	44	50% (38) Cingulate Mid R 50% (20) Frontal Sup Medial R	Middle cingulate & paracingulate gyri R SFG (medial) R
15	4	3.289	0.048	34	22	60	100% (6) Frontal Mid 2 R	MFG R
16	6	3.031	0.048	44	46	-4	50% (12) Frontal Inf Orb 2 R 33% (10) Frontal Inf Tri R 17% (6) Frontal Mid 2 R	IFG (pars orbitalis) R IFG (triangular part) R MFG R
17	2	2.815	0.050	52	28	28	100% (10) Frontal Inf Tri R	IFG (triangular part) R

** with TFCE and) FWE-R correction at a significance level of .05. SFG. Superior Frontal Gyrus; MFG. Middle Frontal Gyrus; IFG. Inferior Frontal Gyrus; POG. Posterior Orbital Gyrus; LOG. Lateral Orbital Gyrus; AOG. Anterior Orbital Gyrus.*

When exploring the positive association between PSS10 scores and left amygdala seed-based connectivity, we found no significant result for the statistical significance of $\alpha = 0.05$. Nonetheless, when changing statistical significance for $\alpha = 0.1$ to further investigate the tendency of association, we found a cluster peaked in the SFG ($x = 24$, $y = 56$, $z = 14$, in mm; cluster size = 36; peak p-value = 0.065 and cluster mean p-value = 0.07). Interestingly, this cluster overlaps with cluster number 1 reported above (Figure 1), which has been shown to have the highest connectivity strength with the right amygdala. A visual representation of these results is presented in Supplementary Figure A1.

There were no significant negative associations between PSS10 scores and right amygdala seed-based connectivity, nor between PSS10 and left amygdala seed-based connectivity.

4.3. Dynamic Functional Connectivity

The LEiDA analysis revealed a particular pattern of phase-locking between brain areas whose probability of occurrence was negatively associated with PSS10 scores (detected for a partition into K = 16 clusters, cluster c = 4, with $p_{corr} = 0.0306$ corrected for the number of independent patterns compared and controlled for age and sex). Interestingly, the same functional subsystem obtained with K = 19, C = 4 also survived statistical correction (see Supplementary Figure A2 for details about all states found and Supplementary Table A2 for all the p-values and correlation coefficients).

As shown in Figure 2A, this pattern is characterized by a phase shift in the fMRI signals of the left and right hippocampus, the left and right amygdala, the left and right parahippocampal gyrus, and the left superior and middle temporal pole. We note that the sign of phase projections is arbitrary and that the vector is bidirectional, meaning simply that when this pattern occurs the brain areas with a given sign increase their fMRI signal, while the areas with opposite sign decrease their fMRI signal or vice-versa.

This pattern of activity where the amygdala and hippocampus are in anti-phase with the rest of the brain was found to occur significantly more often in participants with lower perceived stress (Figure 2B). Conversely, participants with high stress scores expressed this pattern less often. Interestingly, these results not only align but also provide insights into the findings from the seed-based analysis. Indeed, in the LEiDA analysis, the pattern occurring less often in participants with higher perceived stress is a pattern where the right amygdala (red arrow in Figure 2A) is strongly phase shifted with respect to the areas in blue.

In subfigures B1 and B2 of Figure 2, an example of two subjects with distinct PSS10 scores are presented (Subject 1 with PSS10 = 30, and Subject 2 with PSS10 = 4). By focusing on the gray patches (which identify the periods of state occurrence), we observed that the significant state was less dominant in stressed Subject 1 (only 2 small periods) than in the non-stress Subject 2 (5 times and in more extended periods). In addition, when looking at the BOLD signals, a higher synchronization is observed in stress Subject 1 than in non-stressed Subject 2. Interestingly, desynchronization is particularly noticed during the periods of state occurrence. These differences are enhanced when looking to the right amygdala (represented in the red line) and comparing it to the majority of the seed-based regions (dark blue line).

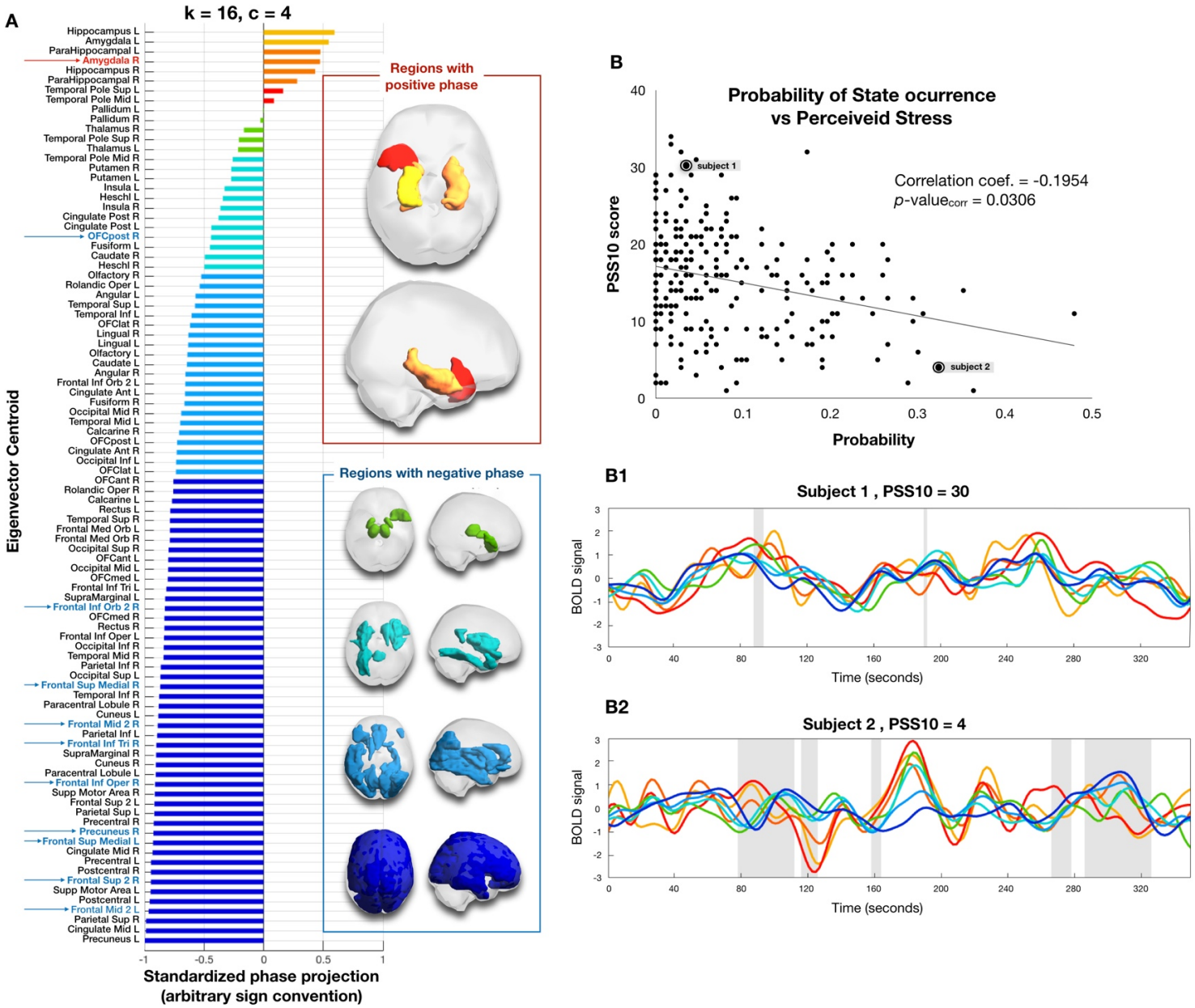

Figure 2. Lower perceived stress relates to more counterbalanced activity between amygdala-hippocampus and the rest of the brain. **A)** The functional phase-locking pattern represented by the cluster centroid V_c obtained for k = 16, c = 4. Elements in $V_c(n)$ are sorted in descending order and colored (from orange to dark blue) according to their relative phase shift. The arrows on the left indicate the seed region (red) and the significant clusters (blue) from the seed-based analysis. On the right, a 3D rendering of the brain regions color-coded according to $V_c(n)$. **B)** The probability of occurrence of this pattern is plotted against PSS10 scores for all 252 subjects, as well as the trendline of the negative association found. **B1-B2)** For two representative subjects, the BOLD signals averaged across subsystems with the same color in panel A. The grey patches in the background highlight the time points when this pattern was detected, revealing clearly more occurrence for the subject with lower perceived stress. Notably, even when this pattern is not detected, there is clearly less synchronicity between the fMRI signals in subject 2.

5. Discussion

In the present study, we used a sizeable cohort of healthy subjects of several ages to explore the interaction of perceived stress with the brain's static and dynamic connectivity. Static connectivity results show that increases in perceived stress are associated with stronger right amygdala connectivity with several frontal cortical nodes. On the other hand, the dynamic analysis revealed the existence of a functional state involving the amygdala and hippocampi, in which the probability of occurrence was found to negatively associate with the PSS10 scores.

The hypothesis that PSS10 scores are associated with right amygdala connectivity was verified mainly in the right prefrontal cortex, right precuneus, and right anterior and middle cingulate. In addition, although not achieving statistical significance, a tendency of increased connectivity between the left amygdala and right PFC was also observed. These results confirm the relevance of the pattern of connectivity between the amygdala and frontal cortical regions when processing emotional stimuli. Interestingly, this association between subjective psychological state and prefrontal-amygdala connectivity has been observed in previous work (Cerqueira et al. 2008; Killgore, 2013).

Curiously, our data also highlight the relevance of distinct patterns of brain hemispheric connectivity in stress response, as suggested by previous literature. Indeed, a previous study has shown that the right PFC activity is associated with increased emotionality (positively associating with amygdala activity), whereas the left PFC relates with the downregulation of negative emotions (negatively associating with amygdala activity) (Johnstone et al., 2007). Another study reveals that increases in self-reported sleep were negatively associated with distress severity and right amygdala-prefrontal FC, whereas no significant results were observed on the left hemisphere (Killgore, 2013). Moreover, in a meta-analysis on brain activity in response to stress, the bias of the right hemisphere activation of the neural correlates of stress is also noticed, particularly in the right superior temporal gyrus (STG) and IFG (Kogler et al., 2015). Therefore, our data seems to reflect the contrast between the right hemisphere dominance on stress regulation and emotional processing, contrasting to the left prominence on linguistic and motor functions (Cerqueira et al., 2008).

Our findings contrast with a research with a smaller sample size, in which the right amygdala-ventromedial prefrontal cortex (vmPFC) FC was negatively related in young adults, without significant correlations being observed in adults (Wu et al., 2018). Furthermore, inconsistencies are emphasized by another study in

which stronger resting-state connectivity between the left, and not the right, amygdala and (bilateral) regions such as MFG, anterior cingulate and thalamus, is observed in subjects with higher levels of discrimination (Clark et al., 2018).

From a higher-level perspective, our seed-based results show alterations in the frontoparietal network, which is known to be involved in several regulation processes (Banks et al., 2007; Marek and Dosenbach, 2018). Most importantly, changes in fronto-limbic and fronto-parietal circuits have been linked to numerous stress-related psychopathologies (Banks et al., 2007; Berboth and Morawetz, 2021; Cerullo et al., 2012; Johnson et al., 2018; Li et al., 2015; Marek and Dosenbach, 2018). Indeed, rather than hamper specific individual brain regions' mechanisms, stress affects the connectivity within brain circuits causing a global impact at the neuromatrix (Sousa, 2016). To confirm the stress repercussions at the network level, the study of dynamic connectivity is of value.

Whereas static connectivity tells us, on average, how synchronized were two brain regions (spatial resolution but no temporal definition), the dynamic analysis identifies brain states resulting from spontaneous fluctuations of brain activity, thus providing spatiotemporal information (Bassett and Sporns, 2017; Biswal et al., 1995; Menon and Krishnamurthy, 2019).

Using LEiDA, besides the identification of most dominant brain states, it is possible to distinguish which patterns (or states) associate with variables of interest (Cabral et al., 2017; Magalhães et al., 2021). Herein, our results show that increases in perceived stress are negatively associated with the occurrence of a functional state in which subcortical regions, including the amygdala and hippocampus, are shifted from the other regions of the brain, with the most significant shifts being observed in PFC regions.

A previous study on clinical stressed subjects demonstrated differential dynamic activation of right frontal areas, relating it to a PFC dysfunction and, consequently, to a diminished ability to downregulate amygdala activity (Kolassa et al., 2007). Using a combination of static and dynamic techniques, another research highlighted the activity of frontal and parietal regions as biomarkers of negative stress (García-Martínez et al., 2020).

When combining static with dynamic connectivity results, we demonstrate that the increase of perceived stress matches an increase in amygdala connectivity, alongside a reduction in the occurrence of the amygdala anti-phase state. Importantly, it is during this anti-phase state that major desynchronization in healthy subjects is observed. Indeed, denoting that state transitions seem to occur in periods of

intermediate synchronization or desynchronization (not in the extremes), our results follow previous evidences supporting the critical brain hypothesis (Fontenele et al., 2019). In short, criticality claims that neurons networks operate close to a critical point, easily crossing to a state in which the activity gradually increases, or to a phase in which the activity rapidly fades away (Beggs and Timme, 2012). Notably, several processing functions are optimized at this critical point, with the ability of the brain to be critical (and therefore shifting across phases) considered fundamental on healthy subjects (Beggs and Timme, 2012).

This study has limitations. Its cross-sectional, rather than longitudinal, design is one of the most significant drawbacks of our research. However, if on one side we cannot infer any causality regarding brain dynamics and perceived stress associations (limitation), on the other hand we were able to identify characteristics of a stressed brain that persist across the lifespan (advantage). The conductance of dynamic data-driven analysis (LEiDA) is still quite novel and in the present study confined to a non-clinical cohort. In light of these issues, future research should focus on expanding the current observations to broader cohorts and in a longitudinal perspective.

In the present study we explored the relationship between perceived stress and brain connectivity in a large cohort of healthy subjects with a broad age range. Our data reveals that increases in perceived stress were associated with altered patterns of both static and dynamic amygdala connectivity with frontal cortical regions. More specifically, we show that increased perceived stress is directly associated with increased amygdala connectivity with frontal cortical regions, which is driven by a reduced occurrence of an activity pattern where the signals in the amygdala and the hippocampus evolve in opposite directions with respect to the rest of the brain. In summary, these results reinforce the detrimental effect of in-phase synchronicity between subcortical and cortical brain areas, but also demonstrate the protective effect of counterbalanced activity between brain subsystems.

6. Data Accessibility statement

The data that support the findings of this study are available from the corresponding author upon reasonable request.

7. Code availability

FSL software is available by the authors at https://fsl.fmrib.ox.ac.uk/fsl/fslwiki/FslInstallation and LEiDA scripts at GitHub (https://github.com/juanitacabral/LEiDA).

8. CRediT author statement

Conceptualization: IC, NS. **Methodology**: IC, SF, JC, NS. **Software**: IC, SF, JC. **Validation**: IC, LA, TCC, CL, MPP, JC. **Formal analysis**: IC, SF, JC. I**nvestigation**: LA, TCC, AC, SF, CPN, JMS, NG, RS, JR, PMarques, PSM, AJR, PM, RM, MPP. **Resources**: AJR, NCS, PM, NS. **Data Curation**: AC, RM. **Writing - Original Draft**: IC. **Writing - Review & Editing**: JC, NS. **Visualization**: IC, JC, NS. **Supervision**: NS. **Project administration**: NS. **Funding acquisition**: AJR, NCS, PM, NS.

9. Acknowlegments

This work was funded by National funds, through the Foundation for Science and Technology (FCT) [projects UIDB/50026/2020, UIDP/50026/2020, PTDC/MED-NEU/29071/2017]; by BIAL foundation [grants PT/FB/BL-2016-206, BIAL 30-16]; Fundação Calouste Gulbenkian [contract grant P-139977]; and the European Commission (FP7) [contract HEALTH-F2-2010-259772].

Fellowship grants supported IC, LA, and AC through the FCT [grants number SFRH/BD/133006/2017, SFRH/BD/101398/2014, NORTE-08-5369-FSE-000041] from the Health Science program.
JC is funded by FCT grant CEECIND/03325/2017.

10. Appendix A. Supplementary data

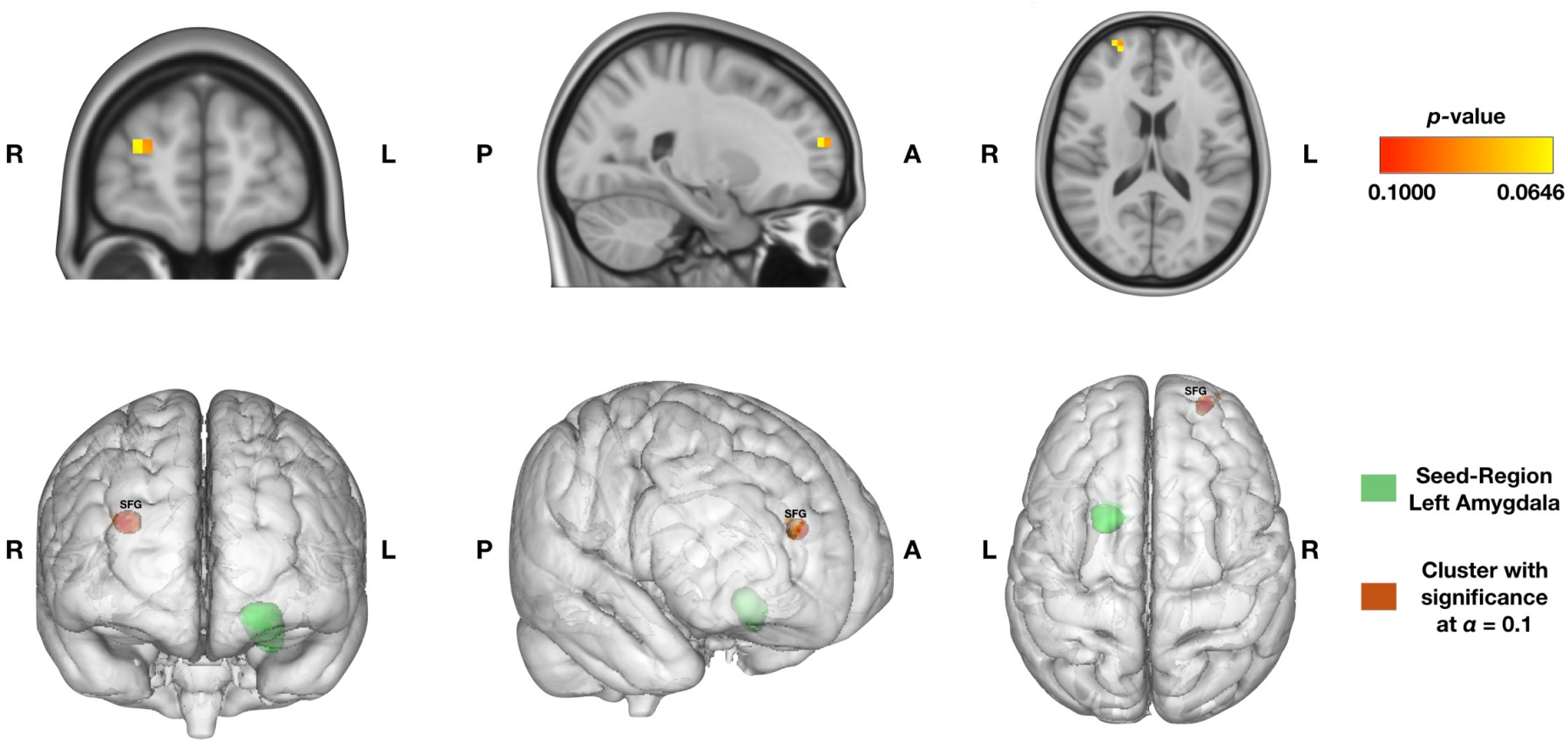

Supplementary Figure A1. Association of the left amygdala seed-based connectivity with PSS10 scores for a statistical significance of $\alpha = 0.1$. Left amygdala seed-based analyses did not reveal statistical significance for $\alpha = 0.05$. When changing statistical significance for $\alpha = 0.1$ to explore the tendency of association between PSS10 scores and the left amygdala seed-based connectivity, a cluster in the Superior Frontal Gyrus (SFG) [peak in $x = 24$, $y = 56$, $z = 14$ (in mm); cluster size = 36; cluster mean p-value = 0.07] was found. Importantly, this cluster overlaps with the cluster number 1 of Figure 1, which has shown the highest connectivity strength with right amygdala when exploring the positive associations of right amygdala seed-based connectivity with PSS10 scores.

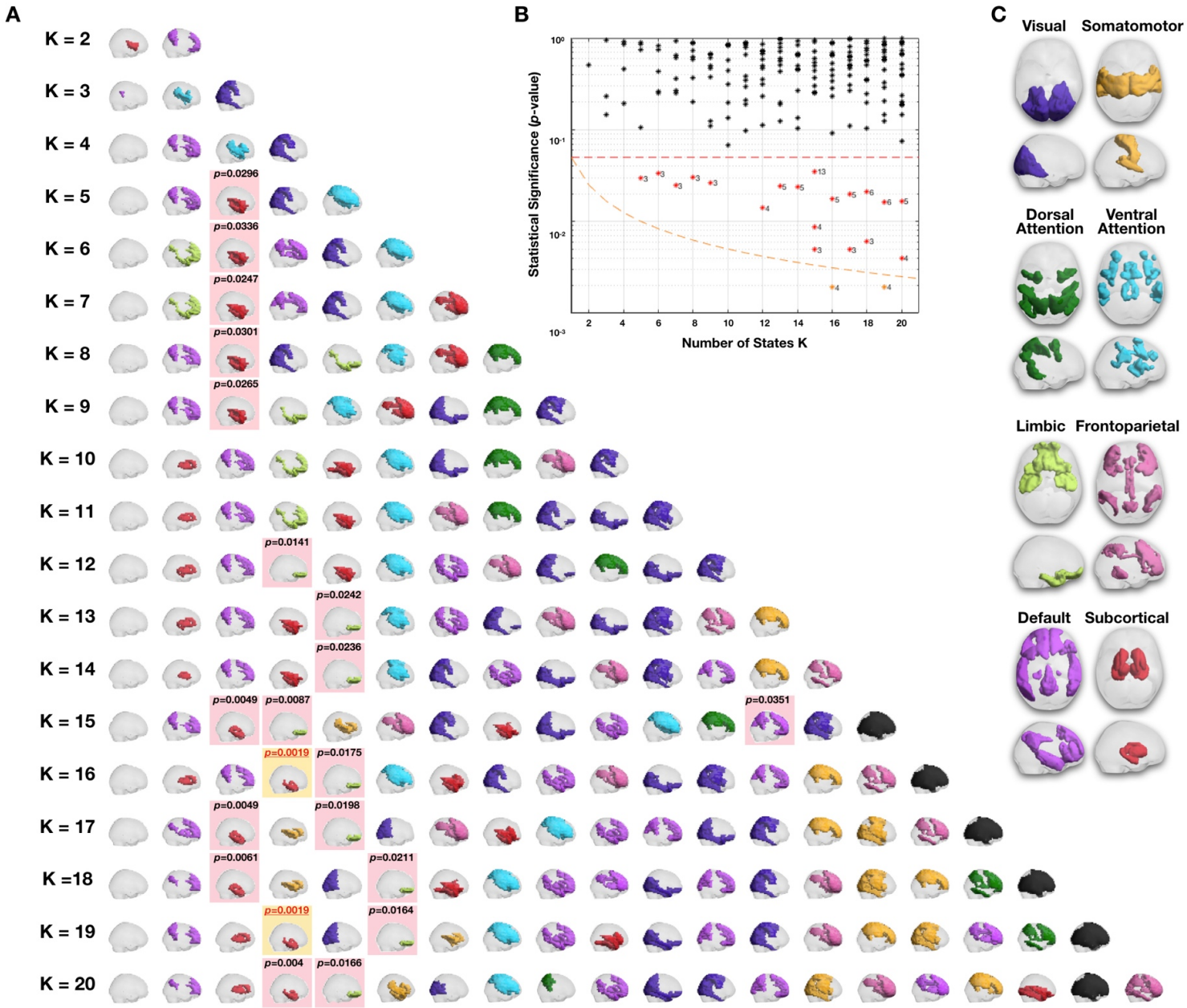

Supplementary Figure A2. Results from the association of LEiDA states with the PSS10 scores. Phase lock states of LEiDA analysis and significance for state probability for all k's between 2 and 20. **A)** Sagittal view over a mesh of the areas composing each state colored according to most represented resting state network (RSN). The background of states with significance surviving a threshold of $p < 0.05$ are colored in light red with the representation of the respective *p*-value. States surviving a threshold of $p < 0.05$ after multiple comparisons correction have their background colored in dark yellow with underlined *p*-values. **B)** Plots of the uncorrected *p*-values for each state of all k iterations. The red line indicates the threshold of $p < 0.05$, and the orange line represents the threshold for significance after multiple comparisons correction for the number of k states. **C)** Color code of each RSN. Representation of the 7 Yeo RSN, plus an additional subcortical network

Supplementary Table A1. Descriptive statistics of cortical, subcortical, and global brain volumes (in mm³). Volumes presented below are representative of a Portuguese population and were computed using the *fMRIprep* FreeSurfer derivatives.

	Left Hemisphere		Right Hemisphere	
	Mean	Standard Deviation	Mean	Standard Deviation
Cortical ROI				
Banks of the Superior Temporal Sulcus	2382	484	2182	408
Caudal Anterior-Cingulate Cortex	1806	444	1978	490
Caudal Middle Frontal Gyrus	6269	1266	6082	1243
Cuneus Cortex	2968	516	3304	651
Entorhinal Cortex	1995	358	1971	380
Fusiform Gyrus	9292	1270	9142	1347
Inferior Parietal Cortex	11836	2226	14302	2591
Inferior Temporal Gyrus	11192	1865	10897	1739
Isthmus–Cingulate Cortex	2531	430	2385	427
Lateral Occipital Cortex	11331	1752	11715	1846
Lateral Orbital Frontal Cortex	7808	1080	7418	1074
Lingual Gyrus	6422	1071	6928	1138
Medial Orbital Frontal Cortex	5117	720	5363	710
Middle Temporal Gyrus	11026	1945	11771	1964
Parahippocampal Gyrus	2060	282	1921	265
Paracentral Lobule	3413	477	3830	561
Pars Opercularis	4696	888	3865	742
Pars Orbitalis	2376	396	2749	465
Pars Triangularis	3604	741	4117	826
Pericalcarine Cortex	2218	447	2513	499
Postcentral Gyrus	9242	1473	8975	1441
Posterior-Cingulate Cortex	3139	559	3204	533
Precentral Gyrus	13166	1785	13075	1785
Precuneus Cortex	9386	1490	9828	1606
Rostral Anterior Cingulate Cortex	2579	538	1911	420
Rostral Middle Frontal Gyrus	15134	2770	15469	2826
Superior Frontal Gyrus	22286	3552	21491	3491
Superior Parietal Cortex	12556	2111	12238	2059
Superior Temporal Gyrus	12118	1963	11284	1829
Supramarginal Gyrus	11197	2187	10001	1848
Frontal Pole	917	160	1079	181
Temporal Pole	2370	337	2474	328
Transverse Temporal Cortex	1117	234	883	171
Insula	7142	904	7174	1018
Subcortical ROI				
Thalamus Proper	7281	1021	7089	971
Caudate	3578	481	3705	497
Putamen	4903	666	4900	640
Pallidum	1949	261	1869	240
Hippocampus	3752	408	3841	417
Amygdala	1352	210	1432	221
Accumbens	593	122	528	110

Global Volumes	**Mean**	**Standard Deviation**
eTIV	1.56x10⁶	1.65x10⁵
GM	6.27x10⁵	7.77x10⁴
WM	4.58x10⁵	5.86x10⁴

ROI. Region-of-interest; eTIV. Estimated Intracranial Volume; GM. Gray matter; WM. White matter.

Supplementary Table A2. Results from the probability of state occurrence associated with PSS10 scores. Representation of the uncorrected and corrected statistical significance, plus the correlation coefficient for each K clustering level (lines) and S state (columns), in first, second and third rows, respectively. Statistical significance was stablished for α = 0.05. Statistically significant *p*-values are presented in bold and underlined. Multiple comparisons correction was made considering the number of states for each k clustering level. States that survive correction for multiple comparisons are highlighted in gray.

	S1	S2	S3	S4	S5	S6	S7	S8	S9	S10	S11	S12	S13	S14	S15	S16	S17	S18	S19	S20
K=2	0.5056	0.5056	-	-	-	-	-	-	-	-	-	-	-	-	-	-	-	-	-	-
	1.0111	1.0111	-	-	-	-	-	-	-	-	-	-	-	-	-	-	-	-	-	-
	-0.0423	0.0423	-	-	-	-	-	-	-	-	-	-	-	-	-	-	-	-	-	-
K=3	0.2314	0.1474	0.9530	-	-	-	-	-	-	-	-	-	-	-	-	-	-	-	-	-
	0.6941	0.4421	2.8590	-	-	-	-	-	-	-	-	-	-	-	-	-	-	-	-	-
	0.0760	-0.0919	-0.0037	-	-	-	-	-	-	-	-	-	-	-	-	-	-	-	-	-
K=4	0.4643	0.8645	0.1946	0.9186	-	-	-	-	-	-	-	-	-	-	-	-	-	-	-	-
	1.8571	3.4580	0.7784	3.6745	-	-	-	-	-	-	-	-	-	-	-	-	-	-	-	-
	0.0465	0.0108	-0.0823	0.0065	-	-	-	-	-	-	-	-	-	-	-	-	-	-	-	-
K=5	0.1049	0.8599	**0.0296**	0.8978	0.7393	-	-	-	-	-	-	-	-	-	-	-	-	-	-	-
	0.5246	4.2994	0.1479	4.4889	3.6965	-	-	-	-	-	-	-	-	-	-	-	-	-	-	-
	0.1028	-0.0112	-0.1376	0.0082	-0.0212	-	-	-	-	-	-	-	-	-	-	-	-	-	-	-
K=6	0.2513	0.2637	**0.0336**	0.4358	0.7458	0.8314	-	-	-	-	-	-	-	-	-	-	-	-	-	-
	1.5078	1.5821	0.2015	2.6146	4.4745	4.9882	-	-	-	-	-	-	-	-	-	-	-	-	-	-
	0.0728	0.0710	-0.1345	-0.0495	-0.0206	0.0135	-	-	-	-	-	-	-	-	-	-	-	-	-	-
K=7	0.2508	0.2653	**0.0247**	0.3593	0.6052	0.6548	0.9336	-	-	-	-	-	-	-	-	-	-	-	-	-
	1.7559	1.8574	0.1728	2.5151	4.2363	4.5839	6.5350	-	-	-	-	-	-	-	-	-	-	-	-	-
	0.0729	0.0707	-0.1421	-0.0582	-0.0329	0.0284	0.0053	-	-	-	-	-	-	-	-	-	-	-	-	-
K=8	0.3675	0.7383	**0.0301**	0.6196	0.2008	0.8796	0.8953	0.5817	-	-	-	-	-	-	-	-	-	-	-	-
	2.9400	5.9064	0.2406	4.9566	1.6067	7.0368	7.1625	4.6537	-	-	-	-	-	-	-	-	-	-	-	-
	0.0572	-0.0212	-0.1372	-0.0315	0.0812	-0.0096	-0.0084	0.0350	-	-	-	-	-	-	-	-	-	-	-	-
K=9	0.3774	0.6756	**0.0265**	0.1113	0.6559	0.4725	0.4969	0.6069	0.1252	-	-	-	-	-	-	-	-	-	-	-
	3.3969	6.0803	0.2385	1.0016	5.9030	4.2524	4.4722	5.4623	1.1265	-	-	-	-	-	-	-	-	-	-	-
	0.0561	-0.0266	-0.1403	0.1010	0.0283	-0.0456	0.0432	0.0327	-0.0972	-	-	-	-	-	-	-	-	-	-	-
K=10	0.4382	0.8404	0.3110	0.1990	0.0683	0.8519	0.5725	0.4399	0.8247	0.1337	-	-	-	-	-	-	-	-	-	-
	4.3819	8.4039	3.1100	1.9898	0.6834	8.5190	5.7249	4.3992	8.2468	1.3369	-	-	-	-	-	-	-	-	-	-
	0.0492	0.0128	-0.0643	0.0815	-0.1155	0.0119	0.0359	0.0491	-0.0141	-0.0951	-	-	-	-	-	-	-	-	-	-
K=11	0.3865	0.8755	0.3481	0.2086	0.0968	0.7859	0.6595	0.2956	0.8998	0.8428	0.1896	-	-	-	-	-	-	-	-	-
	4.2513	9.6306	3.8294	2.2943	1.0651	8.6452	7.2550	3.2515	9.8974	9.2712	2.0851	-	-	-	-	-	-	-	-	-
	0.0550	0.0100	-0.0596	0.0798	-0.1053	0.0173	-0.0280	0.0664	-0.0080	-0.0126	-0.0832	-	-	-	-	-	-	-	-	-
K=12	0.4970	0.7384	0.4743	**0.0141**	0.1116	0.6730	0.7171	0.3547	0.8525	0.3164	0.5814	0.2309	-	-	-	-	-	-	-	-
	5.9642	8.8604	5.6915	0.1692	1.3390	8.0764	8.6052	4.2564	10.2302	3.7968	6.9768	2.7705	-	-	-	-	-	-	-	-
	0.0432	-0.0212	-0.0455	0.1551	-0.1009	0.0268	-0.0230	-0.0588	0.0118	0.0636	-0.0350	-0.0760	-	-	-	-	-	-	-	-
K=13	0.5045	0.8762	0.4326	0.1233	**0.0242**	0.7930	0.5634	0.9803	0.5946	0.7152	0.1957	0.1885	0.9734	-	-	-	-	-	-	-
	6.5582	11.3910	5.6239	1.6034	0.3150	10.3095	7.3248	12.7440	7.7296	9.2971	2.5445	2.4499	12.6548	-	-	-	-	-	-	-
	0.0424	-0.0099	-0.0499	-0.0977	0.1425	0.0167	-0.0367	0.0016	-0.0338	-0.0232	-0.0821	0.0835	0.0021	-	-	-	-	-	-	-
K=14	0.4527	0.6724	0.6435	0.1030	**0.0236**	0.9326	0.8351	0.5018	0.6596	0.4586	0.4949	0.1350	0.8354	0.2648	-	-	-	-	-	-
	6.3380	9.4137	9.0083	1.4424	0.3307	13.0559	11.6911	7.0251	9.2351	6.4197	6.9284	1.8896	11.6953	3.7072	-	-	-	-	-	-
	0.0477	-0.0269	-0.0294	-0.1034	0.1431	0.0054	-0.0132	0.0427	-0.0280	-0.0471	-0.0434	-0.0948	0.0132	0.0708	-	-	-	-	-	-
K=15	0.2545	0.4433	**0.0049**	**0.0087**	0.3044	0.3727	0.9498	0.4965	0.9160	0.7207	0.2528	0.5938	**0.0351**	0.2517	0.5434	-	-	-	-	-
	3.8169	6.6493	0.0738	0.1310	4.5664	5.5907	14.2463	7.4482	13.7402	10.8100	3.7916	8.9071	0.5271	3.7756	8.1516	-	-	-	-	-
	0.0723	0.0487	-0.1773	0.1655	-0.0652	-0.0566	0.0040	-0.0432	0.0067	0.0227	0.0726	0.0339	-0.1333	-0.0728	0.0386	-	-	-	-	-
K=16	0.2312	0.6542	0.8872	**0.0019**	**0.0175**	0.6660	0.3430	0.9021	0.5265	0.3922	0.8820	0.2850	0.0925	0.8998	0.4526	0.6851	-	-	-	-
	3.7000	10.4669	14.1944	**0.0306**	0.2805	10.6555	5.4882	14.4328	8.4242	6.2758	14.1126	4.5602	1.4793	14.3965	7.2412	10.9614	-	-	-	-
	0.0760	0.0285	-0.0090	-0.1954	0.1501	0.0274	-0.0602	0.0078	0.0402	-0.0543	0.0094	-0.0679	-0.1066	0.0080	0.0477	0.0258	-	-	-	-
K=17	0.2678	0.3937	**0.0049**	0.5108	**0.0198**	0.6232	0.3103	0.6356	0.5017	0.8136	0.1108	0.7020	0.9991	0.9647	0.2657	0.4675	0.5784	-	-	-
	4.5520	6.6936	0.0835	8.6828	0.3370	10.5942	5.2749	10.8047	8.5285	13.8317	1.8831	11.9337	16.9855	16.4001	4.5172	7.9477	9.8335	-	-	-
	0.0704	0.0542	-0.1774	-0.0418	0.1473	-0.0312	-0.0644	-0.0301	0.0427	0.0150	-0.1011	0.0243	0.0001	0.0028	-0.0707	0.0462	0.0353	-	-	-
K=18	0.1967	0.5779	**0.0061**	0.5138	0.7342	**0.0211**	0.2459	0.5634	0.7794	0.3455	0.9336	0.1048	0.8727	0.5092	0.3470	0.9326	0.3561	0.6627	-	-
	3.5400	10.4015	0.1093	9.2492	13.2164	0.3791	4.4253	10.1408	14.0296	6.2189	16.8046	1.8861	15.7089	9.1647	6.2457	16.7860	6.4089	11.9278	-	-
	0.0819	0.0354	-0.1731	-0.0415	-0.0216	0.1458	-0.0737	0.0367	0.0178	-0.0599	0.0053	-0.1028	0.0102	0.0419	-0.0597	-0.0054	0.0586	0.0277	-	-
K=19	0.2060	0.7003	0.5723	**0.0019**	0.5893	**0.0164**	0.1468	0.2918	0.9207	0.4512	0.8606	0.1235	0.8488	0.9136	0.9951	0.3268	0.6225	0.3257	0.7414	-
	3.9131	13.3050	10.8729	**0.0366**	11.1958	0.3110	2.7890	5.5434	17.4932	8.5736	16.3515	2.3466	16.1272	17.3577	18.9065	6.2089	11.8279	6.1884	14.0862	-
	0.0803	0.0245	0.0359	-0.1952	-0.0343	0.1517	-0.0920	0.0669	0.0063	-0.0479	0.0112	-0.0977	0.0121	0.0069	-0.0004	-0.0623	-0.0313	0.0624	0.0210	-
K=20	0.2346	0.3944	0.8635	**0.0040**	**0.0166**	0.1845	0.1895	0.4597	0.1463	0.9138	0.5165	0.8642	0.0748	0.2037	0.9810	0.7250	0.8957	0.4009	0.6816	0.6596
	4.6929	7.8884	17.2691	0.0795	0.3322	3.6899	3.7891	9.1938	2.9262	18.2753	10.3298	17.2834	1.4961	4.0736	19.6209	14.4994	17.9147	8.0173	13.6314	13.1924
	0.0754	0.0541	0.0109	-0.1815	0.1514	-0.0842	-0.0833	0.0470	0.0921	0.0069	0.0412	0.0109	-0.1129	-0.0807	0.0015	-0.0224	-0.0083	-0.0534	0.0261	0.0280

11. Conflict of interest statement

The authors declared that they had no conflicts of interest concerning their authorship or the publication of this article.

12. References

Alonso Martínez, S., Deco, G., Ter Horst, G.J., Cabral, J., 2020. The Dynamics of Functional Brain Networks Associated With Depressive Symptoms in a Nonclinical Sample. Front. Neural Circuits 14, 570583. https://doi.org/10.3389/fncir.2020.570583

Archer, J.A., Lee, A., Qiu, A., Chen, S.-H.A., 2018. Functional connectivity of resting-state, working memory and inhibition networks in perceived stress. Neurobiol. Stress 8, 186–201. https://doi.org/10.1016/j.ynstr.2017.01.002

Arnold Anteraper, S., Triantafyllou, C., Sawyer, A.T., Hofmann, S.G., Gabrieli, J.D., Whitfield-Gabrieli, S., 2014. Hyper-Connectivity of Subcortical Resting-State Networks in Social Anxiety Disorder. Brain Connectivity 4, 81–90. https://doi.org/10.1089/brain.2013.0180

Avants, B., Epstein, C., Grossman, M., Gee, J., 2008. Symmetric diffeomorphic image registration with cross-correlation: Evaluating automated labeling of elderly and neurodegenerative brain. Medical Image Analysis 12, 26–41. https://doi.org/10.1016/j.media.2007.06.004

Avvenuti, G., Leo, A., Cecchetti, L., Franco, M.F., Travis, F., Caramella, D., Bernardi, G., Ricciardi, E., Pietrini, P., 2020. Reductions in perceived stress following Transcendental Meditation practice are associated with increased brain regional connectivity at rest. Brain Cogn. 139, 105517. https://doi.org/10.1016/j.bandc.2020.105517

Banks, S.J., Eddy, K.T., Angstadt, M., Nathan, P.J., Phan, K.L., 2007. Amygdala–frontal connectivity during emotion regulation. Soc Cogn Affect Neurosci 2, 303–312. https://doi.org/10.1093/scan/nsm029

Bassett, D.S., Sporns, O., 2017. Network neuroscience. Nat Neurosci 20, 353–364. https://doi.org/10.1038/nn.4502

Beggs, J.M., Timme, N., 2012. Being Critical of Criticality in the Brain. Front. Physio. 3. https://doi.org/10.3389/fphys.2012.00163

Behzadi, Y., Restom, K., Liau, J., Liu, T.T., 2007. A component based noise correction method (CompCor) for BOLD and perfusion based fMRI. NeuroImage 37, 90–101. https://doi.org/10.1016/j.neuroimage.2007.04.042

Berboth, S., Morawetz, C., 2021. Amygdala-prefrontal connectivity during emotion regulation: A meta-analysis of psychophysiological interactions. Neuropsychologia 153, 107767. https://doi.org/10.1016/j.neuropsychologia.2021.107767

Bergdahl, J., Larsson, A., Nilsson, L.-G., Ahlström, K.R., Nyberg, L., 2005. Treatment of chronic stress in employees: subjective, cognitive and neural correlates. Scand J Psychol 46, 395–402. https://doi.org/10.1111/j.1467-9450.2005.00470.x

Betensky, J.D., Robinson, D.G., Gunduz-Bruce, H., Sevy, S., Lencz, T., Kane, J.M., Malhotra, A.K., Miller, R., McCormack, J., Bilder, R.M., Szeszko, P.R., 2008. Patterns of stress in schizophrenia. Psychiatry Research 160, 38–46. https://doi.org/10.1016/j.psychres.2007.06.001

Biswal, B., Zerrin Yetkin, F., Haughton, V.M., Hyde, J.S., 1995. Functional connectivity in the motor cortex of resting human brain using echo-planar mri. Magn. Reson. Med. 34, 537–541. https://doi.org/10.1002/mrm.1910340409

Brewin, C.R., Andrews, B., Valentine, J.D., 2000. Meta-analysis of risk factors for posttraumatic stress disorder in trauma-exposed adults. Journal of Consulting and Clinical Psychology 68, 748–766. https://doi.org/10.1037/0022-006X.68.5.748

Bryant, R.A., 2019. Post-traumatic stress disorder: a state-of-the-art review of evidence and challenges. World Psychiatry 18, 259–269. https://doi.org/10.1002/wps.20656

Cabral, J., Vidaurre, D., Marques, P., Magalhães, R., Silva Moreira, P., Miguel Soares, J., Deco, G., Sousa, N., Kringelbach, M.L., 2017. Cognitive performance in healthy older adults relates to spontaneous switching between states of functional connectivity during rest. Sci Rep 7, 5135. https://doi.org/10.1038/s41598-017-05425-7

Caetano, I., Amorim, L., Soares, J.M., Ferreira, S., Coelho, A., Reis, J., Santos, N.C., Moreira, P.S., Marques, P., Magalhães, R., Esteves, M., Picó-Pérez, M., Sousa, N., 2021. Amygdala size varies with stress perception. Neurobiology of Stress 14, 100334. https://doi.org/10.1016/j.ynstr.2021.100334

Carvalho, A.F., Firth, J., Vieta, E., 2020. Bipolar Disorder. N Engl J Med 383, 58–66. https://doi.org/10.1056/NEJMra1906193

Cerqueira, J.J., Almeida, O.F.X., Sousa, N., 2008. The stressed prefrontal cortex. Left? Right! Brain, Behavior, and Immunity 22, 630–638. https://doi.org/10.1016/j.bbi.2008.01.005

Cerqueira, J.J., Mailliet, F., Almeida, O.F.X., Jay, T.M., Sousa, N., 2007. The Prefrontal Cortex as a Key Target of the Maladaptive Response to Stress. Journal of Neuroscience 27, 2781–2787. https://doi.org/10.1523/JNEUROSCI.4372-06.2007

Cerullo, M.A., Fleck, D.E., Eliassen, J.C., Smith, M.S., DelBello, M.P., Adler, C.M., Strakowski, S.M., 2012. A longitudinal functional connectivity analysis of the amygdala in bipolar I disorder across mood states: A longitudinal functional connectivity analysis. Bipolar Disorders 14, 175–184. https://doi.org/10.1111/j.1399-5618.2012.01002.x

Chen, J.E., Lewis, L.D., Chang, C., Tian, Q., Fultz, N.E., Ohringer, N.A., Rosen, B.R., Polimeni, J.R., 2020. Resting-state "physiological networks." NeuroImage 213, 116707. https://doi.org/10.1016/j.neuroimage.2020.116707

Clark, U.S., Miller, E.R., Hegde, R.R., 2018. Experiences of Discrimination Are Associated With Greater Resting Amygdala Activity and Functional Connectivity. Biol. Psychiat.-Cogn. Neurosci. Neuroimag. 3, 367–378. https://doi.org/10.1016/j.bpsc.2017.11.011

Cox, R.W., Hyde, J.S., 1997. Software tools for analysis and visualization of fMRI data. NMR in Biomedicine 10, 171–178. https://doi.org/10.1002/(SICI)1099-1492(199706/08)10:4/5<171::AID-NBM453>3.0.CO;2-L

Dale, A.M., Fischl, B., Sereno, M.I., 1999. Cortical Surface-Based Analysis: I. Segmentation and Surface Reconstruction. NeuroImage 9, 179–194. https://doi.org/10.1006/nimg.1998.0395

Davidson, J.R.T., Hughes, D., Blazer, D.G., George, L.K., 1991. Post-traumatic stress disorder in the community: an epidemiological study. Psychol. Med. 21, 713–721. https://doi.org/10.1017/S0033291700022352

Esteban, O., Markiewicz, C.J., Blair, R.W., Moodie, C.A., Isik, A.I., Erramuzpe, A., Kent, J.D., Goncalves, M., DuPre, E., Snyder, M., Oya, H., Ghosh, S.S., Wright, J., Durnez, J., Poldrack, R.A., Gorgolewski, K.J., 2018. fMRIPrep: a robust preprocessing pipeline for functional MRI. Nat Methods 16, 111–116. https://doi.org/10.1038/s41592-018-0235-4

Esteban, O., Markiewicz, C.J., Burns, C., Goncalves, M., Jarecka, D., Ziegler, E., Berleant, S., Ellis, D.G., Pinsard, B., Madison, C., Waskom, M., Notter, M.P., Clark, Daniel, Manhães-Savio, A., Clark, Dav, Jordan, K., Dayan, M., Halchenko, Y.O., Loney, F., Salo, T., Dewey, B.E., Johnson, H., Bougacha, S., Keshavan, A., Yvernault, B., Hamalainen, C., Christian, H., Ćirić, R., Dubois, M., Joseph, M., Cipollini, B., Tilley II, S., Visconti di Oleggio Castello, M., Wong, J., De La Vega, A., Kaczmarzyk, J., Huntenburg, J.M., Clark, M.G., Benderoff, E., Erickson, D., Kent, J.D., Hanke, M., Giavasis, S., Moloney, B., Nichols, B.N., Tungaraza, R., Frohlich, C., Wassermann, D., de Hollander, G., Eshaghi, A., Millman, J., Mancini, M., Nielson, D.M., Varoquaux, G., Watanabe, A., Mordom, D., Guillon, J., Koudoro, S., Chetverikov, A., Rokem, A., Acland, B., Forbes, J., Markello, R., Gillman, A., Kong, X.-Z., Geisler, D., Salvatore, J., Gramfort, A., Doll, A., Buchanan, C., DuPre, E., Liu, S., Schaefer, A., Kleesiek, J., Sikka, S., Schwartz, Y., Lee, J.A., Mattfeld, A., Richie-Halford, A., Liem, F., Perez-Guevara, M.F., Heinsfeld, A.S., Haselgrove, C., Durnez, J., Lampe, L., Poldrack, R., Glatard, T., Tabas, A., Cumba, C., Pérez-García, F., Blair, R., Iqbal, S., Welch, D., Triplett, W., Ghayoor, A., Craddock, R.C., Correa, C., Papadopoulos Orfanos, D., Stadler, J., Warner, J., Sisk, L.M., Falkiewicz, M., Sharp, P., Rothmei, S., Kim, S., Weinstein, A., Kahn, A.E., Kastman, E., Bottenhorn, K., Grignard, M., Perkins, L.N., Contier, O., Zhou, D., Bielievtsov, D., Cooper, G., Stojic, H., Linkersdörfer, J., Waller, L., Renfro, M., Hinds, O., Stanley, O., Küttner, R., Pauli, W.M., Glen, D., Kimbler, A., Meyers, B., Tarbert, C., Ginsburg, D., Haehn, D., Margulies, D.S., Ma, F., Malone, I.B., Snoek, L., Brett, M., Cieslak, M., Hallquist, M., Molina-Romero, M., Bilgel, M., Lee, N., Inati, S., Gerhard, S., Mathotaarachchi, S., Saase, V., Van, A., Steele, C.J., Ort, E., Condamine, E., Lerma-Usabiaga, G., Schwabacher, I., Arias, J., Lai, J., Pellman, J., Huguet, J., WEN, J., Leinweber, K., Chawla, K., Weninger, L., Modat, M., Harms, R., Andberg, S.K., Baratz, Z., Matsubara, K., González Orozco, A.A., Marina, A., Davison, A., Floren, A., Park, A., Cheung, B., McDermottroe, C., McNamee, D., Shachnev, D., Flandin, G., Gonzalez, I., Varada, J., Schlamp, K., Podranski, K., Huang, L., Noel, M., Crusoe, M.R., Pannetier, N., Khanuja, R., Urchs, S., Nickson, T., Huang, L., Broderick, W., Tambini, A., Mihai, P.G., Gorgolewski, K.J., Ghosh, S., 2020. Nipype (software). Zenodo. https://doi.org/10.5281/zenodo.4035081

Esteban, O., Markiewicz, C.J., Goncalves, M., DuPre, E., Kent, J.D., Salo, T., Ciric, R., Pinsard, B., Blair, R.W., Poldrack, R.A., Gorgolewski, K.J., 2021. fMRIPrep (software). Zenodo. https://doi.org/10.5281/zenodo.5569959

Evans, A.C., Janke, A.L., Collins, D.L., Baillet, S., 2012. Brain templates and atlases. NeuroImage 62, 911–922. https://doi.org/10.1016/j.neuroimage.2012.01.024

Everaerd, D.S., Henckens, M.J.A.G., Bloemendaal, M., Bovy, L., Kaldewaij, R., Maas, F.M.W.M., Mulders, P.C.R., Niermann, H.C.M., van de Pavert, I., Przezdzik, I., Fernández, G., Klumpers, F., de Voogd, L.D., 2020. Good vibrations: An observational study of real-life stress induced by a stage performance. Psychoneuroendocrinology 114, 104593. https://doi.org/10.1016/j.psyneuen.2020.104593

Fett, A.-K.J., Lemmers-Jansen, I.L.J., Krabbendam, L., 2019. Psychosis and urbanicity: a review of the recent literature from epidemiology to neurourbanism. Current Opinion in Psychiatry 32, 232–241. https://doi.org/10.1097/YCO.0000000000000486

Figueroa, C.A., Cabral, J., Mocking, R.J.T., Rapuano, K.M., Hartevelt, T.J., Deco, G., Expert, P., Schene, A.H., Kringelbach, M.L., Ruhé, H.G., 2019. Altered ability to access a clinically relevant control network in patients remitted from major depressive disorder. Hum Brain Mapp 40, 2771–2786. https://doi.org/10.1002/hbm.24559

Fonov, V., Evans, A., McKinstry, R., Almli, C., Collins, D., 2009. Unbiased nonlinear average age-appropriate brain templates from birth to adulthood. NeuroImage, Organization for Human Brain Mapping 2009 Annual Meeting 47, S102. https://doi.org/10.1016/S1053-8119(09)70884-5

Fontenele, A.J., de Vasconcelos, N.A.P., Feliciano, T., Aguiar, L.A.A., Soares-Cunha, C., Coimbra, B., Dalla Porta, L., Ribeiro, S., Rodrigues, A.J., Sousa, N., Carelli, P.V., Copelli, M., 2019. Criticality between Cortical States. Phys. Rev. Lett. 122, 208101. https://doi.org/10.1103/PhysRevLett.122.208101

García-Martínez, B., Martínez-Rodrigo, A., Fernández-Caballero, A., Moncho-Bogani, J., Alcaraz, R., 2020. Nonlinear predictability analysis of brain dynamics for automatic recognition of negative stress. Neural Comput & Applic 32, 13221–13231. https://doi.org/10.1007/s00521-018-3620-0

Gispen-de Wied, C.C., 2000. Stress in schizophrenia: an integrative view. European Journal of Pharmacology 405, 375–384. https://doi.org/10.1016/S0014-2999(00)00567-7

Gong, Y., Palmer, S., Gallacher, J., Marsden, T., Fone, D., 2016. A systematic review of the relationship between objective measurements of the urban environment and psychological distress. Environ Int 96, 48–57. https://doi.org/10.1016/j.envint.2016.08.019

Gorgolewski, K., Burns, C.D., Madison, C., Clark, D., Halchenko, Y.O., Waskom, M.L., Ghosh, S.S., 2011. Nipype: A Flexible, Lightweight and Extensible Neuroimaging Data Processing Framework in Python. Front. Neuroinform. 5. https://doi.org/10.3389/fninf.2011.00013

Greve, D.N., Fischl, B., 2009. Accurate and robust brain image alignment using boundary-based registration. NeuroImage 48, 63–72. https://doi.org/10.1016/j.neuroimage.2009.06.060

Hammen, C., 2005. Stress and Depression. Annu. Rev. Clin. Psychol. 1, 293–319. https://doi.org/10.1146/annurev.clinpsy.1.102803.143938

Hölzel, B.K., Carmody, J., Evans, K.C., Hoge, E.A., Dusek, J.A., Morgan, L., Pitman, R.K., Lazar, S.W., 2010. Stress reduction correlates with structural changes in the amygdala. Social Cognitive and Affective Neuroscience 5, 11–17. https://doi.org/10.1093/scan/nsp034

Jenkinson, M., Bannister, P., Brady, M., Smith, S., 2002. Improved Optimization for the Robust and Accurate Linear Registration and Motion Correction of Brain Images. NeuroImage 17, 825–841. https://doi.org/10.1006/nimg.2002.1132

Jenkinson, M., Beckmann, C.F., Behrens, T.E.J., Woolrich, M.W., Smith, S.M., 2012. FSL. NeuroImage 62, 782–790. https://doi.org/10.1016/j.neuroimage.2011.09.015

Johnson, F.K., Delpech, J.-C., Thompson, G.J., Wei, L., Hao, J., Herman, P., Hyder, F., Kaffman, A., 2018. Amygdala hyper-connectivity in a mouse model of unpredictable early life stress. Transl Psychiatry 8, 49. https://doi.org/10.1038/s41398-018-0092-z

Johnstone, T., van Reekum, C.M., Urry, H.L., Kalin, N.H., Davidson, R.J., 2007. Failure to Regulate: Counterproductive Recruitment of Top-Down Prefrontal-Subcortical Circuitry in Major Depression. Journal of Neuroscience 27, 8877–8884. https://doi.org/10.1523/JNEUROSCI.2063-07.2007

Jovanovic, H., Perski, A., Berglund, H., Savic, I., 2011. Chronic stress is linked to 5-HT1A receptor changes and functional disintegration of the limbic networks. Neuroimage 55, 1178–1188. https://doi.org/10.1016/j.neuroimage.2010.12.060

Kaul, D., Schwab, S.G., Mechawar, N., Matosin, N., 2021. How stress physically re-shapes the brain: Impact on brain cell shapes, numbers and connections in psychiatric disorders. Neuroscience & Biobehavioral Reviews 124, 193–215. https://doi.org/10.1016/j.neubiorev.2021.01.025

Kendler, K.S., Karkowski, L.M., Prescott, C.A., 1999. Causal Relationship Between Stressful Life Events and the Onset of Major Depression. AJP 156, 837–841. https://doi.org/10.1176/ajp.156.6.837

Killgore, W.D.S., 2013. Self-Reported Sleep Correlates with Prefrontal-Amygdala Functional Connectivity and Emotional Functioning. Sleep 36, 1597–1608. https://doi.org/10.5665/sleep.3106

Kim, E.Y., Miklowitz, D.J., Biuckians, A., Mullen, K., 2007. Life stress and the course of early-onset bipolar disorder. Journal of Affective Disorders 99, 37–44. https://doi.org/10.1016/j.jad.2006.08.022

Klein, A., Ghosh, S.S., Bao, F.S., Giard, J., Häme, Y., Stavsky, E., Lee, N., Rossa, B., Reuter, M., Chaibub Neto, E., Keshavan, A., 2017. Mindboggling morphometry of human brains. PLoS Comput Biol 13, e1005350. https://doi.org/10.1371/journal.pcbi.1005350

Koenig, J.I., Walker, C.-D., Romeo, R.D., Lupien, S.J., 2011. Effects of stress across the lifespan. Stress 14, 475–480. https://doi.org/10.3109/10253890.2011.604879

Kogler, L., Müller, V.I., Chang, A., Eickhoff, S.B., Fox, P.T., Gur, R.C., Derntl, B., 2015. Psychosocial versus physiological stress — Meta-analyses on deactivations and activations of the neural correlates of stress reactions. NeuroImage 119, 235–251. https://doi.org/10.1016/j.neuroimage.2015.06.059

Kolassa, I.-T., Wienbruch, C., Neuner, F., Schauer, M., Ruf, M., Odenwald, M., Elbert, T., 2007. Altered oscillatory brain dynamics after repeated traumatic stress. BMC Psychiatry 7, 56. https://doi.org/10.1186/1471-244X-7-56

Larabi, D.I., Renken, R.J., Cabral, J., Marsman, J.-B.C., Aleman, A., Ćurčić-Blake, B., 2020. Trait self-reflectiveness relates to time-varying dynamics of resting state functional connectivity and underlying structural connectomes: Role of the default mode network. NeuroImage 219, 116896. https://doi.org/10.1016/j.neuroimage.2020.116896

Lebares, C.C., Guvva, E.V., Olaru, M., Sugrue, L.P., Staffaroni, A.M., Delucchi, K.L., Kramer, J.H., Ascher, N.L., Harris, H.W., 2019. Efficacy of Mindfulness-Based Cognitive Training in Surgery: Additional Analysis of the Mindful Surgeon Pilot Randomized Clinical Trial. JAMA Netw Open 2, e194108. https://doi.org/10.1001/jamanetworkopen.2019.4108

Lederbogen, F., Ulshoefer, E., Peifer, A., Fehlner, P., Bilek, E., Streit, F., Deuschle, M., Tost, H., Meyer-Lindenberg, A., 2018. No association between cardiometabolic risk and neural reactivity to acute psychosocial stress. NeuroImage-Clin. 20, 1115–1122. https://doi.org/10.1016/j.nicl.2018.10.018

Li, M., Huang, C., Deng, W., Ma, X., Han, Y., Wang, Q., Li, Z., Guo, W., Li, Y., Jiang, L., Lei, W., Hu, X., Gong, Q., Ries Merikangas, K., Palaniyappan, L., Li, T., 2015. Contrasting and convergent patterns of amygdala

connectivity in mania and depression: A resting-state study. Journal of Affective Disorders 173, 53–58. https://doi.org/10.1016/j.jad.2014.10.044

Lord, L.-D., Expert, P., Atasoy, S., Roseman, L., Rapuano, K., Lambiotte, R., Nutt, D.J., Deco, G., Carhart-Harris, R.L., Kringelbach, M.L., Cabral, J., 2019. Dynamical exploration of the repertoire of brain networks at rest is modulated by psilocybin. NeuroImage 199, 127–142. https://doi.org/10.1016/j.neuroimage.2019.05.060

Lucassen, P.J., Pruessner, J., Sousa, N., Almeida, O.F.X., Van Dam, A.M., Rajkowska, G., Swaab, D.F., Czéh, B., 2014. Neuropathology of stress. Acta Neuropathol 127, 109–135. https://doi.org/10.1007/s00401-013-1223-5

Lv, H., Wang, Z., Tong, E., Williams, L.M., Zaharchuk, G., Zeineh, M., Goldstein-Piekarski, A.N., Ball, T.M., Liao, C., Wintermark, M., 2018. Resting-State Functional MRI: Everything That Nonexperts Have Always Wanted to Know. AJNR Am J Neuroradiol ajnr;ajnr.A5527v1. https://doi.org/10.3174/ajnr.A5527

Magalhães, R., Barrière, D.A., Novais, A., Marques, F., Marques, P., Cerqueira, J., Sousa, J.C., Cachia, A., Boumezbeur, F., Bottlaender, M., Jay, T.M., Mériaux, S., Sousa, N., 2018. The dynamics of stress: a longitudinal MRI study of rat brain structure and connectome. Mol Psychiatry 23, 1998–2006. https://doi.org/10.1038/mp.2017.244

Magalhães, R., Novais, A., Barrière, D.A., Marques, P., Marques, F., Sousa, J.C., Cerqueira, J.J., Cachia, A., Jay, T.M., Bottlaender, M., Sousa, N., Mériaux, S., Boumezbeur, F., 2019. A Resting-State Functional MR Imaging and Spectroscopy Study of the Dorsal Hippocampus in the Chronic Unpredictable Stress Rat Model. J. Neurosci. 39, 3640–3650. https://doi.org/10.1523/JNEUROSCI.2192-18.2019

Magalhães, R., Picó-Pérez, M., Esteves, M., Vieira, R., Castanho, T.C., Amorim, L., Sousa, M., Coelho, A., Fernandes, H.M., Cabral, J., Moreira, P.S., Sousa, N., 2021. Habitual coffee drinkers display a distinct pattern of brain functional connectivity. Mol Psychiatry. https://doi.org/10.1038/s41380-021-01075-4

Marek, S., Dosenbach, N.U.F., 2018. The frontoparietal network: function, electrophysiology, and importance of individual precision mapping. Dialogues Clin Neurosci 20, 133–140. https://doi.org/10.31887/DCNS.2018.20.2/smarek

Melchior, M., Caspi, A., Milne, B.J., Danese, A., Poulton, R., Moffitt, T.E., 2007. Work stress precipitates depression and anxiety in young, working women and men. Psychol. Med. 37, 1119–1129. https://doi.org/10.1017/S0033291707000414

Menon, S.S., Krishnamurthy, K., 2019. A Comparison of Static and Dynamic Functional Connectivities for Identifying Subjects and Biological Sex Using Intrinsic Individual Brain Connectivity. Sci Rep 9, 5729. https://doi.org/10.1038/s41598-019-42090-4

Novais, A., Monteiro, S., Roque, S., Correia-Neves, M., Sousa, N., 2017. How age, sex and genotype shape the stress response. Neurobiology of Stress 6, 44–56. https://doi.org/10.1016/j.ynstr.2016.11.004

Pêgo, J.M., Sousa, J.C., Almeida, O., Sousa, N., 2009. Stress and the Neuroendocrinology of Anxiety Disorders, in: Stein, M.B., Steckler, T. (Eds.), Behavioral Neurobiology of Anxiety and Its Treatment, Current Topics in Behavioral Neurosciences. Springer Berlin Heidelberg, Berlin, Heidelberg, pp. 97–118. https://doi.org/10.1007/7854_2009_13

Popoli, M., Yan, Z., McEwen, B.S., Sanacora, G., 2012. The stressed synapse: the impact of stress and glucocorticoids on glutamate transmission. Nat Rev Neurosci 13, 22–37. https://doi.org/10.1038/nrn3138

Power, J.D., Barnes, K.A., Snyder, A.Z., Schlaggar, B.L., Petersen, S.E., 2012. Spurious but systematic correlations in functional connectivity MRI networks arise from subject motion. NeuroImage 59, 2142–2154. https://doi.org/10.1016/j.neuroimage.2011.10.018

Power, J.D., Mitra, A., Laumann, T.O., Snyder, A.Z., Schlaggar, B.L., Petersen, S.E., 2014. Methods to detect, characterize, and remove motion artifact in resting state fMRI. NeuroImage 84, 320–341. https://doi.org/10.1016/j.neuroimage.2013.08.048

Ritchie, H., Roser, M., 2018. Urbanization. Our World in Data.

Rolls, E.T., Joliot, M., Tzourio-Mazoyer, N., 2015. Implementation of a new parcellation of the orbitofrontal cortex in the automated anatomical labeling atlas. NeuroImage 122, 1–5. https://doi.org/10.1016/j.neuroimage.2015.07.075

Shin, L.M., Liberzon, I., 2010. The Neurocircuitry of Fear, Stress, and Anxiety Disorders. Neuropsychopharmacol 35, 169–191. https://doi.org/10.1038/npp.2009.83

Smith, S.M., Jenkinson, M., Woolrich, M.W., Beckmann, C.F., Behrens, T.E.J., Johansen-Berg, H., Bannister, P.R., De Luca, M., Drobnjak, I., Flitney, D.E., Niazy, R.K., Saunders, J., Vickers, J., Zhang, Y., De Stefano, N., Brady, J.M., Matthews, P.M., 2004. Advances in functional and structural MR image analysis and implementation as FSL. NeuroImage 23, S208–S219. https://doi.org/10.1016/j.neuroimage.2004.07.051

Soares, J.M., Magalhães, R., Moreira, P.S., Sousa, A., Ganz, E., Sampaio, A., Alves, V., Marques, P., Sousa, N., 2016. A Hitchhiker's Guide to Functional Magnetic Resonance Imaging. Front. Neurosci. 10. https://doi.org/10.3389/fnins.2016.00515

Soares, J.M., Marques, P., Alves, V., Sousa, N., 2013a. A hitchhiker's guide to diffusion tensor imaging. Front. Neurosci. 7. https://doi.org/10.3389/fnins.2013.00031

Soares, J.M., Sampaio, A., Ferreira, L.M., Santos, N.C., Marques, F., Palha, J.A., Cerqueira, J.J., Sousa, N., 2012. Stress-induced changes in human decision-making are reversible. Transl Psychiatry 2, e131–e131. https://doi.org/10.1038/tp.2012.59

Soares, J.M., Sampaio, A., Ferreira, L.M., Santos, N.C., Marques, P., Marques, F., Palha, J.A., Cerqueira, J.J., Sousa, N., 2013b. Stress Impact on Resting State Brain Networks. PLoS ONE 8, e66500. https://doi.org/10.1371/journal.pone.0066500

Soares, J.M., Sampaio, A., Marques, P., Ferreira, L.M., Santos, N.C., Marques, F., Palha, J.A., Cerqueira, J.J., Sousa, N., 2013c. Plasticity of resting state brain networks in recovery from stress. Front. Hum. Neurosci. 7. https://doi.org/10.3389/fnhum.2013.00919

Sousa, N., 2016. The dynamics of the stress neuromatrix. Mol Psychiatry 21, 302–312. https://doi.org/10.1038/mp.2015.196

Sousa, N., Lukoyanov, N.V., Madeira, M.D., Almeida, O.F.X., Paula-Barbosa, M.M., 2000. Reorganization of the morphology of hippocampal neurites and synapses after stress-induced damage correlates with behavioral improvement. Neuroscience 97, 253–266. https://doi.org/10.1016/S0306-4522(00)00050-6

Szabo, C.P., 2018. Urbanization and mental health: a developing world perspective. Current Opinion in Psychiatry 31, 256–257. https://doi.org/10.1097/YCO.0000000000000414

Taren, A.A., Gianaros, P.J., Greco, C.M., Lindsay, E.K., Fairgrieve, A., Brown, K.W., Rosen, R.K., Ferris, J.L., Julson, E., Marsland, A.L., Bursley, J.K., Ramsburg, J., Creswell, J.D., 2015. Mindfulness meditation training alters stress-related amygdala resting state functional connectivity: a randomized controlled trial. Soc. Cogn. Affect. Neurosci. 10, 1758–1768. https://doi.org/10.1093/scan/nsv066

Taren, A.A., Gianaros, P.J., Greco, C.M., Lindsay, E.K., Fairgrieve, A., Brown, K.W., Rosen, R.K., Ferris, J.L., Julson, E., Marsland, A.L., Creswell, J.D., 2017. Mindfulness Meditation Training and Executive Control Network Resting State Functional Connectivity: A Randomized Controlled Trial. Psychosom Med 79, 674–683. https://doi.org/10.1097/PSY.0000000000000466

Tustison, N.J., Avants, B.B., Cook, P.A., Yuanjie Zheng, Egan, A., Yushkevich, P.A., Gee, J.C., 2010. N4ITK: Improved N3 Bias Correction. IEEE Trans. Med. Imaging 29, 1310–1320. https://doi.org/10.1109/TMI.2010.2046908

Tzourio-Mazoyer, N., Landeau, B., Papathanassiou, D., Crivello, F., Etard, O., Delcroix, N., Mazoyer, B., Joliot, M., 2002. Automated Anatomical Labeling of Activations in SPM Using a Macroscopic Anatomical Parcellation of the MNI MRI Single-Subject Brain. NeuroImage 15, 273–289. https://doi.org/10.1006/nimg.2001.0978

Vohryzek, J., Deco, G., Cessac, B., Kringelbach, M.L., Cabral, J., 2020. Ghost Attractors in Spontaneous Brain Activity: Recurrent Excursions Into Functionally-Relevant BOLD Phase-Locking States. Front. Syst. Neurosci. 14, 20. https://doi.org/10.3389/fnsys.2020.00020

Walker, E., Mittal, V., Tessner, K., 2008. Stress and the Hypothalamic Pituitary Adrenal Axis in the Developmental Course of Schizophrenia. Annu. Rev. Clin. Psychol. 4, 189–216. https://doi.org/10.1146/annurev.clinpsy.4.022007.141248

Welberg, L., 2014. A REDD line from stress to depression. Nat Rev Neurosci 15, 350–350. https://doi.org/10.1038/nrn3749

Williams, L.M., 2016. Precision psychiatry: a neural circuit taxonomy for depression and anxiety. The Lancet Psychiatry 3, 472–480. https://doi.org/10.1016/S2215-0366(15)00579-9

Winkler, A.M., Ridgway, G.R., Webster, M.A., Smith, S.M., Nichols, T.E., 2014. Permutation inference for the general linear model. NeuroImage 92, 381–397. https://doi.org/10.1016/j.neuroimage.2014.01.060

Wong, W., Cabral, J., Rane, R., Ly, R., Kringelbach, M.L., Feusner, J.D., 2021. Effects of visual attention modulation on dynamic functional connectivity during own-face viewing in body dysmorphic disorder. Neuropsychopharmacol. 46, 2030–2038. https://doi.org/10.1038/s41386-021-01039-w

Woolrich, M.W., Jbabdi, S., Patenaude, B., Chappell, M., Makni, S., Behrens, T., Beckmann, C., Jenkinson, M., Smith, S.M., 2009. Bayesian analysis of neuroimaging data in FSL. NeuroImage 45, S173–S186. https://doi.org/10.1016/j.neuroimage.2008.10.055

Wu, J., Geng, X., Shao, R., Wong, N.M.L., Tao, J., Chen, L., Chan, C.C.H., Lee, T.M.C., 2018. Neurodevelopmental changes in the relationship between stress perception and prefrontal-amygdala functional circuitry. NeuroImage-Clin. 20, 267–274. https://doi.org/10.1016/j.nicl.2018.07.022

Xia, M., Wang, J., He, Y., 2013. BrainNet Viewer: A Network Visualization Tool for Human Brain Connectomics. PLoS ONE 8, e68910. https://doi.org/10.1371/journal.pone.0068910

Yuen, E.Y., Wei, J., Liu, W., Zhong, P., Li, X., Yan, Z., 2012. Repeated Stress Causes Cognitive Impairment by Suppressing Glutamate Receptor Expression and Function in Prefrontal Cortex. Neuron 73, 962–977. https://doi.org/10.1016/j.neuron.2011.12.033

Zhang, Y., Brady, M., Smith, S., 2001. Segmentation of brain MR images through a hidden Markov random field model and the expectation-maximization algorithm. IEEE Trans. Med. Imaging 20, 45–57. https://doi.org/10.1109/42.906424

CHAPTER V

General discussion

1. Discussion

Stress is a significant precursor of several psychiatric diseases (Kim et al., 2007; Lucassen et al., 2014; Sousa, 2016; Welberg, 2014). Notably, the perception of stress is increasing day by day (Fett et al., 2019; Lederbogen et al., 2011), being estimated that 1 out of 5 years is lived with incapacity due to mental disorders (World Health Organization, 2021).

Starting as a multisystemic reaction with the primary involvement of the HPA axis, the stress response usually helps individuals overcome unpredictable situations. However, exposure to chronic stress may cause the dysregulation of internal mechanisms, usually resulting in sustained increases in corticosteroid levels due to HPA hyperactivation (Arborelius et al., 1999; Pêgo et al., 2009). Notably, brain regions enriched by GR (such as the amygdalae and hippocampus) are more susceptible to this persistent GC increase (Sousa et al., 2008). In the long run, these maladaptive stress reactions may exacerbate disease development (Lucassen et al., 2014; Sousa, 2016).

Despite the remote interest of researchers and clinicians in the link between stress and mental health, most stress neuroimage literature relates to clinical samples. Notably, even sharing the same precursor, each neuropsychiatric condition presents unique characteristics. Thus, it is of major relevance to explore how the stressed, however healthy, brain behaves before it crosses the breakout point in which pathology emerges.

With the previous questions in mind, this Thesis aimed to provide new insights into the changes induced by stress (particularly perceived stress) on the healthy brain. Considering the possible emergence of new in-vivo biomarkers, herein, we used a sizeable non-pathological cohort with a broad age range to explore the interaction between PSS10 scores and the brain's structure and functioning. In the following paragraphs, we will describe the primary contributions of this Thesis and discuss how our findings might be incorporated (and enriched) the current literature on the field. For easy understanding and contextualization, major results of each Chapter were combined with the summary table of the introductory Chapter 1 (Table 1 of Section 5) in the following Table. We denote that the contributions of this Thesis are highlighted in gray.

Table 1. Contribution of these Thesis findings to the current state-of-the literature related to the impact of perceived stress (measured by PSS10) on the healthy brain.

Type of study	Study	N (Females)	Age (SD)	PSS (SD/*SE)	Methods	Findings in structural and rs-fMRI
Structural cross-sectional	(Li et al., 2014)	304 (166)	19.2 (1.24)	23.10 (6.48*)	WB GMV and WMV (VBM)	↑**PSS:** ↑GMV L/R Parahippocampal G, FC, Entorhinal C; ↓GMV R Insular C; ↓WMV Corpus Callosum
	(Sherman et al., 2016)	40 (27)	67.2 (5.1)	9.53 (5.2)	Amy GMV (ROI)	↑**PSS** ↑Amy (total and L/R)
	(Moreno et al., 2017)	28 (14)	78.41 (4.1)	13.1 (5.1)	PFC, OFC, Hip, Amy GMV and WMV (ROI)	↑**PSS:** ↓Overal R/L PFC; ↓L/R WM in PFC, vlPFC, dlPFC; ↓L WM vmPFC; ↓R WM OFC; ↓L/R GM vlPFC
	(Wu et al., 2020)	26 (13)	36.74 (5.23)	23.38 (8.84)	WB GMV (VBM)	PSS x Age interaction in insula, OFC and L Amy ↑**PSS** ↓OFC, insula, L Amy in adults
	Chapter 2 (Caetano et al., 2021)	50 (35)	24.30 (1.81)	26.2 (7.14)	Subcortical GMV (VBM and ROI)	↑**PSS VBM:** ↑R Amy, R Hip, R Putamen; ↑L Hip, L Amy; ↑R Pallidum, R Accumbens-area ↑**PSS ROI volume:** ↑R Amy, R ant Hip
	Chapter 3 *(in submission)*	272 (157)	38.3 (20.85)	16.5 (7.85)	Amy GMV (ROI)	↑**PSS** ↑R Amy
Structural longitudinal	(Hölzel et al., 2010)	26 (15)	35.2 (6.7)	Pre: 20.7 (5.6) Pos: 15.2 (4.7)	WB GMV (VBM)	↓ **PSS** ↓ R Amy
	(Soares et al., 2012)	Case: 12 (6) Control: 12 (6)	Case: 23.9 (0.70) Control: 23.6 (2.11)	Case Pre > Case Pos Case Pre > Control Case Pos ≈ Control	Corticostriatal GMV (ROI)	**Case Pre vs Controls:** ↑**PSS** ↓ R Caudate ↑L/R Putamen ↓L medial OFC; ↑ Caudate-to-putamen ratio in controls **Case Pre vs Case Pos:** ↓**PSS** caused recovery of Caudate, Putamen and OFC
	(Joss et al., 2020)	21 (16)	26.05 (2.25)	Pre: 22.421 (8.375) Pos: 16.895 (8.055)	Hip GMV (VBM)	↓ **PSS** ↑L Hip
	(Joss et al., 2021)	15 (12)	26.27 (0.47)	Pre: 19.7 (2.91) Pos: 12.5 (2.91)	Amy GMV (VBM)	↓ **PSS** ↑L Amy
	Appendix A *(congress publication)*	21 (10)	24 (1.5)	M1: 21.0 (7.12) M2: 21.6 (7.10) M1 + M2: 21.3 ± 7.03 |PSS1-PSS2| = 5.2 ± 3.97	R Amy GMV (ROI)	**M1:** model not significant **M2:** model significant (but only a trend ↑PSS ↑R Amy) **M1+M2:** model significant and ↑**PSS** ↑**R Amy**
Structural and Functional	(Soares et al., 2013a)	Case: 8 (6) Control: 8 (6)	Case: 23.86 (0.35) Control: 24.25 (1.98)	Case > Control	rs-networks ICA rs-networks GMV (ROI)	↑ **rs-networks FC Case vs Controls (↑PSS) in:** DMN: mPFC, medial OFC, pCC and precuneus; DAN: S parietal, R middle occipital and L medial and SF; VAN: L angular, S parietal and middle F; SMN: L paracentral lobule, precentral, R postcentral and the L cerebellum; VN: Calcarine ↓**rs-networks GMV Case vs Controls (↑PSS) in:** DMN: L pCC, L/R parietal I
	(Soares et al., 2013b)	Case: 6 (3) Control: 6 (3)	Case: 23.83 (0.37) Control: 24.33 (1.24)	Case Pre: 35.50 (2.59) Case Pos: 30.00 (3.03) Control: 30.17 (4.49)	rs-networks ICA rs-networks GMV (ROI)	↓ DMN GMV (L pCC and R Parietal I) in Case Pre vs Controls (↑PSS) ↑ **rs-networks FC Case Pre vs Case Pos (↑PSS) in:** DMN: L aCC, L medial OFC, R precuneus, L Lingual; VAN: L I/S Parietal, R middle and S F; Sensorimotor: L Cerebellum ↓ **rs-networks FC Case Pre vs Case Pos (↑PSS) in:** DAN: R I Parietal, R Supramarginal, R FI opercularis, R Precentral; AN: L Temporal S **≈ PSS but ↑ rs-network FC Case Pos vs Controls in:** DAN: L Occipital S, L Parietal S, R Parietal S, R Postcentral, L middle and S F, L/R F I opercularis, L/R Precentral; VAN: L Parietal I, L/R Angular; Sensorimotor: L/R Precentral, L Paracentral, R Postcentral, L/R Cerebellum **≈ PSS but ↓ rs-network FC Pos < Controls in:** DMN: R ACC; VAN: L/R Parietal I, L Angular, L/R F middle, L F I Triangularis
	(Soares et al., 2017)	104 (52)	65.20 (8.07)	21.49 (8.18)	DMN ICA DMN GMV (ROI)	↑**PSS** (trend for ↓ DMN GMV) ↑DMN FC in L FSG and medial OFC, middle CG, occipital middle G; and in R middle FG, posterior CC and precuneus

Table 1. *(Continuation)*

Type of study	Study	N (Females)	Age (SD)	PSS (SD/*SE)	Methods	Findings in structural and rs-fMRI
Functional	(Taren et al., 2015)	130 (59)	40.15 (6.14)	13.3 (6.1)	Amy seed-based FC	↑**PSS:** ↑FC R Amy - R subgenual ACC; ↑FC L Amy: L subgenual ACC, L parahippocampal G, R S Temporal, L Insula, R Perigenual A Cingulum
	(Archer et al., 2018)	26 (22)	M: 45.04 (13.25) F: 48.81 (15.21)	M: 11.37 (5.68) F: 12.59 (6.04)	Amy, Hip and ACC seed-based FC	↑ **PSS rs-fMRI in Females:** ↑ FC in L ACC - L/R MCG and in R ACC - L/R MCG; ↓ FC in L Hip - L/R Precuneus and in R Hip - L ITG/MTG/FG ↑ **PSS-FC association in F>M in:** L Amy - R Paracentral Lobule and L Hip - L MFG ↑ **PSS-FC association in M>F in**: L /R ACC - L Cerebellum Lobule VIIIA
	(Wu et al., 2018)	Young adults: 22 (9) Adults: 21 (9)	Young adults: 19.55 (0.43) Adults: 35.21 (4.19)	Young adults: 23.14 (6.18) Adults: 21.24 (7.84)	Amy seed-based FC	PSS x Age interaction in R Amy FC with subgenual ACC and vmPFC: **Young adults:** ↑PSS ↓R Amy-vmPFC FC (trend ↓R Amy- subgenual ACC FC) **Adults:** no significant correlations were found
	(McDermott et al., 2019)	22 (14)	71.2 (9.61)	9.7 (6.6)	Hip seed-based FC	↓**PSS** ↑ FC L Hip - L Parietal Lobe
	Chapter 4 (in submission)	252 (143)	39.2 (21.20)	15.4 (6.82)	Amy seed-based FC LEiDA (dynamic FC)	↑**PSS** ↑R Amy FC: PFC (mainly R), R Precuneus, R anterior and middle cingulate Trend ↑**PSS** ↑L Amy - R PFC FC ↑**PSS** ↓occurrence of an activity pattern in which amygdala and hippocampus signals evolve in opposite directions with respect to the rest of the brain

As a starting point for this Thesis, a review of the neuroimaging studies regarding the effects of perceived stress (measured by PSS10) on the morphology and function of the healthy brain was performed (Chapter 1, Section 5). Interestingly, a clear link between stress perception and the brain's structure (and functioning) was observed, albeit revealing some disparities. For example, whereas some studies showed positive associations with subcortical regions, such as the amygdala and hippocampus (Hölzel et al., 2010; Sherman et al., 2016), others failed in showing these associations (Joss et al., 2021, 2020; Moreno et al., 2017; Wu et al., 2020).

As a way of clarifying discrepancies observed in the literature, we decided to design a robust study that considered the use of distinct volumetric techniques as a way of increasing the trustfulness of results. Thus, in Chapter 2, we explored the association between perceived stress and the volumetry of subcortical regions (which are the most predisposal to be affected), using FSL-VBM and FreeSurfer methods. In line with the works of Hölzel and Sherman (Hölzel et al., 2010; Sherman et al., 2016), we saw that increased levels of perceived stress (measured by PSS10) positively associate with the volume of the right amygdala, with a similar trend on the left hemisphere not being replicated in FreeSurfer Analysis (which was more restrictive than the FSL-VBM). Furthermore, a significant association with the anterior hippocampal volumes was observed, which seems to complement Li et al.'s observations regarding the parahippocampal-PSS10 association (Li et al., 2014). Notably, the work of Chapter 2 confirmed the great physiological relevance of the PSS10 metric, as well as the strong link between stress perception and amygdala size, in which we decided to focus on.

Following the hint of Chapter 2 (i.e., the replicability of the amygdala-PSS10 link across FSL-VBM and FreeSurfer methods), we decided to uphold our conclusions by reevaluating a subgroup of 21 participants 8 months after the first assessment (Work presented in Appendix A – 34th ECNP Congress Poster). Shortly after having two acquisitions per subject, we explored the association of amygdala volume and PSS levels in: a) moment 1; b) moment 2; c) and combining the data from both moments. When analyzing moments 1 and 2 individually, only a positive trend of association was observed. Importantly, when gathering all the MRI acquisitions in the same analysis as a way of increasing the statistical power (Goulet and Cousineau, 2019), the dependence between amygdala size and PSS scores was (statistically significantly) highlighted. Therefore, these results seem to indicate that this positive relationship is stable across time, at least in young adults.

Although considering the importance of the studies mentioned above (and their particular contribution to set aside some of the discrepancies observed in the literature), stress has become pervasive, and it is no longer limited to a specific age range or life stage. Notably, the association between amygdala size and stress perception was observed in young (Hölzel et al., 2010) and older adults (Sherman et al., 2016) individually, but none of these studies considered stress and life as a continuum. Therefore, in Chapter 3, using a sizeable cohort with a broad age range, we were able to add the life span component, which is missed by the narrow age-ranged studies like the ones presented in the literature (Hölzel et al., 2010; Li et al., 2014; Moreno et al., 2017; Sherman et al., 2016). Indeed, being a transversal study across life instead of a longitudinal one, Chapter's 3 work was the first evaluating the interaction between the amygdala-PSS link and age, considering a representative population from young adults to elderly subjects. Herein, we show that besides stability across time, the association between stress perception and amygdala volume is also stable across age. Interestingly, significance was only observed in the right amygdala, highlighting the right hemisphere's prominence on emotional and affective functions, which has previously been discussed in Chapter 2 (Cerqueira et al., 2008). Notably, our findings continue to contradict Wu et al. observations, with no interactions between this association and age being observed (Wu et al., 2020). Nonetheless, the sample size of our cohort, which is particularly emphasized when compared with the study of Wu and colleagues (Wu et al., 2020), as well as the use of the more restrictive technique (FreeSurfer), supports the robustness of this study, as well as the confidence that we have on our results.

At this point, with irrefutable evidence on the association between amygdala size and stress perception, we decided to investigate how stress relates to brain functioning (and particularly on the interaction between perceived stress and amygdala connectivity). Interestingly, excluding the previous works developed by our group (in which an Independent Component Analysis was used to ascertain the impact of stress in resting-state networks) (Soares et al., 2017, 2013b, 2013a), all other groups have focused their functional investigations in seed-based connectivity analysis, mainly in the amygdala and hippocampus (key regions involved in the stress response) (Archer et al., 2018; McDermott et al., 2019; Taren et al., 2015; Wu et al., 2018, p. 201). Therefore, in Chapter 5, we started by conducting an amygdala seed-connectivity analysis using the same sizeable cohort. Herein, we saw that increases in perceived stress are followed by increases in amygdala connectivity with frontal regions, which reinforces the pathological effect of in-phase synchronicity between subcortical and cortical regions. Notably, this result seems to go in line with the Taren et al. (Taren et al., 2015) observations but, again, are not

consistent with Wu's research (Wu et al., 2018). Although our result withstands a relevant pattern of static connectivity (Banks et al., 2007; Berboth and Morawetz, 2021; Johnson et al., 2018), they do not provide any information about the temporal dynamics of the brain, which are crucial to evaluate the stress repercussions at the neuromatrix (Sousa, 2016). Therefore, and considering that no other work in the literature has explored the association of PSS10 scores with brain functional dynamics, we decided to disseminate the effects of perceived stress on brain functioning using LEiDA. This whole-brain data-driven method revealed that perceived stress is associated with a reduced occurrence of a pattern in which the amygdala and hippocampal signals grow in opposite directions to the rest of the brain. Importantly, this new finding is of great relevance as it shows the protective effect of counterbalanced (i.e., phase-shifted) activity between brain subsystems (Alonso Martínez et al., 2020; Figueroa et al., 2019).

Altogether, our findings highlight the involvement of the amygdala and hippocampus in stress response (both at morphological and at functional levels). Indeed, morphological associations in the hippocampus were not as strong as amygdala observations. However, when considering solely the anterior hippocampus in FreeSurfer analysis, results showed significance (see Chapter 2 for details). Indeed, there is a dichotomy between the functional role of anterior (more emotional) and posterior (more cognitive) components of the hippocampus (Pinto et al., 2015; Strange et al., 2014). This contrast deeply relates with hippocampal molecular, structural, and circuitry levels, in which the amygdala also has a crucial role (Wang, 2017; Zhang et al., 2021).

Briefly, the amygdala is composed of three main subnuclei: the basolateral amygdala (BLA), the central amygdala (CeA), and the medial amygdala (MeA). Notably, each sub-compartment has distinguished functions, mediating excitatory (BLA, anxiogenic) or inhibitory (CeA and MeA, anxiolytic) indirect pathways, which will ultimately result in the activation or deactivation of the HPA axis (see the supplementary material of (Picó-Pérez et al., 2019) and the work of (Zhang et al., 2021) for details). The hippocampus can also be transversally divided into three main sections: CA1, CA3, and dentate gyrus (DG) (Wang, 2017). Importantly, in situations of chronic stress, there is a circuit-specific remodeling of BLA excitatory projections to the ventral hippocampus (Zhang et al., 2021), and particularly to the ventral CA1 portion (Wang, 2017), in which synaptic outgrowth, input integration, and neuronal activity, will ultimately cause increased anxiety (Sousa and Almeida, 2012; Zhang et al., 2021). Moreover, it has also been shown that ventral CA1-PFC inputs are activated in anxiety-related behaviors (Ciocchi et al., 2015). Thus, our morphological results can be a consequence of this neuronal remodeling, with LEiDA findings providing

new insights on how increases in stress perception levels condition the amygdala-hippocampal subsystem.

In summary, this Thesis revealed the existence of a strong link between amygdala size and stress perception, which positive association is stable across time, and across age. It also shows that increases in perceived stress relate to increases in amygdala-cortical connectivity and decreases in the occurrence of a pattern of counterbalanced activity between the amygdala-hippocampus subsystem and the rest of the brain. Therefore, the initial hypothesis of this Thesis was verified, with stress perception exhibiting a substantial interaction both with brain morphology and functioning.

2. Future perspectives

This Thesis provided new insights on how perceived stress impacts brain morphology and functioning. However, there is still a large spectrum of questions we would like to address in future studies. Firstly, we would like to replicate our functional analysis in other cohorts. Considering that LEiDA is a data-driven method, we would like to confirm if the same functional amygdala-hippocampus subsystem is reproducible in other healthy populations. In addition, using LEiDA in clinical cohorts of stress-related diseases could also help us ascertain if this subsystem is a common trait of pathological stress. Other options include the conductance of further research to unravel other/new biomarkers of the stressed brain. Herein, we can opt by exploring new methods (as the analyses of fiber pathways by diffusion tensor tractography) or by reviewing measures that are still undeveloped in the current literature (for instance, WM volumetry)(Li et al., 2014; Moreno et al., 2017). Importantly, we would like to combine all this information to develop a predictive model of stress degree. Then, perform a longitudinal study to evaluate the model's efficacy both as an output for risk assessment and as a tool of therapy improvement.

3. References

Alonso Martínez, S., Deco, G., Ter Horst, G.J., Cabral, J., 2020. The Dynamics of Functional Brain Networks Associated With Depressive Symptoms in a Nonclinical Sample. Front. Neural Circuits 14, 570583. https://doi.org/10.3389/fncir.2020.570583

Arborelius, L., Owens, M., Plotsky, P., Nemeroff, C., 1999. The role of corticotropin-releasing factor in depression and anxiety disorders. Journal of Endocrinology 160, 1–12. https://doi.org/10.1677/joe.0.1600001

Archer, J.A., Lee, A., Qiu, A., Chen, S.-H.A., 2018. Functional connectivity of resting-state, working memory and inhibition networks in perceived stress. Neurobiol. Stress 8, 186–201. https://doi.org/10.1016/j.ynstr.2017.01.002

Banks, S.J., Eddy, K.T., Angstadt, M., Nathan, P.J., Phan, K.L., 2007. Amygdala–frontal connectivity during emotion regulation. Soc Cogn Affect Neurosci 2, 303–312. https://doi.org/10.1093/scan/nsm029

Berboth, S., Morawetz, C., 2021. Amygdala-prefrontal connectivity during emotion regulation: A meta-analysis of psychophysiological interactions. Neuropsychologia 153, 107767. https://doi.org/10.1016/j.neuropsychologia.2021.107767

Caetano, I., Amorim, L., Soares, J.M., Ferreira, S., Coelho, A., Reis, J., Santos, N.C., Moreira, P.S., Marques, P., Magalhães, R., Esteves, M., Picó-Pérez, M., Sousa, N., 2021. Amygdala size varies with stress perception. Neurobiology of Stress 14, 100334. https://doi.org/10.1016/j.ynstr.2021.100334

Cerqueira, J.J., Almeida, O.F.X., Sousa, N., 2008. The stressed prefrontal cortex. Left? Right! Brain, Behavior, and Immunity 22, 630–638. https://doi.org/10.1016/j.bbi.2008.01.005

Ciocchi, S., Passecker, J., Malagon-Vina, H., Mikus, N., Klausberger, T., 2015. Selective information routing by ventral hippocampal CA1 projection neurons. Science 348, 560–563. https://doi.org/10.1126/science.aaa3245

Fett, A.-K.J., Lemmers-Jansen, I.L.J., Krabbendam, L., 2019. Psychosis and urbanicity: a review of the recent literature from epidemiology to neurourbanism. Current Opinion in Psychiatry 32, 232–241. https://doi.org/10.1097/YCO.0000000000000486

Figueroa, C.A., Cabral, J., Mocking, R.J.T., Rapuano, K.M., Hartevelt, T.J., Deco, G., Expert, P., Schene, A.H., Kringelbach, M.L., Ruhé, H.G., 2019. Altered ability to access a clinically relevant control network in patients remitted from major depressive disorder. Hum Brain Mapp 40, 2771–2786. https://doi.org/10.1002/hbm.24559

Goulet, M.-A., Cousineau, D., 2019. The Power of Replicated Measures to Increase Statistical Power. Advances in Methods and Practices in Psychological Science 2, 199–213. https://doi.org/10.1177/2515245919849434

Hölzel, B.K., Carmody, J., Evans, K.C., Hoge, E.A., Dusek, J.A., Morgan, L., Pitman, R.K., Lazar, S.W., 2010. Stress reduction correlates with structural changes in the amygdala. Social Cognitive and Affective Neuroscience 5, 11–17. https://doi.org/10.1093/scan/nsp034

Johnson, F.K., Delpech, J.-C., Thompson, G.J., Wei, L., Hao, J., Herman, P., Hyder, F., Kaffman, A., 2018. Amygdala hyper-connectivity in a mouse model of unpredictable early life stress. Transl Psychiatry 8, 49. https://doi.org/10.1038/s41398-018-0092-z

Joss, D., Khan, A., Lazar, S.W., Teicher, M.H., 2021. A pilot study on amygdala volumetric changes among young adults with childhood maltreatment histories after a mindfulness intervention. Behavioural Brain Research 399, 113023. https://doi.org/10.1016/j.bbr.2020.113023

Joss, D., Lazar, S.W., Teicher, M.H., 2020. Effects of a mindfulness based behavioral intervention for young adults with childhood maltreatment history on hippocampal morphometry: a pilot MRI study with voxel-based morphometry. Psychiatry Res Neuroimaging 301, 111087. https://doi.org/10.1016/j.pscychresns.2020.111087

Kim, E.Y., Miklowitz, D.J., Biuckians, A., Mullen, K., 2007. Life stress and the course of early-onset bipolar disorder. Journal of Affective Disorders 99, 37–44. https://doi.org/10.1016/j.jad.2006.08.022

Lederbogen, F., Kirsch, P., Haddad, L., Streit, F., Tost, H., Schuch, P., Wüst, S., Pruessner, J.C., Rietschel, M., Deuschle, M., Meyer-Lindenberg, A., 2011. City living and urban upbringing affect neural social stress processing in humans. Nature 474, 498–501. https://doi.org/10.1038/nature10190

Li, H., Li, W., Wei, D., Chen, Q., Jackson, T., Zhang, Q., Qiu, J., 2014. Examining brain structures associated with perceived stress in a large sample of young adults via voxel-based morphometry. NeuroImage 92, 1–7. https://doi.org/10.1016/j.neuroimage.2014.01.044

Lucassen, P.J., Pruessner, J., Sousa, N., Almeida, O.F.X., Van Dam, A.M., Rajkowska, G., Swaab, D.F., Czéh, B., 2014. Neuropathology of stress. Acta Neuropathol 127, 109–135. https://doi.org/10.1007/s00401-013-1223-5

McDermott, K., Ren, P., Lin, F., 2019. The mediating role of hippocampal networks on stress regulation in amnestic mild cognitive impairment. Neurobiology of Stress 10, 100162. https://doi.org/10.1016/j.ynstr.2019.100162

Moreno, G.L., Bruss, J., Natalie, L.D., 2017. Increased perceived stress is related to decreased prefrontal cortex volumes among older adults. Journal of Clinical and Experimental Neuropsychology 313–325. https://doi.org/10.1080/13803395.2016.1225006

Pêgo, J.M., Sousa, J.C., Almeida, O., Sousa, N., 2009. Stress and the Neuroendocrinology of Anxiety Disorders, in: Stein, M.B., Steckler, T. (Eds.), Behavioral Neurobiology of Anxiety and Its Treatment, Current Topics in Behavioral Neurosciences. Springer Berlin Heidelberg, Berlin, Heidelberg, pp. 97–118. https://doi.org/10.1007/7854_2009_13

Picó-Pérez, M., Ipser, J., Taylor, P., Alonso, P., López-Solà, C., Real, E., Segalàs, C., Roos, A., Menchón, J.M., Stein, D.J., Soriano-Mas, C., 2019. Intrinsic functional and structural connectivity of

emotion regulation networks in obsessive-compulsive disorder. Depress Anxiety 36, 110–120. https://doi.org/10.1002/da.22845

Pinto, V., Costa, J.C., Morgado, P., Mota, C., Miranda, A., Bravo, F.V., Oliveira, T.G., Cerqueira, J.J., Sousa, N., 2015. Differential impact of chronic stress along the hippocampal dorsal–ventral axis. Brain Struct Funct 220, 1205–1212. https://doi.org/10.1007/s00429-014-0713-0

Sherman, S.M., Cheng, Y.-P., Fingerman, K.L., Schnyer, D.M., 2016. Social support, stress and the aging brain. Soc Cogn Affect Neurosci 11, 1050–1058. https://doi.org/10.1093/scan/nsv071

Soares, J.M., Marques, P., Magalhães, R., Santos, N.C., Sousa, N., 2017. The association between stress and mood across the adult lifespan on default mode network. Brain Struct Funct 222, 101–112. https://doi.org/10.1007/s00429-016-1203-3

Soares, J.M., Sampaio, A., Ferreira, L.M., Santos, N.C., Marques, F., Palha, J.A., Cerqueira, J.J., Sousa, N., 2012. Stress-induced changes in human decision-making are reversible. Transl Psychiatry 2, e131–e131. https://doi.org/10.1038/tp.2012.59

Soares, J.M., Sampaio, A., Ferreira, L.M., Santos, N.C., Marques, P., Marques, F., Palha, J.A., Cerqueira, J.J., Sousa, N., 2013a. Stress Impact on Resting State Brain Networks. PLoS ONE 8, e66500. https://doi.org/10.1371/journal.pone.0066500

Soares, J.M., Sampaio, A., Marques, P., Ferreira, L.M., Santos, N.C., Marques, F., Palha, J.A., Cerqueira, J.J., Sousa, N., 2013b. Plasticity of resting state brain networks in recovery from stress. Front. Hum. Neurosci. 7. https://doi.org/10.3389/fnhum.2013.00919

Sousa, N., 2016. The dynamics of the stress neuromatrix. Mol Psychiatry 21, 302–312. https://doi.org/10.1038/mp.2015.196

Sousa, N., Almeida, O.F.X., 2012. Disconnection and reconnection: the morphological basis of (mal)adaptation to stress. Trends in Neurosciences 35, 742–751. https://doi.org/10.1016/j.tins.2012.08.006

Sousa, N., Cerqueira, J.J., Almeida, O.F.X., 2008. Corticosteroid receptors and neuroplasticity. Brain Research Reviews 57, 561–570. https://doi.org/10.1016/j.brainresrev.2007.06.007

Strange, B.A., Witter, M.P., Lein, E.S., Moser, E.I., 2014. Functional organization of the hippocampal longitudinal axis. Nat Rev Neurosci 15, 655–669. https://doi.org/10.1038/nrn3785

Taren, A.A., Gianaros, P.J., Greco, C.M., Lindsay, E.K., Fairgrieve, A., Brown, K.W., Rosen, R.K., Ferris, J.L., Julson, E., Marsland, A.L., Bursley, J.K., Ramsburg, J., Creswell, J.D., 2015. Mindfulness meditation training alters stress-related amygdala resting state functional connectivity: a randomized controlled trial. Soc. Cogn. Affect. Neurosci. 10, 1758–1768. https://doi.org/10.1093/scan/nsv066

Wang, J.-Z., 2017. From Structure to Behavior in Basolateral Amygdala-Hippocampus Circuits. Frontiers in Neural Circuits 11, 8.

Welberg, L., 2014. A REDD line from stress to depression. Nat Rev Neurosci 15, 350–350. https://doi.org/10.1038/nrn3749

World Health Organization, 2021. Mental health [WWW Document]. URL https://www.who.int/westernpacific/health-topics/mental-health (accessed 12.4.21).

Wu, J., Geng, X., Shao, R., Wong, N.M.L., Tao, J., Chen, L., Chan, C.C.H., Lee, T.M.C., 2018. Neurodevelopmental changes in the relationship between stress perception and prefrontal-amygdala functional circuitry. NeuroImage-Clin. 20, 267–274. https://doi.org/10.1016/j.nicl.2018.07.022

Wu, J., Tong, H., Liu, Z., Tao, J., Chen, L., Chan, C.C.H., Lee, T.M.C., 2020. Neurobiological effects of perceived stress are different between adolescents and middle-aged adults. Brain Imaging and Behavior. https://doi.org/10.1007/s11682-020-00294-7

Zhang, W.-H., Zhang, J.-Y., Holmes, A., Pan, B.-X., 2021. Amygdala Circuit Substrates for Stress Adaptation and Adversity. Biological Psychiatry 89, 847–856. https://doi.org/10.1016/j.biopsych.2020.12.026

APPENDIX A

34th ECNP Congress Poster

Inês Caetano, Liliana Amorim, José Miguel Soares, Sónia Ferreira, Ana Coelho, Joana Reis, Nadine Correia Santos, Pedro Silva Moreira, Paulo Marques, Ricardo Magalhães, Madalena Esteves, Maria Picó-Pérez, Nuno Sousa

Abstract selected for publication and in-person poster presentation
at 34th ECNP Congress, 1-5 October 2021
Winner of ECNP Excellence Award 2021
(ePoster available on the online congress platform)

(In publication in a supplement of European Neuropsychopharmacology (ENP) Journal)

Amygdala size associates with stress perception

Background: Stress is largely understood as an individual and subjective perception. Indeed, depending on its type, duration, and individual vulnerability, the variable response of the subject to the stressor can be partially measured. In our group's recent work, we have shown an association between amygdala size and perceived stress, in a healthy cohort of young adults [1]. Herein we uphold our conclusions by observing a similar association in a subset of participants that have performed a second MRI scan in a different moment.

Methods: In the present study, 21 healthy participants recruited at the School of Medicine, University of Minho, performed two individual evaluation sessions, with, at least, 8 months of span. In each session, a psychological characterization using the 10-items Perceived Stress Scale (PSS) [2] was made as well as a structural MRI scan. The imaging sessions were conducted at Hospital of Braga (Braga, Portugal) on a clinical approved Siemens Magnetom Avanto 1.5 T MRI scanner (Siemens Medical Solutions, Erlangen, Germany), using a 12-channel receive-only head coil. The 3D magnetization prepared rapid gradient echo (MPRAGE) were acquired with a repetition time (TR) = 2.7 s, echo time (TE) = 2.73 ms, 176 sagittal slices with no gap, field-of-view (FoV) = 256 mm, flip angle (FA) = 8°, in-plane resolution = 1.2 × 1.2 mm2 and slice thickness = 1.2 mm. After visual inspection, image preprocessing was made using fMRIPrep version 1.4.1 [3]. Then, the FreeSurfer derivatives of the fMRIPrep were used to compute individual volumes. For statistical analysis, both the SPSS version 23 (IBM, SPSS, Chicago, IL, USA), and JASP version 0.11.1 were used. For exploring the association between amygdala and perceived stress, multilinear regression models with volume as the dependent variable and PSS scores, age and sex as independent variables were established.

Results: Between the first and the second moment, the psychological state of the subjects differed (mean PSS difference = 2.6 +/- 3.8). The model computed exclusively with the data acquired on first sessions shows a positive association tendency between amygdala size and perceived stress scores, not achieving statistical significance (N = 21, PSS = 21.048 +/- 7.124; R = 0.431, Adj R^2 = 0.186, p = 0.310). On the second sessions model (N = 21, PSS = 21.571 +/- 7.03; R= 0.605, Adj R^2 = 0.255, p = 0.047), the statistical significance of the PSS independent term shows a positive association without achieving significance (B = 0.001, t = 2.025, p = 0.059). Including both sessions on a global model (N = 42, PSS = 21.310 +/- 7.031; R = 0.488, Adj R^2 = 0.178, p = 0.015), the positive association between amygdala volumes and perceived stress is verified (B = 0.001, t = 2.031, p = 0.049).

Conclusions: Our results sustain our previous work conclusions, in which a positive association between amygdala size and perceived stress scores is observed. Importantly, this relationship is observed when including subjects assessed at different timepoints, with distinct perceived stress levels.

References:

[1] Caetano, I., Amorim, L., Soares, J.M., Ferreira, S., Coelho, A., Reis, J., Santos, N.C., Moreira, P.S., Marques, P., Magalhães, R., Esteves, M., Picó-Pérez, M., Sousa, N., 2021. Amygdala size varies with stress perception. Neurobiology of Stress 14, 100334. doi:10.1016/j.ynstr.2021.100334

[2] Cohen, S., Kamarck, T., Mermelstein, R., 1983. A Global Measure of Perceived Stress. Journal of Health and Social Behavior 24, 385. doi:10.2307/2136404

[3] Esteban, O., Markiewicz, C.J., Blair, R.W., Moodie, C.A., Isik, A.I., Erramuzpe, A., Kent, J.D., Goncalves, M., DuPre, E., Snyder, M., Oya, H., Ghosh, S.S., Wright, J., Durnez, J., Poldrack, R.A., Gorgolewski, K.J., 2018. fMRIPrep: a robust preprocessing pipeline for functional MRI. Nature Methods 16, 111–116. doi:10.1038/s41592-018-0235-4

No conflict of interest

Topics:

Healthy Brain/ Prevention/ Course alteration

In vivo neuroimaging

Stress-related disorders

APPENDIX B

Ongoing work

Effects of perceived stress on brain morphometry and functioning: A systematic review of neuroimaging findings

Inês Caetano, Rita Vieira, Maria Picó-Pérez, Nuno Sousa

PROSPERO 2021 CRD42021278981

Available at

https://www.crd.york.ac.uk/prospero/display_record.php?ID=CRD42021278981

PROSPERO
International prospective register of systematic reviews

NHS National Institute for Health Research

UNIVERSITY of York
Centre for Reviews and Dissemination

Systematic review

*Fields that have an **asterisk (*)** next to them means that they **must be answered. Word limits** are provided for each section. You will be unable to submit the form if the word limits are exceeded for any section. Registrant means the person filling out the form.*

1. * Review title.

Give the title of the review in English

Effects of perceived stress on brain morphometry and functioning: A systematic review of neuroimaging findings.

2. Original language title.

For reviews in languages other than English, give the title in the original language. This will be displayed with the English language title.

3. * Anticipated or actual start date.

Give the date the systematic review started or is expected to start.

29/06/2021

4. * Anticipated completion date.

Give the date by which the review is expected to be completed.

01/02/2022

5. * Stage of review at time of this submission.

Tick the boxes to show which review tasks have been started and which have been completed. Update this field each time any amendments are made to a published record.

Reviews that have started data extraction (at the time of initial submission) are not eligible for inclusion in PROSPERO. If there is later evidence that incorrect status and/or completion date has been supplied, the published PROSPERO record will be marked as retracted.

This field uses answers to initial screening questions. It cannot be edited until after registration.

The review has not yet started: No

Review stage	Started	Completed
Preliminary searches	Yes	No
Piloting of the study selection process	Yes	No
Formal screening of search results against eligibility criteria	Yes	No
Data extraction	No	No
Risk of bias (quality) assessment	No	No
Data analysis	No	No

Provide any other relevant information about the stage of the review here.

6. * Named contact.

The named contact is the guarantor for the accuracy of the information in the register record. This may be any member of the review team.

Inês Caetano

Email salutation (e.g. "Dr Smith" or "Joanne") for correspondence:

Inês Caetano

7. * Named contact email.

Give the electronic email address of the named contact.

ines.caetano91@gmail.com

8. Named contact address

Give the full institutional/organisational postal address for the named contact.

Escola de Medicina, Universidade do Minho, Campus de Gualtar, 4710-057 Braga, Portugal.

9. Named contact phone number.

Give the telephone number for the named contact, including international dialling code.

00351253 604 800

10. * Organisational affiliation of the review.

Full title of the organisational affiliations for this review and website address if available. This field may be completed as 'None' if the review is not affiliated to any organisation.

Life and Health Sciences Research Institute (ICVS), School of Medicine, University of Minho; ICVS-3Bs PT Government Associate Laboratory, Braga/Guimarães, Portugal

Organisation web address:

https://www.med.uminho.pt/en ; http://icvs.uminho.pt/default.aspx

11. * Review team members and their organisational affiliations.

Give the personal details and the organisational affiliations of each member of the review team. Affiliation refers to groups or organisations to which review team members belong. **NOTE: email and country now MUST be entered for each person, unless you are amending a published record.**

Inês Caetano. Life and Health Sciences Research Institute (ICVS), School of Medicine, University of Minho; ICVS-3Bs PT Government Associate Laboratory, Braga/Guimarães, Portugal
Rita Vieira. Life and Health Sciences Research Institute (ICVS), School of Medicine, University of Minho; ICVS-3Bs PT Government Associate Laboratory, Braga/Guimarães, Portugal
Maria Picó-Pérez. Life and Health Sciences Research Institute (ICVS), School of Medicine, University of Minho; ICVS-3Bs PT Government Associate Laboratory, Braga/Guimarães, Portugal
Nuno Sousa. Life and Health Sciences Research Institute (ICVS), School of Medicine, University of Minho; ICVS-3Bs PT Government Associate Laboratory, Braga/Guimarães, Portugal

12. * Funding sources/sponsors.

Details of the individuals, organizations, groups, companies or other legal entities who have funded or sponsored the review.

This work is funded by National funds, through the Foundation for Science and Technology (FCT) - project UIDB/50026/2020 and UIDP/50026/2020; and by the projects NORTE-01-0145-FEDER-000013 and NORTE-01-0145-FEDER-000023, supported by Norte Portugal Regional Operational Programme (NORTE 2020), under the PORTUGAL 2020 Partnership Agreement, through the European Regional Development Fund (ERDF). IC and RV are supported by fellowship grants through the FCT (grants number SFRH/BD/133006/2017 and PD/BDE/150619/2020).

Grant number(s)

State the funder, grant or award number and the date of award

13. * Conflicts of interest.

List actual or perceived conflicts of interest (financial or academic).

None

14. Collaborators.

Give the name and affiliation of any individuals or organisations who are working on the review but who are not listed as review team members. **NOTE: email and country must be completed for each person, unless you are amending a published record.**

15. * Review question.

State the review question(s) clearly and precisely. It may be appropriate to break very broad questions down into a series of related more specific questions. Questions may be framed or refined using PI(E)COS or similar where relevant.

What is the effect of perceived stress in brain morphometry? What is the effect of perceived stress in brain function?

16. * Searches.

State the sources that will be searched (e.g. Medline). Give the search dates, and any restrictions (e.g. language or publication date). Do NOT enter the full search strategy (it may be provided as a link or attachment below.)

The searches will be restricted to human subjects, English language, and research article in ISI Web Knowledge, PubMed and Scopus databases. No restrictions on date, setting or country will be applied. Moreover, searches adapted to the syntax and subjects heading of each database. Searches will be conducted twice: (1) initially to identify articles for screening; (2) immediately after the final analysis, to identify new articles published since the initial search. A comprehensive strategy limited to Title/Abstract was elaborated including the following key terms "Prolonged stress; Chronic stress; perceived stress; stress perception; perception of stress; PSS; PSS10; PSS-10; 10-PSS; 10-item PSS; Psychological stress; Psychosocial stress; Occupational stress; Psychological distress; Neuroimag* ; volum*; magnetic resonance imaging; MRI; resting state; resting-state; functional MRI; fMRI; connectivity; structural MRI; gray matter; grey matter; morphology; morphometry; seed-based; VBM; FreeSurfer; FSL; brain connectivity". The search will be conducted until January 2022.

17. URL to search strategy.

Upload a file with your search strategy, or an example of a search strategy for a specific database, (including the keywords) in pdf or word format. In doing so you are consenting to the file being made publicly accessible. Or provide a URL or link to the strategy. Do NOT provide links to your search **results**.

https://www.crd.york.ac.uk/PROSPEROFILES/278981_STRATEGY_20210915.pdf

Alternatively, upload your search strategy to CRD in pdf format. Please note that by doing so you are consenting to the file being made publicly accessible.

Do not make this file publicly available until the review is complete

18. * Condition or domain being studied.

Give a short description of the disease, condition or healthcare domain being studied in your systematic review.

There are opposite perspectives regarding the effects of stress in brain morphology and functioning. Interestingly, part of these differences can be justified by the use of different study approaches and methodologies. Differences on stress concept, measurements and software used in the analysis are examples of these variations. Particularly, the use of clinical populations leads to distinct results across studies. Interestingly, there is still a lack in stress studies regarding healthy participants. Therefore, in this review we aim to unravel the association between perceived stress and brain fingerprint, both at structural and functional levels, before the development of any neuropsychiatric disease.

19. * Participants/population.

Specify the participants or populations being studied in the review. The preferred format includes details of both inclusion and exclusion criteria.

This review will include participants with 18+ years, without any neuropsychiatric disorder or any other

comorbidity of the central nervous system, at different levels of stress.

20. * Intervention(s), exposure(s).

Give full and clear descriptions or definitions of the interventions or the exposures to be reviewed. The preferred format includes details of both inclusion and exclusion criteria.

This review will include studies where participants perceived stress was measures with Perceived Stress Scale (PSS). Studies where subjects without pathology are exposed to stress (psychological stress, psychosocial stress, occupational stress, job-related stress, stress), will also be included.

21. * Comparator(s)/control.

Where relevant, give details of the alternatives against which the intervention/exposure will be compared (e.g. another intervention or a non-exposed control group). The preferred format includes details of both inclusion and exclusion criteria.

The studies included must be included in one of these topics: 1) Regression analyses with PSS; 2) Stressed vs non-stress, with PSS as group division criteria (or, at least, as confirmation).

22. * Types of study to be included.

Give details of the study designs (e.g. RCT) that are eligible for inclusion in the review. The preferred format includes both inclusion and exclusion criteria. If there are no restrictions on the types of study, this should be stated.

Correlational studies (relationship between PSS and brain), longitudinal, experimental and clinical trial studies (before and after being exposed to stress or stress-free intervention).

23. Context.

Give summary details of the setting or other relevant characteristics, which help define the inclusion or exclusion criteria.

24. * Main outcome(s).

Give the pre-specified main (most important) outcomes of the review, including details of how the outcome is defined and measured and when these measurement are made, if these are part of the review inclusion criteria.

The primary outcomes are neuroimaging biomarkers of increased perceived stress (volumetric and functional changes that associates with PSS). The secondary outcomes will unveil brain regions plastic to alterations in stress-related conditions.

Measures of effect

Please specify the effect measure(s) for you main outcome(s) e.g. relative risks, odds ratios, risk difference, and/or 'number needed to treat.

25. * Additional outcome(s).

List the pre-specified additional outcomes of the review, with a similar level of detail to that required for main outcomes. Where there are no additional outcomes please state 'None' or 'Not applicable' as appropriate to the review

Additional outcomes will include the identification of variables/features associated with increased healthy

resilience to stress (both copying mechanisms and factors that contribute to individual ability to deal with stress).

Measures of effect

Please specify the effect measure(s) for you additional outcome(s) e.g. relative risks, odds ratios, risk difference, and/or 'number needed to treat.

26. * Data extraction (selection and coding).

Describe how studies will be selected for inclusion. State what data will be extracted or obtained. State how this will be done and recorded.

Inclusion criteria:

• Heathy adult with 18+ years;

• No neuropsychiatric disorder or any other comorbidity of the central nervous system;

• PSS evaluation and neuroimaging markers;

• Comparison between stressed and non-stress subjects (categorization validated by PSS) or correlation between PSS and neuroimaging markers (anatomical and resting-state)

• English language;

• Published on peer-reviewed journals.

Exclusion criteria:

• Psychiatric or neurologic disorders diagnoses;

• Post-mortem studies;

• N 10.

• Gray literature;

• Case series, case reports, conference abstracts, protocol papers, letters, editorials, opinion pieces, theoretical papers, reviews, and studies with purely quantitative designs

Study Selection:

As stated above, after the primary searchers, the results will be upload to Zotero to remove duplicates. Afterwards, a two-step screening process will be implemented (Level 1 assessment). Titles and abstracts of all publications will be screened against the eligibility criteria. If a decision cannot be made based on the title and abstract, the article will be retained for full-text screening. At level 2 assessment, full-text of all publications included at first screening will be detailed screened to determine eligibility. Inclusion and exclusion decisions will be saved into an Excel file. Any disagreement between reviewers will be solved through discussion and consensus. Neither of the review authors will be blind to journals title, authors names or institutions. The process of selection will be comprehensively reported using PRISMA flow diagram framework.

Data To extract: Sample size, sex, age, education, PSS scores, methodology (scanner, MRI technique, analysis and software used), and results (e.g., anatomical space, brain coordinates, brain regions, linear regression equations, significance and effect size,...)

27. * Risk of bias (quality) assessment.

State which characteristics of the studies will be assessed and/or any formal risk of bias/quality assessment tools that will be used.

We will use the NIH Study Quality Assessment Tools available at https://www.nhlbi.nih.gov/health-topics/study-quality-assessment-tools .

28. * Strategy for data synthesis.

Describe the methods you plan to use to synthesise data. This **must not be generic text** but should be **specific to your review** and describe how the proposed approach will be applied to your data. If meta-analysis is planned, describe the models to be used, methods to explore statistical heterogeneity, and software package to be used.

The selected articles will be organized following the two approaches used on the research: 1) Regression analyses with PSS; 2) Stressed vs non-stress, with PSS as group division criteria (or, at least, as confirmation). After review, If more than 10 eligible studies were found, grey matter volume and/or fMRI results will be meta-analyzed using the SDM software.

29. * Analysis of subgroups or subsets.

State any planned investigation of 'subgroups'. Be clear and specific about which type of study or participant will be included in each group or covariate investigated. State the planned analytic approach.

Age and sex covariates will be analyzed as factors to unveil differences in PSS-neuroimaging association. If more than 10 studies are eligible in one of those categories, a meta-analysis upon results will also be conducted.

30. * Type and method of review.

Select the type of review, review method and health area from the lists below.

Type of review

Cost effectiveness
No

Diagnostic
No

Epidemiologic

No

Individual patient data (IPD) meta-analysis
No

Intervention
No

Living systematic review
No

Meta-analysis
No

Methodology
No

Narrative synthesis
No

Network meta-analysis
No

Pre-clinical
No

Prevention
No

Prognostic
No

Prospective meta-analysis (PMA)
No

Review of reviews
No

Service delivery
No

Synthesis of qualitative studies
No

Systematic review
Yes

Other
No

Health area of the review

Alcohol/substance misuse/abuse
No

Blood and immune system
No

Cancer
No

Cardiovascular
No

Care of the elderly
No

Child health
No

Complementary therapies
No

COVID-19
No

Crime and justice
No

Dental
No

Digestive system
No

Ear, nose and throat
No

Education
No

Endocrine and metabolic disorders
No

Eye disorders
No

General interest
No

Genetics
No

Health inequalities/health equity
No

Infections and infestations
No

International development
No

Mental health and behavioural conditions
Yes

Musculoskeletal
No

Neurological
No

Nursing
No

Obstetrics and gynaecology
No

Oral health

No

Palliative care
No

Perioperative care
No

Physiotherapy
No

Pregnancy and childbirth
No

Public health (including social determinants of health)
No

Rehabilitation
No

Respiratory disorders
No

Service delivery
No

Skin disorders
No

Social care
No

Surgery
No

Tropical Medicine
No

Urological
No

Wounds, injuries and accidents
No

Violence and abuse
No

31. Language.

Select each language individually to add it to the list below, use the bin icon to remove any added in error.
English

There is not an English language summary

32. * Country.

Select the country in which the review is being carried out. For multi-national collaborations select all the countries involved.

Portugal

33. Other registration details.

Name any other organisation where the systematic review title or protocol is registered (e.g. Campbell, or The Joanna Briggs Institute) together with any unique identification number assigned by them. If extracted data will be stored and made available through a repository such as the Systematic Review Data Repository (SRDR), details and a link should be included here. If none, leave blank.

34. Reference and/or URL for published protocol.

If the protocol for this review is published provide details (authors, title and journal details, preferably in Vancouver format)

Add web link to the published protocol.

Or, upload your published protocol here in pdf format. Note that the upload will be publicly accessible.

No I do not make this file publicly available until the review is complete

Please note that the information required in the PROSPERO registration form must be completed in full even if access to a protocol is given.

35. Dissemination plans.

Do you intend to publish the review on completion?

No

Give brief details of plans for communicating review findings.?

36. Keywords.

Give words or phrases that best describe the review. Separate keywords with a semicolon or new line. Keywords help PROSPERO users find your review (keywords do not appear in the public record but are included in searches). Be as specific and precise as possible. Avoid acronyms and abbreviations unless these are in wide use.

37. Details of any existing review of the same topic by the same authors.

If you are registering an update of an existing review give details of the earlier versions and include a full bibliographic reference, if available.

38. * Current review status.

Update review status when the review is completed and when it is published.New registrations must be ongoing so this field is not editable for initial submission.
Please provide anticipated publication date

Review_Ongoing

39. Any additional information.

Provide any other information relevant to the registration of this review.

40. Details of final report/publication(s) or preprints if available.

Leave empty until publication details are available OR you have a link to a preprint (NOTE: this field is not editable for initial submission). List authors, title and journal details preferably in Vancouver format.

Give the link to the published review or preprint.

(Note: Page 12/12 empty)

Research strategy

Prolonged stress **Chronic stress** perceived stress stress perception perception of stress PSS PSS10 PSS-10 10-PSS 10-item PSS Psychological stress Psychosocial stress Occupational stress Psychological distress	Neuroimag* volum* magnetic resonance imaging MRI resting state **resting-state** functional MRI fMRI connectivity structural MRI gray matter grey matter morphology morphometry **seed-based** **VBM** **FreeSurfer** **FSL** brain connectivity
PUBMED (selection of English and Humans Filter)	(("prolonged stress"[Title/Abstract]) OR ("chronic stress"[Title/Abstract]) OR ("perceived stress"[Title/Abstract]) OR ("stress perception"[Title/Abstract]) OR ("perception of stress"[Title/Abstract]) OR ("PSS"[Title/Abstract]) OR ("PSS10"[Title/Abstract]) OR ("PSS-10"[Title/Abstract]) OR ("10-PSS"[Title/Abstract]) OR ("10-item PSS"[Title/Abstract]) OR ("Psychological stress"[Title/Abstract]) OR ("Psychosocial stress"[Title/Abstract]) OR ("Occupational stress"[Title/Abstract]) OR ("Psychological distress"[Title/Abstract])) AND (("Neuroimag*"[Title/Abstract]) OR ("volum*"[Title/Abstract]) OR ("magnetic resonance imaging"[Title/Abstract]) OR ("MRI"[Title/Abstract]) OR ("resting state"[Title/Abstract]) OR ("resting-state"[Title/Abstract]) OR ("functional MRI"[Title/Abstract]) OR ("fMRI"[Title/Abstract]) OR ("connectivity"[Title/Abstract]) OR ("structural MRI"[Title/Abstract]) OR ("gray matter"[Title/Abstract]) OR ("grey matter"[Title/Abstract]) OR ("morphology"[Title/Abstract]) OR ("morphometry"[Title/Abstract]) OR ("seed-based"[Title/Abstract]) OR ("VBM"[Title/Abstract]) OR ("FreeSurfer"[Title/Abstract]) OR ("FSL"[Title/Abstract]) OR ("brain connectivity"[Title/Abstract])) AND ((humans[Filter]) AND (english[Filter])) AND ((humans[Filter]) AND (english[Filter])) AND ((humans[Filter]) AND (english[Filter]))
SCOPUS (filters: English; neuroscience; article, **review**; human, humans	TITLE-ABS-KEY (("prolonged stress" OR "chronic stress" OR "perceived stress" OR "stress perception" OR "perception of stress" OR "PSS" OR "PSS10" OR "PSS-10" OR "10-PSS" OR "10-item PSS" OR "Psychological stress" OR "Psychosocial stress" OR "Occupational stress" OR "Psychological distress") AND ("Neuroimag*" OR "volum*" OR "magnetic resonance imaging" OR "MRI" OR "resting state" OR "resting-state" OR "functional MRI" OR "fMRI" OR "connectivity" OR "structural MRI" OR "gray matter" OR "grey matter" OR "morphology" OR "morphometry" OR "seed-based" OR "VBM" OR "FreeSurfer" OR "FSL" OR "brain connectivity")) AND (

	LIMIT-TO (SUBJAREA , "NEUR")) AND (LIMIT-TO (DOCTYPE , "ar") OR LIMIT-TO (DOCTYPE , "re")) AND (LIMIT-TO (LANGUAGE , "English")) AND (LIMIT-TO (EXACTKEYWORD , "Human") OR LIMIT-TO (EXACTKEYWORD , "Humans"))
ISI Web Knowl English	(#1 OR #2) AND SU=(Neurosciences & Neurology OR Radiology, Nuclear Medicine & Medical Imaging) TI/AB = (("prolonged stress" OR "chronic stress" OR "perceived stress" OR "stress perception" OR "perception of stress" OR "PSS" OR "PSS10" OR "PSS-10" OR "10-PSS" OR "10-item PSS" OR "Psychological stress" OR "Psychosocial stress" OR "Occupational stress" OR "Psychological distress") AND ("Neuroimag*" OR "volum*" OR "magnetic resonance imaging" OR "MRI" OR "resting state" OR "resting-state" OR "functional MRI" OR "fMRI" OR "connectivity" OR "structural MRI" OR "gray matter" OR "grey matter" OR "morphology" OR "morphometry" OR "seed-based" OR "VBM" OR "FreeSurfer" OR "FSL" OR "brain connectivity"))